CHARACTERIZING INOCULUM DENSITY AND PLANT PHENOTYPIC VARIATION AT HIGH SPATIAL RESOLUTION

A Dissertation

by

ROY L. DAVIS II

Submitted to the Graduate and Professional School of
Texas A&M University
in partial fulfillment of the requirements for the degree of

DOCTOR OF PHILOSOPHY

Chair of Committee,	Thomas M. Chappell
Committee Members,	Won-Bo Shim
	Olufemi J. Alabi
	Micky M. Eubanks
Head of Department,	Leland S. Pierson III

May 2022

Major Subject: Plant Pathology

ABSTRACT

Agroecosystems, even when crops are planted in monoculture, are complex and characterized by heterogeneity. Disease incidence and inoculum density vary across space and time, but explanation for this variation enhances prediction and management of disease. In many plant pathosystems, such variation is not always well characterized if it is observed at all. Advancements in precision agriculture technologies provide the opportunity to describe variation in near real-time and to more rapidly respond to the threat of disease. Innovative approaches to data collection and analysis are required to fully realize the capabilities of these technologies through high-throughput detection or high-resolution remote sensing, and to improve management by describing and explaining variation in disease and inoculum density. To enhance the value of remote sensing, an unsupervised machine learning technique, finite mixture modeling, was applied to more efficiently estimate plant height by accounting for spatial variability in height, at scale, through aerial imagery. Finite mixture models were fit to three-dimensional point cloud data to estimate plant height in different terrains. This method was effective at estimating height and robust to variation associated with topography. To enhance the value of cotton variety trials, the spatial and temporal variation of soilborne *Fusarium oxysporum* f. sp. *vasinfectum* race 4 was described. First, a DNA-based method to quantify soilborne inoculum was developed and validated using spike-in experiments in environmental soils. Next, this quantitative PCR-based method was utilized to describe the pathogen at high spatial resolution in a research field in Fabens,

Texas. Spatial statistical techniques were used to determine the spatial autocorrelation of inoculum density in this field, and the results indicated that temporal factors should also affect the efficiency of variety trials. To describe the temporal variation in inoculum density, a longitudinal study was devised to test the effect of cotton cultivar and other organic matter in an environmental growth chamber. Empirical characterization of the heterogeneity in plant pathosystems is necessary for the development of more robust predictive epidemiological models. High-resolution data and the models that use those data are a necessary component associated with management and precision agriculture. Empirical characterization of heterogeneity in field is an essential for the development of more robust predictive epidemiological models.

DEDICATION

This dissertation is dedicated to my family for their love and support. Without that foundation, pursuing this degree would have been more difficult.

This dissertation is also dedicated Mrs. Tara Nye, Dr. Christopher Havran, and Dr. L. Michael Larsen who all inspired me to follow this career path.

ACKNOWLEDGEMENTS

I would like to thank my advisor and committee chair Dr. Thomas Chappell, for accepting me as his first student and for challenging me to become a better researcher. I am fortunate to have had a dedicated advisor during my time as a graduate student. I am grateful for his guidance and mentoring. I would like to acknowledge my committee members, Dr. Won-Bo Shim, Dr. Olufemi Alabi, and Dr. Micky Eubanks, for their contributions to my development as a scholar throughout my degree program.

Additionally, I would like to thank the faculty and staff of the Department of Plant Pathology and Microbiology for their invaluable support throughout my time at Texas A&M University. To my collaborators and contributors, I am sincerely grateful for your help and input.

Finally, to my lab mates, I would like to thank each of you for the good times we had and the laughs we shared. I genuinely value the bond that we built over the years. I will carry these experiences and the inside jokes with me into the future.

CONTRIBUTORS AND FUNDING SOURCES

Contributors

This research herein was supervised by a dissertation committee consisting of Dr. Thomas M. Chappell (advisor and committee chair), Dr. Won-Bo Shim, and Dr. Olufemi J. Alabi of the Department of Plant Pathology and Microbiology, and Dr. Micky D. Eubanks of the Department of Entomology.

Unmanned aircraft system image data used in Chapter II were provided by Dr. Young-Ki Jo of the Department of Plant Pathology and Microbiology and Dr. Fugen Dou, of the Department of Soil & Crop Sciences. Drone mission for data collected at the Beaumont AgriLife Research and Extension Center were flown by Eric Pitts. Dr. Jeremy K. Greene, of the Clemson University Department of Plant and Environmental Sciences, provided unmanned aircraft system image data captured at Amerson's Nursery and the Clemson Edisto Research and Education Center. In addition, Dr. Greene provided crop measurements acquired in the field. These data were published in 2020 in *Agronomy*.

Dr. Thomas M. Chappell and Dr. Thomas Isakeit contributed to research in Chapter III, which was published in 2022 in *Plant Disease*. Initial fungal isolates used for this study were provided by Dr. Thomas Isakeit, Dr. Terry Wheeler, and Dr. Won-Bo Shim. Cyrena Petersen, Dr. Thomas Isakeit, Heather Elkins-Arce, Joel Arce, Cynthia Sanchez, and Jensen Hayter assisted in the collection of soil samples which were used to generate data used in Chapter III and Chapter IV.

All other work herein was completed by the candidate independently.

Funding Sources

Funding for this research was provided by the College of Agriculture and Life Sciences of Texas A&M University, the Texas Energy & Sustainability Alliance for Graduate Education and the Professoriate Mini-Grant, Cotton Incorporated grant number 19-165, and the United State Department of Agriculture through Hatch Project TEX09705.

NOMENCLATURE

AGL	Above ground level
ANCOVA	Analysis of covariance
BIC	Bayesian information criterion
C_q	Cycle of quantitation
ddPCR	Droplet digital polymerase chain reaction
E	qPCR efficiency
FMM	Finite mixture modeling
FOL	*Fusarium oxysporum* f. sp. *lycopersici*
FOV1	*Fusarium oxysporum* f. sp. *vasinfectum* race 1
FOV4	*Fusarium oxysporum* f. sp. *vasinfectum* race 4
FV	*Fusarium verticilliodes*
GLM	Generalized linear model
GPS	Global positioning satellite
LARS	Low altitude remote sensing
m	Meters
p	p-value
PHO84	Phosphate permase gene
qPCR	Quantitative polymerase chain reaction
r	Pearson correlation coefficient
R^2	Coefficient of determination

RGB	Red-Green-Blue (color channels)
SAS	Statistical analysis system
Tfo1	FOV4 CA-9 transposase gene
UAS	Unmanned aircraft systems
Z	Z-score
μ	Mean

TABLE OF CONTENTS

Page

LIST OF FIGURES

Page

LIST OF TABLES

Page

CHAPTER I

INTRODUCTION

Dimension of the Disease Triangle

The description of the epidemiology of plant diseases is enhanced by first understanding the factors that directly affect the growth and development of plants within the constraints of their ecosystems. Plants are sessile organisms, meaning that during their life cycles they are constrained to the conditions of their surroundings, and they must adapt to those conditions to survive to maturity and produce seeds for future propagation. In an agricultural setting the end goal – production of seed, fiber, fuel, or food – is dependent upon the use of a specific crop. Nevertheless, host plants, whether wild or domesticated, are subject to the conditions of their ecosystems. Whether wild or domesticated, conditions such as variable weather, nutrient availability, or pathogen inoculum density are common, though interactions between these conditions and plants are not always well understood. The disease triangle, a foundational concept in plant pathology, was designed for the purpose of better understanding the interactions between host plants and the outside factors that can lead to the onset of disease.

As a conceptual construct, the disease triangle is commonly utilized to describe the requirement of three factors for the onset of plant disease: hosts, their pathogens, and the environment. Specifically, disease manifestation is brought about by the interaction of a susceptible host and a virulent pathogen under conducive environmental conditions (Stevens 1960; Scholthof 2007). The utility of the disease triangle is that it decomposes

the complex biological interactions underlying pathogenesis into a readily understandable format to describe how epidemics start and why they manifest (Scholthof 2007; Grulke 2011). While this concept is useful in the visualization of disease, nuances within each of the points of the triangle are lost when the describing the most basic conditions necessary for disease manifestation. The construct of the disease triangle is a useful tool to understand the initiation of disease, but to describe disease epidemics other factors that affect disease progression and severity must also be considered.

The disease triangle is limited to the instance of pathogenesis, whereas plant disease epidemics are variable and complex, involving many causes that can be modeled as dimensions. Alongside the host, pathogen, and environment, other aspects such as time and spatial aggregation also affect disease progression. To overcome the limitations of this construct, the outside factors that act upon each of the three sides must be better understood. Studying these inputs in relation to one of the facets of the disease triangle helps to reveal causes of variation in plant disease. By focusing on a specific facet of the disease triangle in relation to a specific plant pathosystem, explanatory models can be developed to describe disease under different conditions. The research described herein focuses on spatial and temporal patterns of variation and investigates the processes that causes the variation. These are the processes that govern heterogeneity of pathogen distribution, related to disease and inoculum density in relevant agricultural settings. Prior to undertaking studies that focus specifically on the pathogen facet of the disease triangle, the interactions between the three constituent parts of the disease triangle must be better understood.

Environmental Factors Affecting Inoculum Density

Of the three facets of the disease triangle, the environment encompasses a wide array of conditions that could affect the onset and progression of diseases in plants. Foremost among environmental conditions that are considered when modeling disease is the weather. Climatic conditions such as rainfall, temperature, humidity, or wind can directly affect the movement of a pathogen (Liu & He 2019). Though some weather conditions are erratic, the range of conditions that dictate the initiation of disease can be reliably used to predict disease where host and pathogen are present. For instance, the dispersal of *Puccinia graminis* f. sp. *tritici*, the causal agent of wheat leaf and stem rust, is dependent on both wind and relative moisture (Eversmeyer & Kramer 2000). The source of primary inoculum of urediniospores is windborne; these spores are carried by the prevailing winds where they eventually land on a new host. Following a rainfall event, when relative moisture is higher, urediniospores release at a lower rate compared to days with dryer conditions (Eversmeyer & Kramer 2000). Environmental conditions not only play a role in dispersion of spores, but also in delaying the dispersion of those same spores. Weather conditions also play a role in the movement of soilborne pathogens. Heavy rains can cause localized flooding, moving soil, and thereby potentially transporting inoculum, between and within fields. The outcome of this movement is the establishment of new disease loci or expansion of existing ones. Overall, the role of weather in spatial and temporal heterogeneity of inoculum cannot not be overstated.

The soil in which a host is planted also plays a major role in disease development, especially the physical and chemical properties. Physical characteristics of soil are major determinants of how pathogens or other soil-inhabiting organisms such as nematodes move. Specifically, soil type, texture, and pore size can create more conducive or inhibitory conditions affecting the movement and growth of soilborne pathogens (Voroney & Heck 2015). For example, pore size, the amount of space between individual soil particles, may affect the percolation of water carrying inoculum either down into the soil or between adjacent plots. Soil biochemistry varies between locations and involves components such as nutrient availability, pH, and organic matter; each of these can directly affect the growth and development both hosts and pathogens (Grulke 2011; Chappelka & Grulke 2015; Chenu et al. 2015; Ojiambo et al. 2017). Organic matter, for instance, can be used to fuel the saprophytic (a form of non-pathogenic) growth of soilborne fungi ensuring survival during potentially detrimental conditions (Chenu et al. 2016). Soil moisture can also play a role in pathogen movement. The water content of the soil can directly affect the establishment and growth of pathogens (Liu & He 2009).

Rhizosphere inhabiting microorganisms can also affect the interactions between hosts and pathogens, in some cases these can lead to soils that can suppress disease (Termorshuizen 2016). Other bacteria or fungi may operate as endophytes within their hosts, with some providing beneficial enhancements (Ballestrini et al. 2015; Santoyo et al. 2016; Wani et al. 2015). Endophytic organisms live within their hosts without the manifestation of visible symptoms and in doing so, some may prove beneficial by

enhancing drought or salinity tolerance, or by enhancing resistance to a variety of stressors (Ballestrini et al. 2015; Santoyo et al. 2016; Wani et al. 2015). Other rhizosphere inhabitants, like *Trichoderma* species, are known to inhibit the growth of other pathogenic microorganisms as a form of biocontrol (Ballestrini et al. 2015). Despite the benefits of some ubiquitous rhizosphere inhabitants, others, such as *Fusarium* or *Rhizoctonia* species, may be pathogenic on a multitude of crops (Ballestrini et al. 2015).

Host-related Factors Affecting Inoculum Density

Due to the prevalence of monoculture cropping practices, agricultural ecosystems have relatively low variability in the genetic resistance of a host population (Burdon and Thrall 2007). With reduced resistance variation in a host population, there is higher risk that an arriving specific, aggressive pathogen race or strain could have a major detrimental effect on yield (Burdon and Thrall 2007). The susceptibility of a host plant has a direct effect on its survival when presented with high disease pressure. Host susceptibility can be regulated by gene-for-gene interactions, where compatibility (disease) or incompatibility (no disease) is determined by resistance genes (*R*) of the host and avirulence genes (*Avr*) of the pathogen (Thrall & Burdon 2002; Thrall et al. 2016). Resistance is either qualitative, often due to a single gene conferring resistance, or quantitative, potentially the result of multiple minor genes determining resistance in combination (Burdon & Thrall 2003). Host populations evolve stronger defensive capabilities in response to the selection imposed by infection by pathogens. Certain pathogen-associated molecular patterns (PAMPs), such as fungal chitin or flagellin in

bacteria, are detected by pathogen recognition receptors (PRR) in plants leading to PAMP-triggered immunity (PTI) (Shan et al. 2007; Anderson et al. 2010). Host plants are able to defend against infection using PTI (Shan et al. 2007; Anderson et al. 2010). In response, pathogen populations evolve to evade or suppress host defenses using effectors. Plants react with effector triggered immunity (ETI), including mechanisms such as stomatal closure or hypersensitive response to limit the pathogen's spread in the plant (Shan et al. 2007; Anderson et al. 2010). The antagonistic coevolution that characterizes pathosystems causes these systems to demonstrate how tenuous resistance can be when a pathogen is actively evolving to overwhelm or bypass host defenses. Though the best defense against plant diseases is robust genetic resistance, even this does not necessarily preclude a pathogen from infecting. Furthermore, resistance in crops may be incomplete or potentially come with a fitness cost that is only known when it is grown under relevant environmental conditions. And although a resistant host may not be affected to the degree that a susceptible host would, a resistant plant may yet be colonized by or infected with a pathogen and not succumb to disease. There is still a chance for nominally resistant and tolerant cultivars to amplify inoculum by acting as reservoirs for the pathogen.

The underlying molecular mechanisms involved in the coevolution of hosts and pathogens are used to develop genetic resistance for agricultural crops. New lines are developed that have been selectively bred for resistance; distribution of plants from these lines into agroecosystems in turn results in selective pressure for pathogen populations to evolve virulence (Burdon & Thrall 1999). In other words, breeding efforts can directly

influence the evolution of pathogen populations leading to epidemics. For example, the emergence of Race T of *Cochliobolus heterostrophus* in the United States in response to the widespread use of the Texas male sterile cytoplasm maize, which to the southern corn leaf blight epidemic of the early 1970s (Bruns 2017). Comparatively, in natural host populations disease is a function of a pathogen's ability to arrive at new, susceptible hosts through dispersal events (Burdon & Thrall 1999). Natural pathogen populations experience evolution due to genetic drift, movement between neighboring populations, and selection pressure (Burdon & Thrall 1999; Seabloom et al. 2015). The artificiality of agricultural coevolution, however, demonstrates that the change in the pathogen is dependent on how frequently a trait is present in the host population (Burdon & Thrall 1999).

Plants inhabiting natural ecosystems have the advantage of biodiversity and variability in genotypes (Alexander 1989). When compared to the spatially uniform planting patterns in agricultural operations, wild hosts are more likely to be either randomly dispersed or aggregated (Alexander 1989). And, depending on the mode through which a pathogen moves and is transmitted, establishment may be more difficult in these environments because of the relative sparseness or spatial discontinuity of susceptible hosts. A related concept in disease ecology is the dilution effect hypothesis, in which increased biodiversity is expected to reduce disease risk through multiple different mechanisms (Keesing 2006; Keesing et al. 2006; Citavello et al. 2015). In agricultural ecosystems, densely populated monocultures are more conducive to the transmission of a pathogen between proximal, susceptible hosts (Termorshuizen 2016),

and large uniformly planted monocultures alongside cultivation practices that aid in the dispersal of pathogens, have the potential to increase inoculum and the likelihood of epidemics (Leclerc et al. 2013; Liu & He 2019). Monoculture settings also allow for the perpetual survival especially of soilborne pathogens either saprophytically or in overwintering structures, subsequently leading to increased disease pressure in the future (Bennett et al. 2011). In addition, cultivation practices that are used to maintain uniformity, such as tillage or fertilization, may make the environment more conducive for epidemic spread (Alexander 1989). Despite evidence supporting the dilution effect hypothesis, increasing biodiversity in agricultural settings is not strategically financially feasible enough for growers to employ. Instead, understanding the spatial make-up of inoculum and its modes of movement are the best methods that can be utilized to control potential disease epidemics.

Pathogen-related Factors Determining Inoculum Density.

Agricultural ecosystems are characterized by the heterogeneity of inoculum and disease, which is caused in part by the mechanisms through which inoculum moves (Plantegenest et al. 2007; Papaix et al. 2015). Spatial and temporal variation in inoculum density determines whether a susceptible host and a virulent pathogen will interact and if disease will manifest. However, inoculum density does not always correlate with the amount of disease appearing in a given host population during a growing season (Berbegal et al. 2007; Hao et al. 2009). Inoculum density is dynamic due to multiple interconnected environmental and biological factors that benefit pathogen dispersion, establishment, and proliferation. These factors may be a direct result of the host or

environment acting on the pathogen, or they may be pathogen-related survival strategies. Viral pathogens survive in host plants, other viruses are able to replicate within their vectors ensuring survival and future transmission (Jeger 2020). Bacterial pathogens can overwinter in hosts tissues, soil, or in vectors (Schuster & Coyne 1974). Fungal pathogens have developed multiple survival strategies such as teliospores for rusts and smuts, which are overwintering forms used to subsist during periods when conditions are not conducive for pathogenesis (Brown 1997). Many soilborne fungal pathogens utilize different strategies to survive. For example, thick-walled chlamydospores can overwinter in soil until exudates from hosts signal the active growth (Brown 1997). Other fungi are able to survive in the interim as saprophytes, on plant debris or other organic material found in soils (Brown 1997). Dispersal patterns of infectious propagules are dependent on the methods a pathogen uses to infest its hosts. Understanding the differences in dispersion patterns is useful in modeling the movement of pathogens.

The movement of inoculum can broadly be classified into two categories: density-dependent and frequency-dependent transmission. Density-dependent transmission is the spread of infectious propagules through mass action, where transmission of inoculum is directly related to host population density (Keesing 2006; Ostfeld & Keesing 2012; Young et al. 2017). The pathogen is readily infectious while passively moving between proximal hosts, an example of this is the movement of windborne spores or the infectious spread of soilborne pathogens. Consequently, density-dependent transmission of inoculum can be considered additive (Young et al. 2017). Frequency-dependent transmission refers to the movement of inoculum through

outside means, such as through water or translocation of soil by field implements, over short and long distances. The more frequently propagules are transmitted, the more likely the pathogen is to establish and for disease to manifest (Keesing 2006; Ostfeld & Keesing 2012; Young et al. 2017). Frequency-dependent transmission has mostly been used to describe vector-borne diseases (Ostfeld & Keesing 2012). Movement of inoculum is interconnected and relies on both density- and frequency-dependent transmission through either short-range or long-distance movement.

Understanding that the modes of inoculum movement are interconnected, statistical techniques can be employed to describe the spatial patterns of inoculum in fields. Spatial autocorrelation quantitatively describes the relationship between states in locations in an *n*-dimensional (usually 2) space as a function of distance between the locations. Moran's I is an index used to represent spatial autocorrelation as a quantity ranging from -1 to +1. Values of Moran's I allow the spatial distribution of inoculum to be described as uniform (-1), random (0), or clustered (+1), where randomness is typically assumed as the null hypothesis for testing (Madden 1989). Uniformly dispersed pathogens are not expected unless inoculum density is equally and consistently high (Madden 1989). When observations are truly randomly dispersed, then there is no spatial autocorrelation because each observation of inoculum is independent (Madden 1989). A pathogen with a clustered spatial pattern is autocorrelated, where observations are dependent on others as a function of spatial aggregation (Madden 1989). The degree to which inoculum is spatially autocorrelated is dependent upon its mechanisms of initial dispersal and subsequent spread. For instance, a windborne pathogen is likely be

randomly distributed due to how it is transported because of the entropy that results from diffusion. Conversely, soilborne pathogens are more likely to be spatially aggregated because of density-dependent spread and growth from an initial inoculum locus.

The modes of inoculum movement can be more simply described as the translocation of inoculum from a source, such as an infested field or infected tree, to a sink, an area where a pathogen can potentially propagate under conducive conditions. Each individual host plant or each disease locus is occupied by a group of pathogens that shifts through space and time due to vegetative growth and reproduction, and due to movement (Burdon & Thrall 1999; Plantegenest et al. 2007; Alexander 2010). This source-sink model of inoculum movement helps to illustrate the importance of understanding the spatial and temporal variation of a pathogen by describing establishment and spread of inoculum as a function of movement. An understanding of how inoculum disperses or is transmitted throughout its environment is necessary for developing explanatory and spatiotemporally resolved models of inoculum density (Plantegenest et al. 2007; Ojiambo et al. 2017). These models can then be used to develop better management strategies for implementation and intervention. However, before these models can be developed, it is useful to measure inoculum density using different quantitative methods for the purposes of calibration and validation.

Quantifying Variation in Agricultural Ecosystems

Innovation is required to enhance comprehension of the spatial and temporal dynamics that lead to heterogeneity in agricultural ecosystems. Precision agriculturecontinues to increase efficiency of crop management by monitoring and

analyzing field conditions at high resolution, and especially benefits from such innovative methods related to observation and measurement. Improvement of methods through which variability is detected and quantified is required to describe epidemics. In the realm of quantification, innovations with different types of technology will increase detection capabilities to determine where symptoms or heterogeneity exists, with consequent benefits to the efficiency and sensitivity of scouting for disease.

Imaging platforms such as unmanned aircraft systems and related technologies have been utilized for whole field imaging to describe the phenotypic variation associated with factors such as differential nutrient input (Yin et al. 2011) or disease (Zhang et al. 2018). Techniques have been developed to measure phenotypes such as height, using structure-from-motion algorithms, biomass (Diaz-Varela et al. 2015; Li et al. 2020), and to estimate crop yield (Gracia-Romero et al. 2017). Such techniques have opened the door for quantifying the number of diseased plants at the field scale. For example, Liu et al. (2019) used red-green-blue images and hue-saturation-intensity system to detect powdery mildew of wheat (*Blumeria graminis* f sp. *tritici*) by calculating different indices describing color. The logarithm of the red color index was the best measure of color to detect incidence of powdery mildew in images (Liu et al. 2019). Others have pioneered techniques utilizing supervised machine learning to describe the variation in phenotypes using pattern recognition, in which an algorithm is trained to detect certain patterns associated with diseases, such as discoloration or lesion shape (Kalischuk et al. 2019; Liu et al. 2019). Innovations such as these, especially those related to the detection of pathogens using aerial imagery, provide increased options,

efficiency, and scalability for scouting for disease. These techniques are all useful for finding disease and they can be used as precursors for analyses to quantify inoculum density.

Empirical characterization of inoculum density is enhanced when data are of high spatial resolution through measurement at scale. Disease assays have been used for this purpose to describe the variation in symptom severity across different inoculum densities. Though disease symptoms are useful for locating inoculum in space, they are not always the most reliable predictor for inoculum density, especially when the relationship between disease and inoculum density is dependent on host type and host effects are unknown – the case in variety trials. Quantitative techniques are widely used to describe heterogeneity associated with inoculum density. Prior to the advent of molecular techniques, other methods to quantify inoculum included counting fungal spores or bacterial colonies. Methods such as high-pressure liquid chromatography to quantify specific compounds or metabolites e.g. fumonisins (Seo et al. 2009), have been widely used to describe variation in inoculum density. Molecular techniques, such as quantitative polymerase chain reaction (qPCR) or sequencing, allow unculturable bacteria and viruses to be directly quantified in both hosts and vectors. Detection of soilborne pathogens using molecular techniques have seen many advancements in quantification using qPCR (Burkhardt et al. 2018; Jiménez-Fernández et al. 2011; Scarlett et al. 2013), and more recently droplet digital PCR (ddPCR). For example, Scarlett et al. (2013) designed primers specific to *Fusarium oxysporum* f. sp. *cucumerinum* to quantify the pathogen from environmental soils. Continued study of

inoculum density variation can be applied to quantifying inoculum not only across space, but also over time. Additional work, however, is still necessary to understand the dependence of reliable inoculum quantification on methods, because some methods may detect both living and dead tissue or genetic material or otherwise not reliably represent infectious inoculum through the use of molecular methods or other proxy.

Conceptual Overview of Dissertation Research

Heterogeneity in agricultural systems is a function of the complex interactions between the spatial and temporal factors that contribute to the establishment, growth, and spread of the pathogen or other factors that affect the development of plants. To describe, understand, and predict heterogeneity in detail for agricultural ecosystems, the spatial and temporal dynamics of both disease and inoculum, and the interplay between them, must be known. To know the spatial and temporal dynamics, the patterns associated with each, and the interplay between them, must be described. The research herein seeks to empirically answer three questions related to the variation in pathosystems across space and time that leads to epidemiologically relevant heterogeneity.

1) What is the spatial distribution of inoculum? The conditions that affect inoculum density and phenotypic expression are expected to be heterogeneous with respect to their spatial configuration. Knowing where disease is and how much inoculum is present are vital to understanding the spatial distribution of inoculum. This question can be further broken down into two parts: detection and quantification. To understand spatial distribution of inoculum, inoculum must first be detected using different means.

The inoculum must then be quantified to describe the potential effect over an expansive spatial scale. In this dissertation, an analytical metric was developed to describe heterogeneity in plant phenotypes independent of topography using UAS-captured image data. Additionally, a method was developed to quantify *Fusarium oxysporum* f. sp. *vasinfectum* race 4 (FOV4) from environmental samples to describe the spatial distribution of inoculum under relevant conditions.

The heterogeneous distribution of inoculum in an agricultural ecosystem is a function of both short-distance spread and long-range transmission through various biological, environmental, and human-mediated modes of movement. Locating inoculum relies on finding the symptoms of disease. By utilizing different technologies, such as low altitude remote sensing, scouting for heterogeneity in an agricultural ecosystem becomes more accessible because a wider range can be viewed as opposed to scouting on foot. The resultant datasets are of high size and resolution, so innovative methods are necessary to efficiently utilize these data for purposes of scouting or estimating phenotypes. In this dissertation, the unsupervised machine learning technique finite mixture modeling (FMM) is utilized for discerning patterns in datasets related to phenotypic variation. Height estimations in the presence of differential nitrogen inputs or across variable topographies were discerned from high resolution red-green-blue image datasets using a structure-from-motion algorithm.

Prior to the use of quantitative techniques, the spatial distribution of inoculum is a black box. While disease symptoms can be used as an indicator for high levels of inoculum, symptom expression may be variable as a function of cultivar tolerance. By

quantifying inoculum, the spatial distribution and associated patterns can be used for the development of management practices. Without knowing the spatial distribution, these tasks prove difficult. A DNA-based quantitative method was developed to quantify soilborne *Fusarium oxysporum* f. sp. *vasinfectum* race 4 to describe the variability of inoculum in-field. A structured sampling plan was developed to account for spatial variation in inoculum density. Description of the spatial autocorrelation of inoculum was determined using Moran's I and other spatial statistical techniques.

2) How does inoculum density vary temporally? Alongside spatial heterogeneity, inoculum also varies as a function of time. The degree to which inoculum varies temporally is dependent on unknown factors. The soilborne fungal pathogen FOV4 is known to be an inoculum density-dependent disease (Hao et al. 2009), but the causes of variation in inoculum density have not been well characterized. Anecdotally, variation in inoculum density has been attributed to amplification of inoculum by susceptible cotton cultivars harboring infection. This research was undertaken to empirically describe the temporal variation in inoculum density by quantifying soilborne FOV4 in field locations and through growth chamber experiments. In the field, soil samples were collected throughout the extent of a cotton variety trial, and inoculum quantity and its spatial autocorrelation over time were analyzed to determine whether inoculum density or its spatial autocorrelation changes through time. The subsequent growth chamber experiment was used to understand what drives variation of inoculum density over time, and to assess the relative importance of saprophytic versus pathogenic growth as functions of organic matter abundance and host susceptibility. The results clarified the

nature of temporal variation in FOV4 inoculum density and they were used to compare between field and growth chamber experiments.

3) Are the spatial and temporal dynamics interdependent? Over the course of a growing season, heterogeneity is expected to be a function of the interplay between causes of spatial and temporal inoculum density variation. To understand this interplay, the patterns associated with heterogeneity of phenotypes, and the spatial and temporal variation in inoculum density must be understood in order to compare them. The ways in which these patterns interact are potentially complex and typically not known in practice, even in the spatially regimented and temporally synchronized operational settings of production or research agriculture. Using the empirical evidence gathered in this dissertation, the interplay between spatial and temporal dynamics of soilborne FOV4 will be discussed by examining patterns resulting from the movement and growth of inoculum. Plant disease epidemiology relies on describing these patterns to infer cause and explain disease epidemics.

When describing the severity of plant disease epidemics, knowing the amount of the pathogen available to initiate infection leading to disease is important. Disease pressure may be either high or low, due in part to the multiple interconnected factors that affect the number of infectious propagules in a given space at a specific time. And though disease pressure may be high at one instance in time, the number of infectious propagules in a field ecosystem is expected to be heterogenous and highly variable at scale (Plantegenest et al. 2007). These infectious propagules are the main determinant of the severity of an epidemic. In many plant pathosystems, the effect of inoculum density

has not been well characterized, in part due to the heterogeneity of inoculum, but also because of the complex interactions that inoculum density has with other aspects of the disease triangle. Gaining a better understanding of the spatiotemporal dynamics of inoculum and heterogeneity of phenotypes will assist in the development of more effective control and management strategies for plant disease epidemics.

This research was commenced to describe heterogeneity in plant phenotypes and inoculum density, each a function of spatial and temporal processes, through empirical observation of relevant agroecosystems and analytical approaches to quantitative estimation. The three questions outlined previously were answered in each of a few different agricultural systems by developing methods of detection using unmanned aircraft systems and by using quantitative, DNA-based techniques to locate disease and inoculum, respectively. High-resolution data were utilized to characterize the spatial structure associated with plant phenotypes and inoculum density and how these vary through time. By using spatially resolved data, while also accounting for variation over time, patterns related to plant phenotypes or inoculum density are more readily recognized. Description of the patterns that emerge from the data, upon empirical investigation, further enhance the predictive ability of models developed using these data. Taken together, answers to these three questions were used to describe the interplay between the spatial and temporal processes leading to heterogeneity relevant to plant disease development. Data generated through these investigations were used to synthesize various inputs into models that explain variation in inoculum density using high resolution datasets. Overall, the research led to techniques that are readily

applicable to precision agriculture, developed and refined through studying heterogeneity relevant to agricultural plant disease.

CHAPTER II

A PRACTICAL APPLICATION OF UNSUPERVISED MACHINE LEARNING FOR ANALYZING PLANT IMAGE DATA COLLECTED USING UNMANNED AIRCRAFT SYSTEMS*

Unmanned aircraft systems are increasingly used in data-gathering operations for precision agriculture, with compounding benefits. Analytical processing of image data remains a limitation for applications. We implement an unsupervised machine learning technique to efficiently analyze aerial image data, resulting in a robust method for estimating plant phenotypes. We test this implementation in three settings: rice fields, a plant nursery, and row crops of grain sorghum and soybeans. We find that unsupervised subpopulation description facilitates accurate plant phenotype estimation without requiring supervised classification approaches such as construction of reference data subsets using geographic positioning systems. Specifically, we apply finite mixture modeling to discern component probability distributions within mixtures, where components correspond to spatial references (for example, the ground) and measurement targets (plants). Major benefits of this approach are its robustness against ground elevational variation at either large or small scale and its proficiency in efficiently returning estimates without requiring in-field operations other than the vehicle overflight. Applications in plant pathosystems where metrics of interest are spectral instead of spatial are a promising future direction.

*__Reproduced from:__ Davis II, R. L., Greene, J. K., Dou, F., Jo, Y. K., and Chappell, T. M. 2020. A practical application of unsupervised machine learning for analyzing plant image data collected using unmanned aircraft systems. *Agronomy.* 10(5): 633. Doi: 10.3390/agronomy10050633.

Introduction

Unmanned aircraft systems (UASs) have been discussed as a cornerstone of precision agriculture (Araus et al. 2018; Araus & Cairns 2014; Maes & Steppe 2019; White et al. 2012; Yang et al. 2017; Zhang & Kovacs 2012), supporting the collection of timely and abundant data at expansive spatial scales through low-altitude remote sensing (LARS). Data collected through LARS are of high resolution and volume and can easily represent spatial scales exceeding the size of current agricultural operations (Haghighattalab et al. 2016; Shi et al. 2016). UAS image collection can be utilized when other means would be logistically limited, for example in flooded-field systems such as rice. Thermal and other spectral data can be collected at increasingly high resolution and detail as imaging technology advances (Bendig et al. 2013; Honkavaara et al. 2012; Liebisch et al. 2015; Su et al. 2018; Torres-Sanchez et al. 2015; Vanegas et al. 2015; Zhang et al. 2018). As beyond-line-of-sight applications become feasible, the potential spatial scale of data collected through LARS becomes practically unlimited. The advancement of LARS applications also makes them useful where financial or logistical resources are limited, providing information with a short turnaround time and low cost for small farms or operations in developing countries (Zhang & Kovacs 2012).

Research concerning LARS is increasing, and work is ongoing to translate this research to applications in commercial agriculture (Jimenez-Brenes et al. 2017; Ota et al. 2015; Su et al. 2018; Yamamoto et al. 2017). LARS techniques have been used to describe various plant metrics in fields, notably plant height (Christensen et al. 2017; Khanna et al. 2015; Madec et al. 2017; Watanabe et al. 2017) and height as a surrogate

for other metrics of economic interest, such as yield (Gracia-Romero et al. 2017; Haghighattalab et al. 2017; Kefauver et al. 2017; Yin et al. 2011). Using UASs, plant height has been studied as a readily measurable response to the uptake of nutrients such as phosphorus (Gracia-Romero et al. 2017) and nitrogen (Anbessa & Juskiw 2012; Kefauver et al. 2017; Vegara-Diaz et al. 2016; Yin et al. 2011). Additional applications of LARS include weed identification and mapping in fields (Borra-Serrano et al. 2015; Pena et al. 2013), characterizing tree canopies (Diaz-Varela et al. 2015), observing tree recovery after pruning (Jimenez-Brenes et al. 2015), and the detection of disease outbreaks (Al-Hiary et al. 2011; Zhang et al. 2018). As LARS technology improves, sophisticated applications of well-established findings are enabled—for example, in 1991, a demonstration established that multispectral measurement could be used to predict aspects of rust severity (Hansen 1991), and since then, applications have advanced commensurate with technology and researchers developing new analytical techniques (Su et al. 2018; Su et al. 2019; Westoby et al. 2012).

Utilization of LARS also faces challenges, especially in the setting of commercial agriculture where users of the technology seek to implement LARS in response to a current need, instead of for the purpose of advancing the underlying technology (Araus et al. 2018; Maes et al. 2019). A major limitation to the practical use of LARS for crop phenotyping is the efficiency of the application of the technology (Araus et al. 2018; Araus & Cairns 2014; Maes et al. 2019; White et al. 2012), such that there is need to streamline the turnaround with data analysis for practical use and rapid output of results. Though the economic feasibility of LARS approaches for producers is

often implied by referring to on-vehicle sensors as “consumer grade,” several analysis steps between image acquisition and result generation are intensive and expensive. A non-trivial problem related to physical characterization of crops is the requirement to have a positional reference for measurement. On-vehicle sensors are photonic in nature and principally record the wavelength and intensity of emissions. A global positioning system (GPS) receiver on a vehicle provides the ability to record the position of a photonic sensor—the three-dimensional orientation of which may also be recorded by accelerometry. Together, photography and positional data can be used by a structure-from-motion algorithm to infer three-dimensional structure from two-dimensional images (Westoby et al. 2012). In common situations where LARS is used to provide physical characterization of a crop, for example the average height of above-ground biomass, there is a requirement for the position of the ground to be known and used for reference (Gracia-Romero et al. 2017; Ota et al. 2015). Approaches to this include equipment- and software-intensive construction of a reference surface using GPS “control points,” or the explicit classification (computer automated or by eye) of plants vs. background for comparison (Haghighattalab et al. 2016; Shi et al. 2016; Zhang et al. 2014). GPS control points constitute references that are of known geospatial position, and also image-recorded position, so that the two can be reconciled in analytical processing (Bendig et al. 2013; Haghighattalab et al. 2016; Ota et al. 2015; Shi et al. 2016; Watanabe et al. 2016; Zhang et al. 2014). The points are effectively anchors for processing algorithms to use in constructing a geospatially explicit rendition of physical objects from imagery. The technique is not without merit, and not without cost.

Here, we focus on addressing these challenges using only image data, without GPS control points for ground surface construction, and without computer vision, obtaining data from visual inputs, for image classification or feature extraction. We test the utility of an unsupervised machine learning technique (hereafter "unsupervised learning") for advancing the analytical use of UAS data acquired by UAS-based LARS, intending to complement improvements in data quality currently being made through engineering. We believe that advancements in the analytical use of data will support optimization of future data collection and interpretation. Attempting to advance the utility of LARS in general, we use data from different agricultural settings and from different LARS platforms. We explore ways of presenting results and the underlying analytical methods of their generation and discuss how each may be optimized to better serve producers' purposes.

Materials and Methods

Sites, Materials, and Data

A field trial of nitrogen fertilizer application rates and timing for rice (*Oryza sativa* L.) crops was conducted in 2017 at the Texas A&M AgriLife Research Center in Beaumont, Texas (**Figure 1**). The project investigated the inbred cultivar Clearfield 272 (Horizon Ag, Memphis, TN), and the hybrid XLP753 (RiceTec Inc., Alvin, Texas). Rice was drill-planted on May 16 and grown with flush irrigation until the four- to five-leaf growth stage, after which a permanent flood (5–10 cm depth) was imposed and maintained until plant maturity. Aerial imagery of rice fields was collected on August 2, 2017 from at 15 m above ground level (AGL). A 245 × 45 m field was divided into six

research blocks, each consisting of forty 4.8 × 1.5 m plots wherein ten experimental treatments were each replicated four times. Nitrogen fertilizer (urea) was applied at four time points: pre-planting, pre-flooding, panicle initiation, and late booting (Table S1). All other field operations followed the 2014 Texas Rice Production Guidelines (Way et al. 2014).

A private nursery (Amerson's Nursery) in Lamar, SC, USA, was aerially photographed, including a diversity of plants on May 13, 2018 (**Figure 2**). Flights were flown at 15 m AGL. Our effort in this instance was to collect and process image data on a variety of plants to investigate the performance and robustness of an analytical approach. Areas populated by shrubs, trees, and potted plants were photographed for this purpose.

At the Clemson University Edisto Research and Educational Center (REC) in Blackville, South Carolina, where a rotational study concerning agriculturally relevant nematodes was underway in 2018, aerial imagery of fields of soybean (Glycine max L.) and grain sorghum (Sorghum bicolor (L.) Moench) was collected on July 23, 2018 (**Figure 3**). Here, our aim was to test approaches for their ability to recover accurate height estimates validated against "ground truth" measurements taken by personnel in the field. Accordingly, rectangular pieces of white cardboard were placed at ground level in these fields to mark locations at which in-field measurements were made on surrounding plants. Five randomly selected plants were measured with a ruler at each of eight such locations (four for grain sorghum and four for soybean), and these measurements were used for comparison with LARS-based estimates of height.

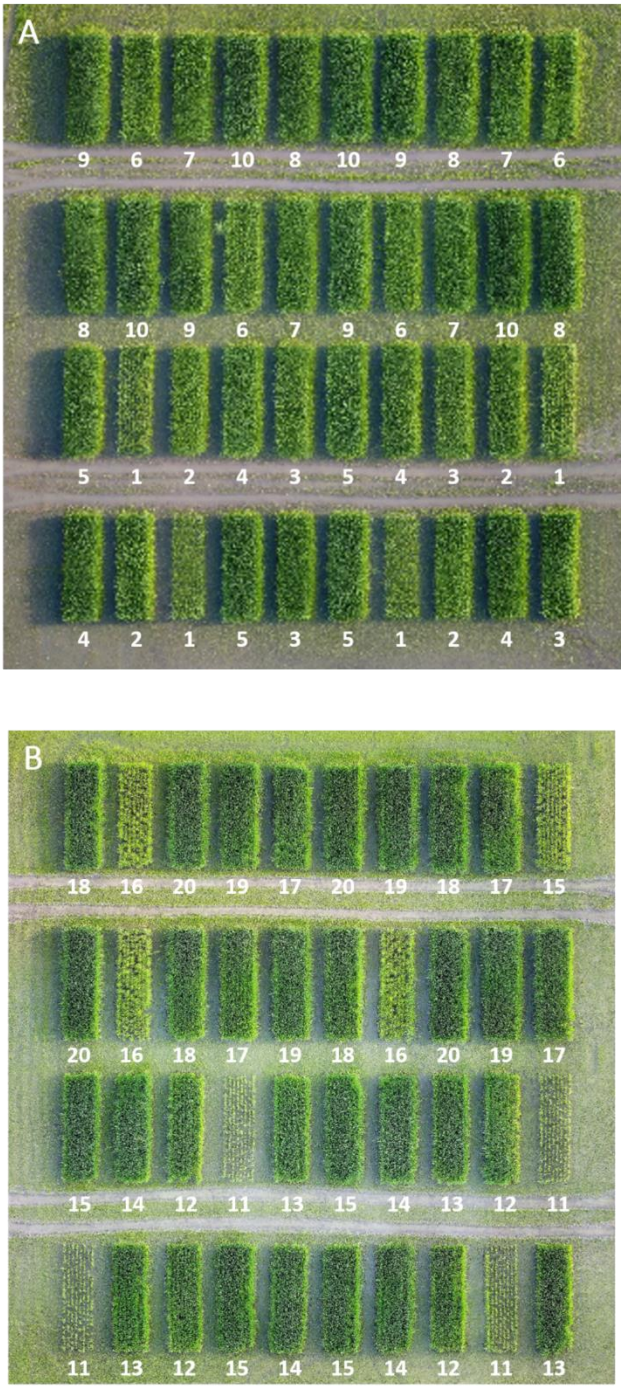

Figure 1. Representative imagery of fields. Rice fields 1 (A) and 2 (B) at the Texas A&M Agrilife Research Center in Beaumont, TX. Treatment numbers, directly below each plot, refer to the amount of nitrogen input (Table S1) during the growing season.

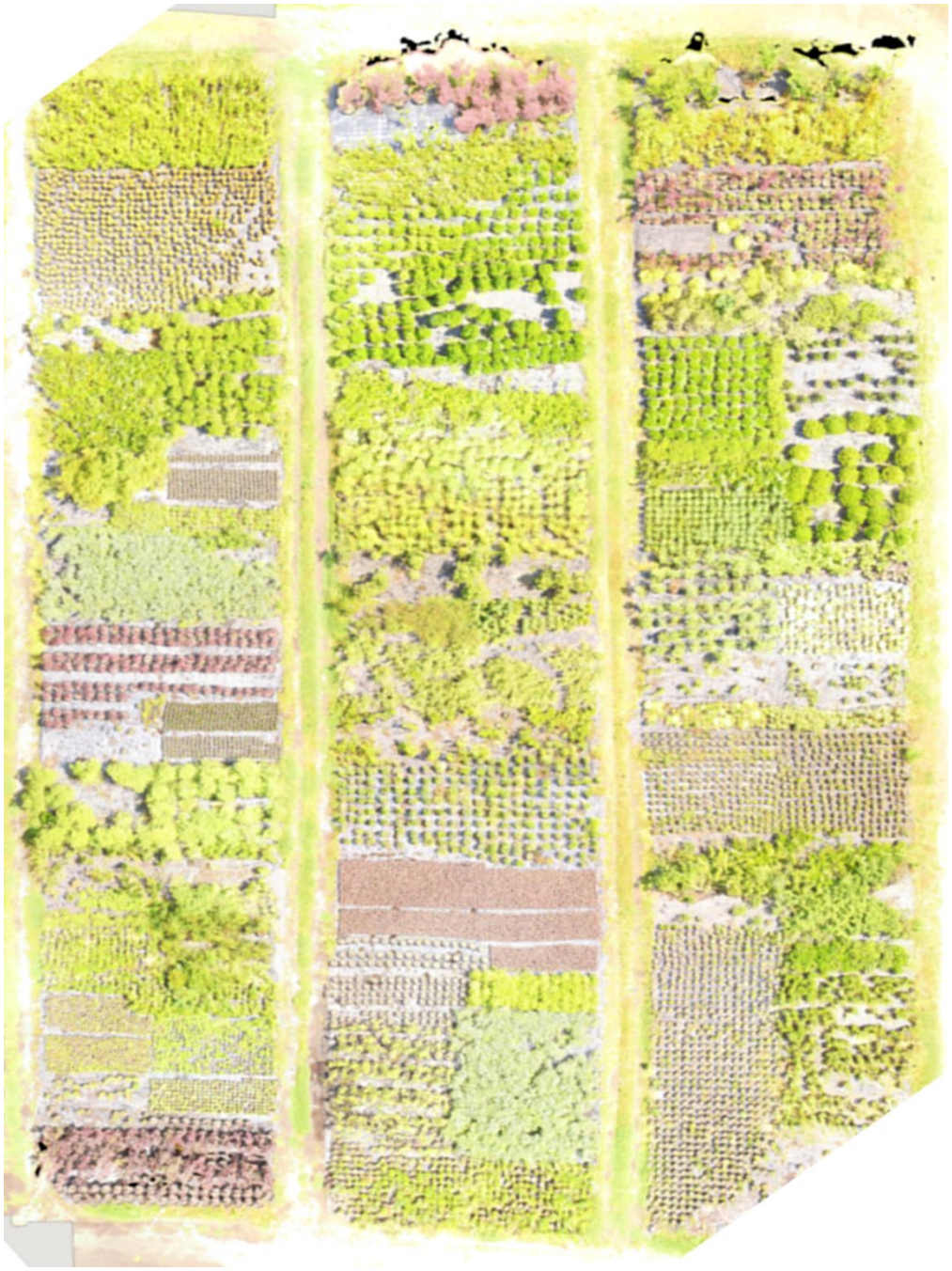

Figure 2. An orthomosaic of Amerson's Nursery in Lamar, SC.

Figure 3. Representative images of the Clemson University Edisto REC, Blackville, SC, soybean (A) and grain sorghum (B) fields.

Unmanned Aircraft Systems

The flight platform used was Dà-Jiāng Innovations (DJI) Phantom 4 (Dà-Jiāng Innovations, Shenzhen, China), with an attached red-green-blue (RGB) camera. The

flight platform used a 30 mm2 CMOS sensor with 12.4 effective megapixels. The viewing angle was 94°, the electronic shutter speeds were 8–1/8000 s, and the image size was 4000 × 3000 pixels. Raw images were stored in digital negative (DNG) format and developed to joint photographic experts group (JPEG) format for analysis. The system used a GPS and global navigation satellite system (GLONASS) for positioning. Images were stored on a micro secure digital (SD) card. Flights were either structured using the flight planning functions of Pix4Dmapper software version 4.1 (Pix4D, Lausanne, Switzerland) or conducted manually. Flights in Texas were planned, involving a double grid pattern with 75% pairwise overlap in both along-track and cross-track directions between sequentially adjacent photographs. Flights in South Carolina were manually directed, involving alternating forward and reverse passes and targeting 80% pairwise overlap between sequentially adjacent photographs in the along-track direction. Degree of overlap was chosen to conform with imaging practices reported in other studies, so that our data acquisition step would be in line with current practices (Haghighattalab et al. 2016, Shi et al. 2016).

Image and Data Processing

For each dataset, images were processed using the structure-from-motion algorithm of Pix4Dmapper software, resulting in point clouds. Point clouds comprise points inferred through the algorithm, in which each point is projected onto a three-dimensional space and has a spectral description. The structure-from-motion algorithm uses a single camera to infer three-dimensional structure in the way that multiscopic vision does, but by processing positional variation of the camera through time as

equivalent to the physical distance between two or more cameras. Point clouds, as tables, were used directly for analysis. Point clouds were visualized as three-dimensional surface plots (**Figure 4**) through the G3D procedure (three-dimensional graphics) of the SAS System v9.4 (SAS Institute, Cary, NC) to confirm point cloud processing success, for data subset delineation, and to visually identify potential anomalies or features that could interfere with or be utilized in analysis. Three-dimensional renderings of data involved latitude and longitude for in-field position and height or spectral (red, green, or blue) indices as the third dimension for visualization. Depictions were used to delineate data subsets representing areas of interest—fields, plots, or subplots in the research settings, and areas of the nursery. Random samples of a given size were taken from the dataset for visualization because the resolution of our raw data was much higher than that required for visualizing general features—in other words, we used a reduced-resolution preview of the full-resolution dataset to identify subareas such as plots or field margins, because these areas were easily identifiable without full-resolution depiction. For example, a point cloud representing the rice field at Beaumont, Texas, includes 3.5 million points, and 35 thousand points were randomly selected from the dataset for use in generating visualizations. Full-resolution point clouds were used for analysis.

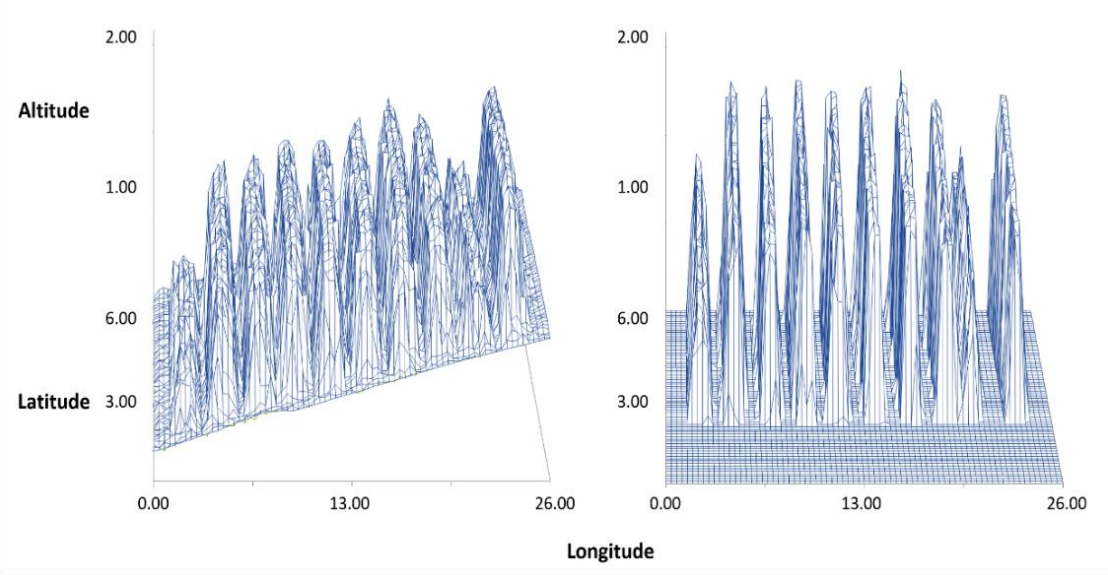

Figure 4. Representations of point cloud data. Subsets of point cloud data describing field N-6 are used to fit the wireframe surface plots shown here on the left, depicting the artifactual slope that formed primarily along the x-axis as a result of image processing without global positioning system (GPS) control points. This slope is marginalized by including the x- and y-axes as covariates in an analysis of covariance (ANCOVA), as shown on the right.

Point clouds were rendered as contour plots using the GCONTOUR procedure of the SAS System v4.3 and visually investigated for quality and representativeness of the depicted area, as compared to images to identify imaged subjects, by eye. Forty plots from the rice research field in Texas were visually identified using a contour map rendered from the point cloud. Treatment information associated with each plot, including timing (date) and amount (kilogram per hectare) of nitrogen addition, was merged with the point cloud dataset by plot for analyzing relationships between treatments and inferred rice plant height. Subsets of point cloud data from Amerson's Nursery were generated on the basis of plant type, following visual identification of areas targeted for analysis, e.g., an area of potted plants, or an area of a given type of

shrub. Subsets of point cloud data from the Edisto REC soybean and grain sorghum fields were generated to investigate how the spatial size of an imaged area can be chosen to optimize the accuracy or precision of estimated plant characteristics: square-shaped sample areas of two, four, eight, sixteen, and thirty-two square meters in area were taken from the whole-field point cloud. Each sample was centered on a reference point indicated by a white piece of cardboard placed at ground level in the field at random. This subsetting was done to emulate a researcher randomly choosing a sample location in a field for inclusion in a dataset.

A preliminary finding guided subsequent methods selection. Initial processing of images using Pix4D to generate point clouds resulted in three-dimensional depictions that included artifacts, specifically slopes that are known to not exist in reality, given that the depicted areas are flooded rice fields and thus necessarily level (**Figure 5**).

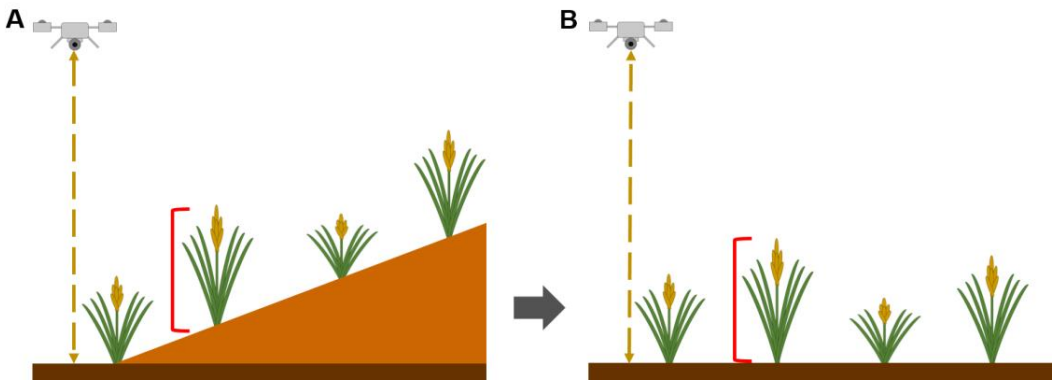

Figure 5. Marginalization of terrain variation to estimate plant height in an idealized setting of flat but sloped terrain. Inclusion of positional variables (e.g., latitude and longitude) as covariates allows terrain variation to be marginalized in a randomized complete block design, as gradients of other variables are addressed in ANCOVA.

The use of GPS control points would result in correcting this issue to a degree proportional to how accurately the points provide for estimating terrain surface. However, in this case, the effect is also easily marginalized by including positional variables (latitude and longitude) as covariates in a generalized linear model of height. For a flat surface (not level, but flat), as was the case for the rice fields, this technique works well. However, for any non-flat surface, terrain variation cannot be described by a linear model without concern that variation in plant height is also being described. The fact that (artifactual) terrain height variation in a special case (rice fields known to be both flat and level) could be marginalized without the use of GPS control points or classification of plants vs. ground suggested that a statistical method could be developed to do this in other cases. We sought a plant height estimation method that would be insensitive to terrain height variation, but without having to describe terrain height variation (as is conventionally done when a digital terrain model is developed). We settled on the unsupervised learning technique of finite mixture modeling, and the following methods were chosen for applying the technique.

Mixture Modeling

To investigate the applicability and performance of mixture modeling to infer plant height, we fit mixtures of frequency distributions to height observations (points in the cloud), irrespective of pixel class (ground vs. plant), using the finite mixture model (FMM) procedure of the SAS System v9.4. A FMM is a statistical model that describes variation in a population made up of a finite number of subpopulations, without classifying individuals' subpopulation membership. Equation 1 relates φ, the

characteristic function of height, h, varying within a given spatial extent and composed of a number, k, of component Gaussian distributions each, i, with location and dispersion parameters, mean, μ, and variance, σ.

$$\varphi_{\mu,\sigma}(h) = \sum_{i=1}^{k} \left(\sqrt{2\pi\sigma_i}\right)^{-1} e^{\left(\frac{-(h-\mu_i)}{2\sigma_i}\right)^2}$$

Equation 1

Initially, we compared mixture models with varying numbers of components (k) in order to confirm that k = 2 for images including plant biomass and the ground was an appropriate parameter value. Our expectation was that two subpopulations of points in the cloud would be detectable through this approach: the ground (terrain between plants visible to the UAS), and plant biomass (aboveground plant tissue). In this initial stage, we fit mixture models for k = 1 to k = 5 and confirmed that k = 2 resulted in best fit by minimizing Schwartz's Bayesian Information Criterion (BIC). In a few instances, the minimum BIC corresponded to k = 3, and visual inspection of histograms of height variation confirmed three distinguishable mixture distribution components. Once we had optimized k for an FMM fit to data from an area of interest, we then proceeded to calculate an average height estimate as the difference between locations (for Gaussian mixture components, μ_i, the means) of "ground" and "plants" distributions. Calculating this difference is possible without needing to classify individual pixels as being members of one or another component distribution. For areas in which the optimal value of k was 3, due to some nursery plants being grown in pots, we estimated plant height as the difference between the "pot" and "plants" distributions. Additional comparisons between

quantile limits of distribution pairs were calculated, expecting that for important reasons other than average plant height, the distribution of height in a given point cloud should vary. For example, plant row spacing or physical architecture should affect depth of visibility into the canopy (**Figure 6**) and this can be addressed by referencing different portions of the "plants" distribution.

Where ground-truth data were available (soybean and grain sorghum fields in South Carolina), plant heights were estimated and thereafter tested for validity as predictors of actual measurements, with this validation being conducted through a regression approach using the generalized linear model (GLM) procedure of the SAS System v9.4: actual heights were regressed against predicted heights.

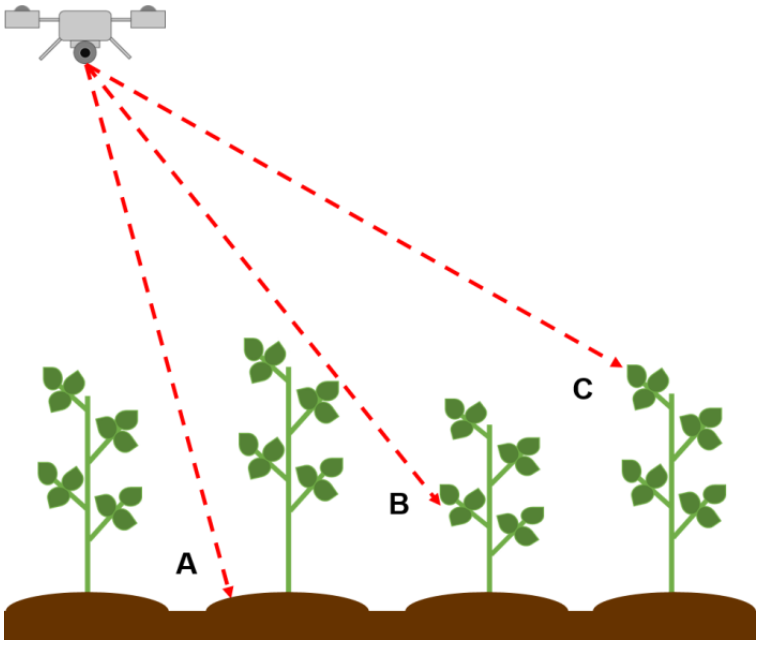

Figure 6. Representation of intermediate plant heights in low-altitude remote sensing (LARS) -derived point clouds. In this image, line-of-sight from the unmanned aerial system (UAS) is depicted for three angles, labeled A, B, and C. The UAS is able to detect the ground (A), the lower leaves of a plant (B), and the top of the plant (C) for the plant spacing shown in the figure. As the space between plants increases (e.g., due to increasing row spacing), the height of points detected at viewing angle (B) will become lower, and the "plants" distribution in a mixture will have a lower mean value, irrespective of actual plant height. This poses a problem for approaches that use one distributional characteristic (e.g., mean or maximum) for multiple plant spacing patterns or architecture. The problem is solved by fitting distributions to latent classes of data and choosing, empirically or analytically, the optimal parameter or quantile for a given application.

Rice Plant Height & Yield – Beaumont, Texas

A generalized linear model describing rice plant height, including treatment number (as a category), latitude, and longitude as independent variables accounted for 85% of height variation for field N- 1, and 87% of height variation for field N-6. **Table 1** includes coefficients estimated for this model, which marginalizes artifactual slope that

arises from image processing and enhances ability to infer differences arising from treatments applied to plots in a randomized complete block design.

This technique results in a level field, confirmed by observing the slope of "ground" area not occupied by rice plots, which is known to be level due to being flooded with water. Height estimates calculated as the difference between FMM mixture components ("ground" and "plants" distributions) are also shown in **Table 1**, confirming that in an idealized situation of level and flat ground (obviating the need to construct a digital surface model or use GPS control points), FMM-derived estimates based on the difference between component means are equivalent to estimates calculated by subtracting a fixed ground position from a plot's average distance from a UAS's sensor. For FMM-based height estimation, a spatial buffer of 0.4 m was added to each plot to ensure adequate representation of the ground in point cloud data.

Table 1. Generalized linear model (GLM)-derived and finite mixture model (FMM)-derived height estimates of rice fields N-1 and N-6. The FMM height estimates were given 0.4 m of ground buffer on each side of the rice plots.

Treatment Number	GLM Estimated Height (m)	FMM Estimated Height (m)
Field N-1		
1	1.05	1.05
2	0.85	0.84
3	0.79	0.79
4	0.77	0.77
5	0.73	0.73
6	0.97	0.97
7	0.86	0.84
8	0.77	0.77
9	0.74	0.73
10	0.69	0.70
Field N-6		
11	0.80	0.80
12	1.21	1.21
13	1.34	1.34
14	1.39	1.39
15	1.36	1.37
16	1.04	1.04
17	1.27	1.32
18	1.31	1.26
19	1.30	1.26
20	1.35	1.35

Multiple Plant Species at Amerson's Nursery – Lamar, South Carolina

Images from Amerson's Nursery were initially processed, as were those from the rice field at Beaumont, Texas, using Pix4D to generate three-dimensional point clouds thereafter analyzed using the FMM procedure of the SAS System. Because the use of FMMs proved well suited to inferring heights of rice plots in the earlier stage of this study, we applied the technique to a variety of plant types to test whether multiple mixture components could be reliably detected across plant types. In this instance FMMs

could be used reliably to detect the presence of three mixture components where appropriate (**Figure 7**), representing ground, pots (being the soil surface contained in a pot), and plants for potted shrubs. Height estimates are generated by calculating the distance between any pair of component means.

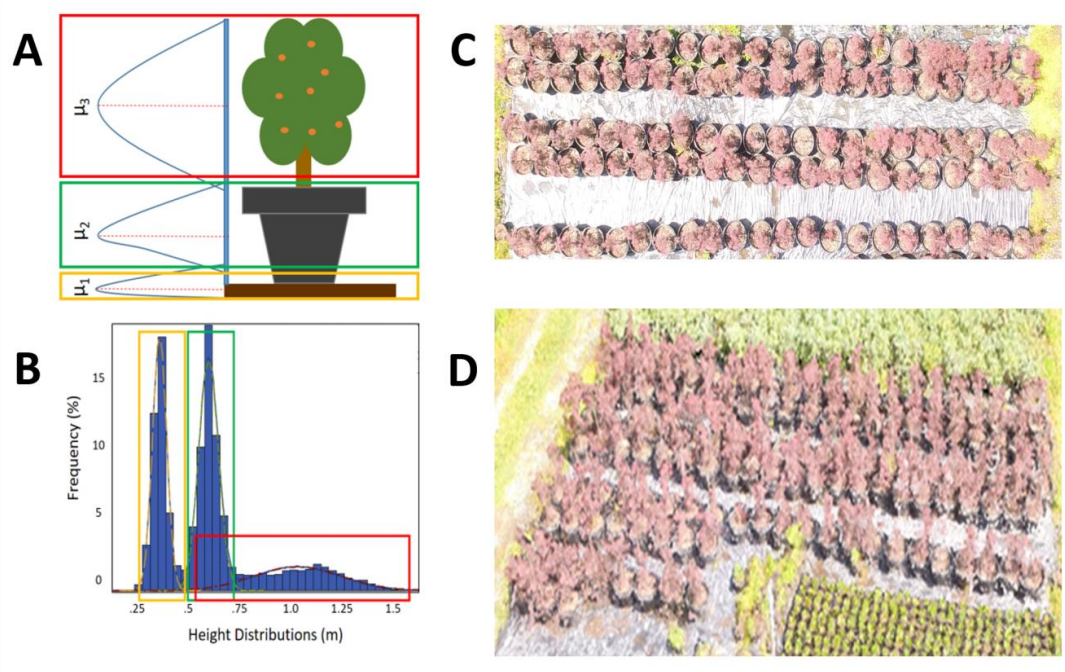

Figure 7. (A) Features in the field are represented accurately by a finite mixture model (FMM). (B) Data from Amerson's Nursery: the first distribution (yellow box) corresponds to the "ground" class of data points in the point cloud, the second distribution (green box) corresponds to the "pots" class of data, and the third distribution (red box) corresponds to the "plants" class of data. Overlap in these distributions results from plant-to-plant, pot-to-pot, and across-ground variation in height. (C) Single aerial image of the area corresponding to data shown in panes (A) and (B). (D) An oblique-angle render of the 3D point cloud from Amerson's Nursery, showing the potted plants' and pots' heights.

Soybean and Grain Sorghum – Blackville, South Carolina

Images from the Edisto REC at Blackville, South Carolina, were processed as before, first using Pix4D and subsequently analyzing point clouds using SAS.

Table 2. Heights estimated from soybean fields using image subsample sizes of four, eight, and sixteen square meters.

	FMM Estimated Heights (m)			
Area	**Field 1**	**Field 2**	**Field 3**	**Field 4**
16 m^2	0.67	0.69	0.67	0.64
8 m^2	0.61	0.67	0.66	0.62
4 m^2	0.54	0.65	0.60	0.68
2 m^2	0.57	0.66	0.61	0.67

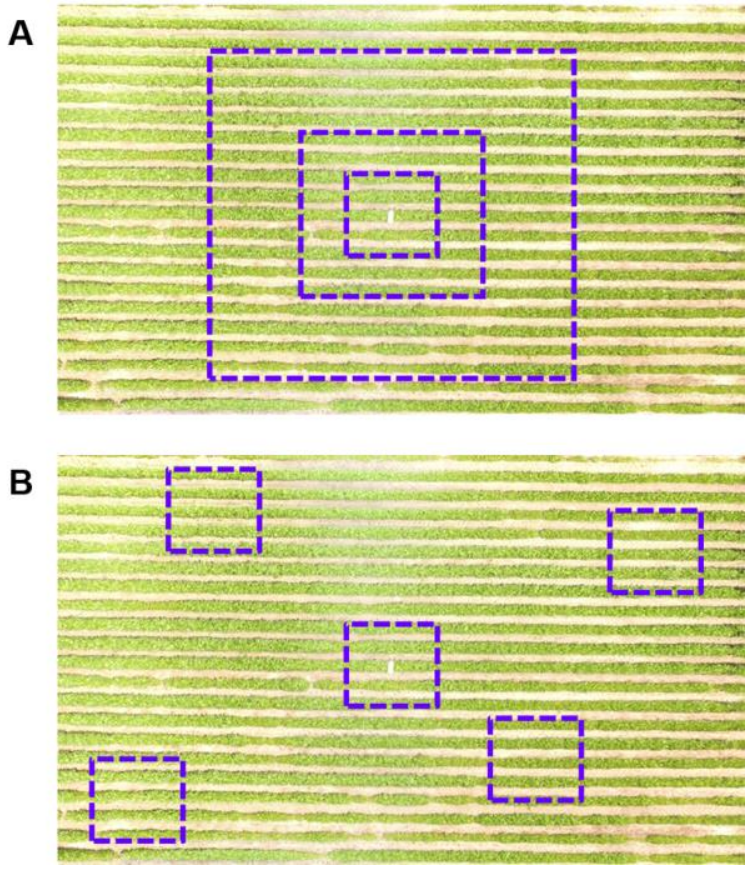

Figure 8. Sampling approaches for generating point cloud data subsets used for estimating soybean height. Two approaches were taken. In the first approach (A), concentric subsets (from 2 to 32 m^2) were delineated around a point at which local ground truth measurements were recorded (indicated by a white board placed at ground level). In the second approach (B), 4 m squares were randomly placed to determine whether estimates derived from random samples throughout the field were representative of ground truth data. Parameter estimates pertaining to one subfield appear in Table 3

Table 3. Representative FMM parameter estimates for a soybean field. μ_1 and μ_2 correspond to the locations of "ground" and "plant" distributions, respectively. σ_1 and σ_2 are respective variances. The difference between μ values is calculated to estimate height, irrespective of the absolute value of μ values. Here, negative height values result due to the global average height being set to zero.

Soybean Field Parameter Estimates				
Area (m^2)	**μ_1**	**μ_2**	**σ_1**	**σ_2**
32 × 32	−0.382	0.255	0.014	0.026
16 × 16	−0.393	0.228	0.005	0.023
8 × 8	−0.391	0.221	0.003	0.019
4 × 4	−0.391	0.221	0.003	0.019
2 × 2	−0.392	0.268	0.019	0.003

Table 4. Estimated soybean heights measured in the field. Median estimated values provided maximum description (R^2 = 0.96) of observed variation.

Estimated Soybean Heights (m)							
Field	**Ave. Obs.**	**Fifth**	**Lower**	**Mean**	**Median**	**Upper**	**Ninety-Fifth**
1	0.49	0.18	0.30	0.59	0.47	0.95	1.05
2	0.53	0.18	0.42	0.62	0.59	1.08	1.20
3	0.47	0.13	0.30	0.71	0.44	1.01	1.10
4	0.44	0.15	0.25	0.83	0.40	0.94	1.02
	R^2	**0.37**	**0.94**	**0.71**	**0.96**	**0.69**	**0.81**

Discussion

This study demonstrates the ability of an unsupervised learning technique to robustly generate useful results from LARS data in agricultural settings, with an emphasis on efficient use of data and rapid output. The approach was to generate three-dimensional point clouds using LARS data collected from different types of agricultural operations and from varying UAS flight patterns, and then to analyze variation without classifying areas or points in the cloud. Implicit in the process of measuring plants for height above ground is differentiation of plants from ground, and many supervised learning analytical approaches address this through classification and subsequent comparison. A conventional approach is to construct the entirety of the "ground" class via linear or other interpolation between GPS control points and treat a spatial subset of point cloud data as the "plants" class. Also common is to construct a surface model from point cloud data, enhancing visualization and summarizing features, but also collapsing variation in a way that prohibits its being analyzed in raw form.

We suggest that a difference between human measurement takers and an aerial sensor can be exploited. Whereas a human on the ground taking a measurement is reliably calibrated (ground position is unlikely to be mistaken), he/she does not record the millions of measurements that are represented in a point cloud assembled from images taken by an aerial sensor. Indeed, the human does not have reason to take millions of measurements because the few taken are likely to be calibrated very accurately. We propose that the aerial imager similarly does not have reason to calibrate relative to ground in the way that the human does because the aerial imager benefits

from the generation of a large number of data points. The calibration of measurements derived from aerial imagery can thus be carried out post-measurement, and through a statistical approach. The volume of data thus generated supports unsupervised learning to infer the distance between two components latent in the resultant distribution of heights (**Table 2**). Results demonstrated that the mean height estimates derived from the FMM are robust to variation in spatial extent being examined (**Table 2**). Furthermore, the FMM-derived height estimates were well correlated (R^2 = 0.71) with in-field human-measured soybean heights (**Table 3**). This process can be generalized to situations in which some background, other than the physical ground, is the reference for comparison. For example, comparisons between colors or temperatures can be made. Such situations include spatial variation in spectral profile arising from disease, stress, or other phenomena of practical interest to agricultural producers. Because the approach does not rely on a priori or computational classification, it negates the consequences of classification error. In an unsupervised learning approach, the difference between plant and ground, or healthy and diseased plants, need only be detectable using analyzed metrics, not defined in terms of what underlies the difference. A producer monitoring a crop for the presence of disease can target areas where two classes of spectral profile are detected for investigation. Because the class-detection result of fitting an FMM does not depend on absolute values, differences between classes can be detected more reliably across varying conditions (lighting, weather, etc.) than may be possible through supervised learning approaches that require reliable classification before analysis. Additionally, FMMs are straightforward to estimate, such that fitting of models for this

purpose can be easily accomplished using many statistical analysis platforms—the technique is not proprietary.

Application of FMMs to the types of problems faced by agricultural producers is fitting because of how the effort-intensive process of classification is (or is not) conducted. Classification of plant vs. ground in this context is not something that directly informs the agricultural producer—the producer can already readily identify ground vs. plant. Instead, classification is required by algorithms that rely on data being classified for supervised learning activities: these algorithms must know the difference between a "ground" point and a "plant" point before inference may be drawn from comparison between classes. Again, this information is not in itself of use to the producer—the producer does not need to know point or pixel class for any purpose outside of the analytical task being undertaken by the relevant algorithm.

The unsupervised machine learning technique used here provides estimates, but with a reduced number of required steps when compared to other approaches that involve the use of GPS control points and their inclusion in analysis. The presence of multiple classes in a dataset is inferred without data needing to be classified. Thus, we expect the approach taken here can be more efficient, simply on the basis of its requiring fewer activities to execute. An approach that involves GPS control points and supervised classification requires, among other things, 1) construction of physical markers to be detected by computer vision algorithms during orthomosaicking; 2) placement of physical markers in target areas, ensuring visibility to aerial cameras by clearing plant biomass or other materials; 3) precisely georeferencing GPS control points by physically

visiting them with GPS equipment; 4) incorporating GPS control points into datasets and constructing terrain maps; 5) subsetting point cloud data to exclude pixels associated with actual terrain, so that statistical characterization of plants can be carried out. There are definitely situations in which these steps are required and advantageous—we highlight the most obvious of these, a situation in which the terrain is not visible to the aerial camera and thus the fitting of FMMs is not possible. However, where these effort-intensive steps are not required, efficiency in phenotyping can be gained by taking an alternative approach that does not require the steps. A consultant or scout operating LARS-based data gathering could collect data in the time it takes to conduct the imaging overflights, process data in the time it takes to assemble a point cloud, and then have an estimate of plant phenotype in the field for discussion with the producer. By fitting FMMs to spatial subsets of data, height estimates can be made precisely despite variable topography of terrain (**Figure 9**). To construct a model of terrain using GPS control points, those points must be numerous enough to support fitting a terrain model that adequately represents variation in a field. If terrain varies appreciably at small spatial scales, then GPS control points must be distributed densely to account for that variation. However, to compare two latent height classes, those classes need only be each adequately represented by data, and not necessarily identified by class. Height estimates for subareas of a field, sampled randomly or with structure, can be averaged to estimate the overall mean height in a field. As in a Riemann sum, the size of these spatial subsets affects the accuracy of the estimate, practically limited in this case by the minimum size at which mixture distribution components can be reliably differentiated and estimated.

We suggest that this approach to LARS data usage combines the well-established practice of random sampling (computing height estimates for multiple data subsets) with the resolution and extent advantages of aerial imagery. Our results demonstrate that small spatial subsets (2 m squares) can be used to generate representative estimates (**Table 3**).

Additionally, **Figure 9** shows how the success of the FMM approach in recovering height estimates means that there is not a need to "level" point clouds or use GPS control points for generating height estimates. Importantly, sources of error or variation that result in a given field not being level can be addressed by the FMM approach regardless of whether those sources are an image-processing artifact, or a real-world sloped or hilly field. Correspondence between GLM- and FMM-derived height estimates (**Table 1**) confirms that the FMM can implicitly account for terrain variation that is explicitly included as covariates in the GLM. Where this covariate information is unavailable, the FMM approach is more useful. Taken together, these considerations underscore the robustness of the unsupervised learning approach to analyzing image data for practical purposes in agriculture.

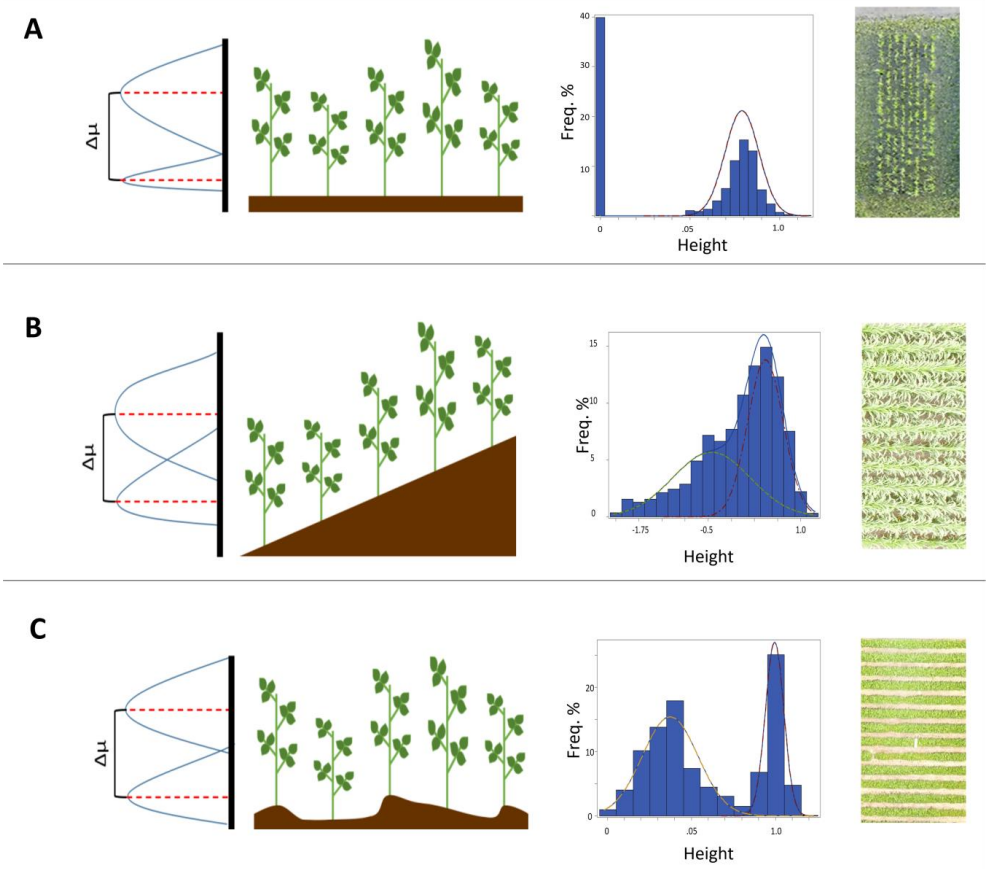

Figure 9. Topography differences do not affect the difference of μ1 and μ2 when estimating height with FMM. Height variance changes dependent on both elevation and plant height variation, but this is independent of the difference between μ1 and μ2. Three scenarios are shown as schematics on the left and are accompanied by real FMM output histograms representing each scenario. Imagery from which FMM output was generated is shown at the right. Scenario (A): flat terrain represented by a rice plot; scenario (B): sloped terrain present in a grain sorghum field; scenario (C): the uneven terrain of a soybean field.

Some situations require GPS control points and comparison between a constructed ground and a point cloud of observations. If the ground is not adequately visible to an aerial sensor, the "ground" component of a mixture distribution cannot be estimated. In such situations, calibration for height estimates cannot be accomplished through the technique used here, and a reference surface must be constructed. Thus, the

application of this technique is limited to situations in which the ground is visible between crop plants—for example, row crops and early developmental stages of field crops. Situations calling for GPS control points and those well suited to application of FMMs are thus to a degree mutually exclusive. Where plants are dense such that canopy can be reasonably represented by a surface, an FMM attempting to differentiate (obscured) ground from plants will fail to return good estimates, and classification is not likely necessary, because all data in a related point cloud would describe plants. For instance, FMMs fit to data from grain sorghum resulted in only one mixture component, corresponding to the dense canopy of the crop when imaged (**Supplemental Figure 4**). In this situation, comparison between the plant canopy surface and a ground surface constructed using GPS control points would be required to estimate height. On the other hand, where plants are spaced such that the ground is visible between them and the canopy is discontinuous instead of being like a surface, an FMM is able to address the issue of classification efficiently without having to classify data points (**Figure 9**). Were explicit classification attempted for comparison of the "plants" points to a constructed ground surface through a supervised learning approach, classification error would result in commensurate phenotype estimate error. In such an approach, excluding generous buffers from analysis to avoid attempting to classify ambiguous data points is not only an additional analysis step with attendant potential for error, but also discards data points that may be informative. Unsupervised learning is more robust in situations to which it is appropriate.

Here, the FMM accounts for overlap between points belonging to each class, without that overlap detrimentally affecting estimates of each class' mean or other distributional parameters. A threshold-based classification method will misclassify at a rate proportional to the overlap between classes, resulting in biased estimates of class means. This bias will increase as a function of the two components' difference in proportional contribution to the mixture, and as a function of the difference between the two components' dispersions. In other words, misclassification is of no consequence to supervised learning-based height estimation if the ground and height classes are equally represented and equally variable in a given dataset. However, as representation and variability differ, misclassification becomes increasingly negative in its impact to such an approach. Again, unsupervised learning accounts for this varying issue more robustly.

Conclusions and Future Work

The analytical method described herein was first explored to estimate rice plot height in the absence of GPS control points. An application of the unsupervised machine learning approach, finite mixture modeling, was developed to reliably estimate plant heights in various terrain configurations. Using imagery data from a nursery, we determined that FMMs could be used to detect latent subpopulations present in the data—specifically, subpopulations that represented the physical ground and plant biomass, allowing expedient estimation of average plant height by calculating the difference between subpopulation mean heights. To validate the application, plant heights were physically measured in the field and compared to the FMM-derived

estimates. Correlation between height estimates derived from the FMM approach and measurements taken on the ground was strong ($R^2 = 0.96$).

Further research should explore additional applications of unsupervised learning to technologically enhanced precision agricultural operations. We suggest that many contemporary applications are utilizing the remarkable resolution and scale of data available through remote sensing, while also involving a constraint that can be overcome: the need for explicit classification or calibration. The need for precise calibration is served by a human taking measurements in a field, and results in measurements that are precise and accurate, so that small sample sizes can be used to reach conclusions. Because LARS data are of such high resolution for an imaged extent, precise calibration (in this case, on the basis of the position of the ground) can be foregone because data are available to support inference on the position of the ground, as we have discussed. We believe that exploiting this type of approach will allow remote sensing and precision agriculture researchers to increase the efficiency of LARS data usage and enable increased focus on new challenges. Additionally, the ability to estimate relevant plant or disease phenotypes in the field without needing to construct a digital terrain model or use GPS control points means that crop managers can harness the benefits of LARS without having to also invest appreciable resources in computation or GPS systems. These investments can in turn be focused where they are required, as in cropping systems that do require GPS-based construction of a reference surface for height or other estimations.

CHAPTER III

DNA-BASED QUANTIFICATION OF *FUSARIUM OXYSPORUM* F. SP. *VASINFECTUM* IN ENVIRONMENTAL SOILS TO DESCRIBE SPATIAL VARIATION IN INOCULUM DENSITY*

Fusarium wilt of cotton, caused by the soilborne fungal pathogen *Fusarium oxysporum* f. sp. *vasinfectum* (FOV), occurs in regions of the United States where cotton (*Gossypium* spp.) is grown. Race 4 of this pathogen (FOV4) is especially aggressive and does not require the co-occurrence of the root knot nematode (*Meloidogyne incognita*) to infect cotton. Its sudden appearance in far-west Texas in 2016 after many years of being restricted to California is of great concern, as is the threat of its continued spread through the cotton-producing regions of the United States. The aim of this research was to analyze the spatial variability of FOV4 inoculum density in the location where FOV4 is locally emerging, using quantitative and droplet digital polymerase chain reaction (qPCR and ddPCR) methods. Soil samples collected from a field with known FOV4 incidence in Fabens, Texas were analyzed. Appreciable variation in inoculum density was found to occur at spatial scales smaller than the size of plots involved in cultivar trial research, and was spatially autocorrelated (Moran's I, $Z = 17.73$, $p < 0.0001$). These findings indicate that for cultivar trials, accounting for the spatial distribution of inoculum either by directly quantifying it or through the use of densely-distributed "calibration checks" is important to the interpretation of results.

*__Reproduced from:__ Davis II, R. L., Isakeit, T., Chappell, T. M. (2022) DNA-based quantification of *Fusarium oxysporum* f. sp. *vasinfectum* in environmental soils to describe spatial variation in inoculum density. *Plant Dis*. Doi: 10.1094/PDIS-08-21-1664-RE.

Introduction

Fusarium oxysporum Schlechtend f. sp. *vasinfectum* (Atk.) W. C. Snyd. & H. N. Hans (FOV) is a soilborne fungal pathogen and the causal agent of Fusarium wilt of cotton (Kim et al. 2005; Davis et al. 2006). Several races of FOV infect cotton (*Gossypium* spp. L), typically in obligate association with the root knot nematode (*Meloidogyne incognita* (Kofoid & White) Chitwood) to establish infection (Armstrong & Armstrong, 1960; Cianchetta et al. 2015). Disease caused by FOV races that require root knot nematode for infection can be managed indirectly through the use of nematicides. But FOV race 4 (FOV4) is able to establish infection in the absence of root knot nematodes, and thus poses an additional challenge to cotton production worldwide (Davis et al. 2006; Cianchetta et al. 2015).

Upon FOV4 colonization of vascular plant tissues, microconidia are produced in the xylem and continue to grow, obstructing movement of water and nutrients (Cox et al. 2019). This leads to the characteristic symptoms of Fusarium wilt of cotton (Davis et al. 2006; Cox et al. 2019) which vary between cotton cultivars (Zhang et al. 2020). Early in the growing season is when symptoms result in the most damage to plants (Halpern et al. 2018). Symptoms include damping off and resultant stand loss (Davis et al. 2006). Further symptoms can occur as the growing season progresses, including chlorosis, wilt, stunting, and leaf necrosis (Davis et al. 2006; Sanogo & Zhang 2016). Vascular staining is a characteristic symptom that can be used to identify FOV4 infection in fields (Davis et al. 2006). In the absence of cotton, thick-walled, overwintering chlamydospores allow

FOV4 to persist for years in field soils (Chawla et al. 2012; Hutmacher et al. 2013; Gordon 2017). Additionally, the fungus can perpetuate on the roots of non-hosts. In the early 2000s, FOV4 was first detected in the San Joaquin Valley of California, in Pima cotton fields that had no previous known incidence of the root knot nematode (Kim et al. 2005). Prior to this detection, the known races of FOV in the United States were limited to those that require root knot nematode injury for infection to occur (Kim et al. 2005; Davis et al. 2006). Following the confirmation of FOV4 in California, efforts were made to prevent spread and to study mechanisms of FOV4 transport (Bennett et al. 2008). The ability of FOV4 to be transmitted on cotton seeds was confirmed (Bennett et al. 2008), and transport via soil has also been indicated as a potential mechanism of spread (Cianchetta et al. 2015). FOV4 was later reported in Texas (Halpern et al. 2018) and in New Mexico (Zhu et al. 2020). FOV4 is currently limited to El Paso and Hudspeth Counties in Texas (Halpern et al. 2018), but threatens Texas' cotton production acreage, which accounts for approximately half of the acreage used to produce cotton in the United States (NASS 2020).

Most races of FOV can be managed through engagement of nematodes. By reducing soilborne nematode populations through planting of nematode-resistant cultivars or use of chemical fumigation, disease associated with nematode-dependent FOV is commensurately reduced (Starr et al. 1989; DeVay et al. 1996). Absent this avenue for reducing FOV-caused disease, resistance to FOV itself becomes key to managing Fusarium wilt (Sanogo & Zhang 2016). Research on FOV4 host plant resistance has resulted in identification of quantitative trait loci and promising

germplasm (Ulloa et al. 2006; Ulloa et al. 2013; Ulloa et al. 2020), and resistance to FOV4 is expected to be polygenic (Wang et al. 2018). Management methods including heat disinfestation (Bennett & Colyer 2010), soil treatments (Bennett et al. 2011), and solarization (Bennett et al. 2012), have been tested; however, control of FOV4 continues to rely principally on limiting the spread of infected seeds, soil, and other plant debris (Davis et al. 2006).

Under controlled greenhouse conditions, Fusarium wilt of cotton has been demonstrated to be an inoculum density-dependent disease (Hao et al. 2009). Thus, in the field, spatial variability in Fusarium wilt incidence could be in large part due to variable inoculum density. Developing strategies to combat the spread of FOV4 will necessitate understanding the distribution and spread of inoculum within and between fields. To study the variability of FOV4 inoculum density at sub-field spatial scales, we used quantitative real-time polymerase chain reaction (qPCR) methods to analyze soils collected directly from affected fields. We implemented DNA-based quantification to estimate inoculum density of FOV4 that had been recently isolated from affected fields. We expect that the diversity of strains present at the onset of an epidemic changes as inter-strain competition (Bell et al. 2019) and other factors affect fungal populations, and set out to describe spatial variability in inoculum at a relatively early phase in local FOV4 establishment.

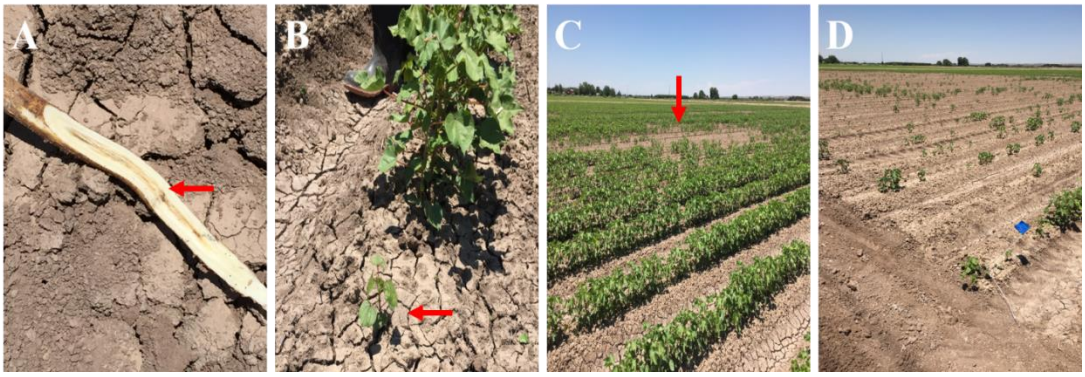

Figure 10. A) The characteristic vascular staining caused by FOV4 infection. B) A stunted cotton plants. C) Inoculum is inconsistent in fields and may cause uneven stands or dead patches. D) Heavily infested cotton fields may have large portions of the field where cotton seedlings do not survive, leading to stand loss across a larger extent of the field.

Materials and Methods

Fungal collections and cultures

DNA to be quantified came from two sources: reference isolates from fungal cultures, and collections of environmental soils. Multiple reference isolates of FOV races 1 (FOV1) and 4 were plated on potato dextrose agar and V8 media. Initial fungal isolates were collected from the roots of infected cotton plants and propagated prior to single spore isolation. FOV isolates from cotton roots were used to begin cultures: FOV1 from plants collected in Rowland and Dawson Counties, Texas, and FOV4 from El Paso County. The race of initial FOV4 cultures was confirmed using the Agdia AmplifyRP Acceler8 kit for FOV4 (Doan et al. 2014), for which specificity to FOV race 4 is indicated with an exception for an Egyptian race 3 isolate, FOV1857 (Crutcher et al. 2016). Isolates of *Fusarium verticilliodes* (FV) and *Fusarium oxysporum* f. sp. *lycopersici* (FOL) were also used to examine PCR primer specificity. A SpectraMax

QuickDrop Micro-Volume Spectrophotometer was used to determine the concentration of fungal DNA in samples.

Soil sample collections

Soil samples were collected in December 2019 and July 2020 from a naturally-infested, commercial cotton field used for trials by Texas A&M AgriLife Research & Extension, located in Fabens, Texas (**Figure 10**). The first group of samples was collected in December 2019 at a time when cotton plants were still present in the field. Presence of FOV4 was confirmed in these fields by symptoms, fungal isolations from roots, and by employing the Agdia AmplifyRP Acceler8 kit for FOV4 (Doan et al. 2014). Soils were collected following a stratified sampling plan, covering the range of damping-off and root rot ratings assigned to cotton plants grown in the field. Single-row cotton plots were 4.9 m in length with 1.0 m of spacing between rows. Thirteen plots were selected for soil collection to represent the range of damping-off ratings made earlier in the season. Three evenly-spaced soil samples were collected from each plot. Approximately 15 g of soil were collected from each plot at a depth of roughly 15 cm in a 50 mL centrifuge tube. The sampling depth of 15 cm was chosen to remain within the root zone of soil, where the likelihood of fungal activity was highest due to root density. Soil was stored in these tubes at room temperature until the time of DNA extraction.

The second group of soil samples was collected in July 2020 from the same commercial cotton field used for trials by Texas A&M AgriLife Research & Extension, in Fabens, Texas. Using the same sampling protocol, collection was expanded to 131 plots to provide greater spatial resolution. The field used for sampling in 2020 was used

for variety trials. A total of 72 Upland cultivars, replicated four times each, in a randomized complete block experimental design, were planted in a spatial arrangement of sixteen rows and eighteen columns (Isakeit & Arce 2021). To generate a data subset of complete spatial coverage at the plot level, soil samples were taken from every plot in five rows of the field (rows 9 through 13). Additional plots were randomly sampled throughout the rest of the field.

DNA extractions

To generate samples to be used as standards, FOV1, FOV4, FV, or FOL mycelia were scraped from plated cultures using blunted, sterile toothpicks. Fungal DNA was extracted from mycelia using a phenol-chloroform based method. Extraction buffer (1 M pH=8 Tris-HCl, 0.5 M EDTA, 20% sodium dodecyl sulfate, 5 M NaCl, and sterile deionized water) and phenol-chloroform were added to a 2 mL screw cap tube containing glass beads and mycelia. The mixture was homogenized for 30 sec by shaking, and then centrifuged at 14,000 RPM for 12 minutes. DNA was precipitated using 100% ethanol at -20 °C for one hour. Following a ten-minute centrifugation, the supernatant was decanted, and the pellet was washed with 70% ethanol and centrifuged again for two minutes. The pellet was dried and suspended in TE buffer (1 M pH=8 Tris-HCl, 0.5 M EDTA, and sterile deionized H_2O). DNA was extracted from field soil samples using the DNeasy PowerSoil Pro kit (Qiagen GmbH, Hilden, Germany), following the manufacturer's protocol: 250 mg field soil samples were processed, yielding 100 µL products ($1x10^{-7}$ to 0.01 ug/mL). Extracted DNA products were stored at 4ºC.

Quantification using qPCR

Primers were designed based on the *Tfo1* transposase gene of the "Fusarium oxysporum f. sp. vasinfectum strain CA-9 transposon *Tfo1* transposase gene, complete cds; and disrupted phosphate permease 84 (*PHO84*) gene" partial sequence (GenBank KT323911) accessioned by Ortiz et al. (2017). The primers for this study were designed using the IDT PrimerQuest Tool (Integrated DNA Technologies Inc.). To first determine which primer pair was best for quantifying FOV4, different annealing temperatures were tested for reactions involving each of several primer pairs using the Bio-Rad CFX Connect QX200 Real-Time PCR System temperature gradient feature. The primer pair selected for further use was the FOV4 A3-2018 forward (5'-CTAGAGTCCTGGTTGATG-3') and reverse (5'-ATATTCCCTGCCGATATG-3') primers, at an optimal annealing temperature of 59°C using genomic DNA extracted from cultured FOV4. The template sequence amplified by this primer pair was within the Tfo1 region as described by Ortiz et al. (2017). The FOV4 A3-2018 primer pair was tested for degree of specificity to FOV4 over other isolates, through PCR amplification. Amplicons resulting from PCR amplification of environmental soils were sequenced (Sanger method, Eton Bioscience, Inc., San Diego, CA) and the sequence results analyzed for similarity with published sequences using the NCBI Basic Local Alignment Search Tool (BLAST) (Altschul et al. 1990).

Soilborne DNA was quantified using a Bio-Rad CFX Connect QX200 Real-Time PCR System. The qPCR master mix used 5 µL SYBR-based Bio-Rad SsoAdvanced

Universal Inhibitor Tolerant SYBR Green Supermix, 1 µL each of forward and reverse primers (0.001 ug of each), and 2 µL of DNase-free water. Supermix was vortexed briefly and placed on ice. The 96-well plates used for reactions were also kept on ice prior to thermal cycling. Reactions included 9 µL of Supermix and 1 µL of template DNA ($1x10^{-7}$ to 0.01 ug/mL) solution and were activated at 95ºC for 3 minutes. Cyclic PCR thermal conditions were 10 s at 95ºC for denaturation, and 10 s at 59ºC for elongation. Reactions were stopped after 35 cycles. A melt curve was created starting at 65ºC, increasing by 0.5ºC at a 5 s interval, and terminating at 95ºC. Following the cycle, temperature was held at 5ºC. Fluorescence was recorded using Bio-Rad CFX Connect Maestro Software for Windows.

Standard curve fitting

To fit standard curves, ten-fold dilution series were generated using genomic DNA extracted from pure cultures, and resulting standards were included in qPCR runs. Genomic DNA was quantified (ng/µL) from 1 µL aliquots of the sample using a SpectraMax QuickDrop Micro-Volume Spectrophotometer (Molecular Devices, San Jose, CA). Reaction efficiency was calculated in the Bio-Rad CFX Connect Maestro Software for Windows program.

Validation through spike recovery

Double-autoclaved field soil samples were used as DNA-background-free matrix for amending with FOV4 fungal material. Cultured FOV4 of 0.010, 0.0250, 0.050, 0.075, and 0.100 g were added to 0.5 g quantities sterile soil. Further validation was performed by spiking dilutions of a conidia suspension into 0.25 g samples of sterile

soil, with the initial suspension concentration (6.75 x 10^5 conidia/μL) determined using a hemocytometer.

Quantification using droplet digital PCR

Droplet digital PCR (ddPCR) was used for corroborating analog qPCR quantifications of soilborne FOV4 inoculum using the Bio-Rad AutoDG QX200 Droplet Digital PCR System following the manufacturer guidelines. The ddPCR is used to quantify genetic material in a sample by classifying whether amplification occurs in each of a large number of reaction partitions, being water-oil emulsion droplets in the case of ddPCR (Hindson et al. 2011). The number of reaction partitions that include at least one template copy (indicated by distinctly higher fluorescence intensity than template-free partitions) is analyzed to estimate the quantity of template molecules in a sample, assuming that the number of copies per droplet is Poisson-distributed (Hindson et al. 2011; Rački et al. 2014). Because of the manner through which target genetic material is amplified during ddPCR, the output from this procedure facilitates estimating DNA concentration in a sample without relying on the fitting of standard curves (Wen et al. 2020). An EvaGreen-based master mix was used for the analysis at a total volume of 22 μL per well, consisting of: 11 μL of QX200 ddPCR EvaGreen Supermix, 1.1 μL of forward and reverse primers (0.001 ug of each), 7.7 μL of DNase-free water, and 1.1 μL of template DNA (1x10^{-7} to 0.01 ug/mL). Following the generation of droplets, the 96-well plate was sealed and transferred to the Bio-Rad C1000 Touch Thermal Cycler for DNA amplification, which begins at 95ºC for 5 min and cycled for 40 times at 95ºC for 30 s for denaturation and for elongation at 60ºC for 1 min. Upon completion of the PCR,

the plate was transferred to the Bio-Rad QX200 Droplet Reader where fluorimetry was used to classify droplets as reaction-positive or -negative. Data output from the QX200 Droplet Reader was collected using Bio-Rad QuantaSoft Software.

Data analysis

The Cq values generated through qPCR were visualized as representations of inoculum density across space, using the G3GRID and G3D procedures of the SAS System version 9.4 (SAS Institute, Cary, NC). The Cq values were also analyzed as a function of template concentration estimates generated through ddPCR, using the GLM procedure of the SAS System version 9.4. The VARIOGRAM procedure of the SAS System was used to estimate Moran's I and to generate semivariograms for the study of spatial structure in inoculum density variation.

Results

Six primer pairs designed for this study were derived from regions including Tfo1 transposase and PHO84 phosphate permease gene sequences (GenBank KT323911) accession by Ortiz et al. (2017) during characterization of an insertion event that distinguished California FOV4 isolates from those of other geographic locations. Primers described by Ortiz et al. (2017) did not amplify FOV4 isolates collected from Texas, potentially due to recent genetic diversification of FOV4 (Bell et al. 2019). We developed additional primer sets based on the sequence results of Ortiz et al. (2017) in search of one that amplifies Texas FOV4 isolates in aggregate efficiently without also appreciably amplifying Texas FOV1, the other FOV race expected to currently occur in Texas cotton fields. A standard curve was fit to translate Cq values to template

concentration estimates (**Figure 11**). If primer pairs resulted in amplification that did not meet general criteria, they were eliminated from this study. Criteria were that amplification of FOV4 templates must be estimated to be 90-105% efficient ($E = 10^{(-1/slope)} - 1$), and that standard curves fit to FOV4 standards must be log-linear with R2 > 0.98. The "2018" primer pair met these criteria and performed best in terms of standard curve determination, and we proceeded with this pair into further analysis. Dilution series of plate-cultured isolates of FV and FOL were not significantly correlated with amplification from the FOV4 A3-2018 primer pair (for FV: $r = -0.149$, $p = 0.8113$; for FOL: $r = -0.375$, $p = 0.4642$).

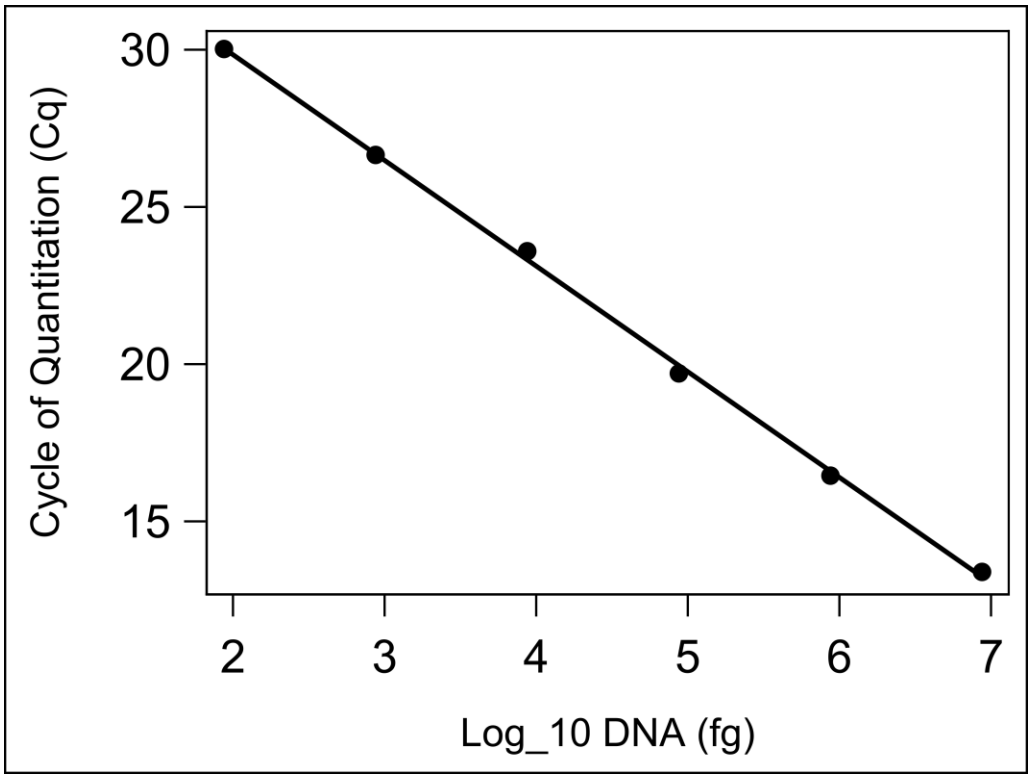

Figure 11. A standard curve was constructed from a ten-fold serial dilution of a genomic DNA extracted from *Fusarium oxysporum* f. sp. *vasinfectum* race 4 (FOV4) harvested from plates. The standard curve was used for absolute quantification in quantitative real-time polymerase chain reaction (qPCR) analyses.

Spike recovery was conducted to study the effectiveness of the quantification method in the presence of soilborne polymerase inhibitors, and co-occurring FOV1. We combined known quantities of FOV4 mycelial tissue or conidia with sterilized environmental soils from the field in Fabens, Texas to simulate unknowns, and examined the method's ability to recover accurate FOV4 quantities. Spike recovery results were used to set the limit of detection, being the smallest amount of template that can be distinguished from a no-template control. In our aggregate data, no-template controls did not result in C_q values lower than 32, so this was set conservatively as the limit of detection. The results of the race 4 quantifications correlated strongly (r = -0.971, p = 0.0059) with the masses of the mycelia mixed with the sterilized soil (**Figure 12**). Estimates of FOV1 template concentration were all below the limit of detection established for FOV4 (C_q values were above 32). Additionally, estimates of FOV1 template concentration were not significantly correlated with FOV1 mycelial mass (r = -0.572, p = 0.2356). Estimates of FOV4 tissue quantity were strongly correlated with conidia concentration generated through a dilution series, from 6.75×10^5 to 6.75×10^1 conidia/μL (r = -0.991, p = 0.001) (**Figure 12**).

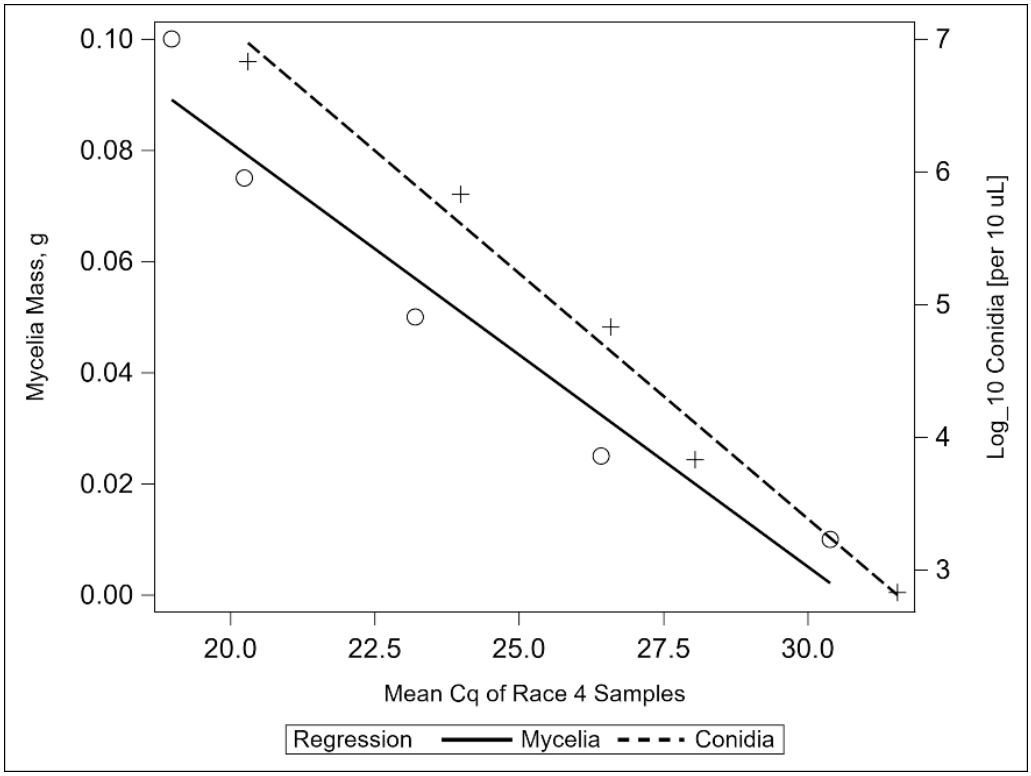

Figure 12. Sterilized soil samples were spiked with mycelia of FOV4 by fresh weight (in grams) or with a dilution series concentrations of conidia to determine how well these quantities could be recovered using qPCR. The resulting cycle of quantification (C_q) values were correlated with the masses of mycelia spiked into the soil samples (r = -0.971, p = 0.0059). Log_{10} conidia concentrations were also correlated with C_q values (r = 0.991, p = 0.0010).

After validating quantifiability of FOV4 in environmental soils, samples from FOV-infested cotton fields were analyzed. Variability in soilborne inoculum density was high (**Figure 13**), ranging from C_q values of 21.46 to below the limit of detection from samples collected in July 2020. The highest quantities of soilborne inoculum density fell between the amounts of DNA present in samples spiked with 0.05 to 0.075 g of mycelia; the lowest were below the quantification for 0.01 g of mycelia. The spike recovery experiment that was used to validate the method represented a realistic range of

inoculum density found in the soil during the peak of the growing season. Soil samples processed from this field had a mean C_q of 28.40 and a variance of 5.83. Field inoculum density was spatially heterogeneous at the spatial scale of experimental plots. Mean and variance of C_q values were not correlated ($r = 0.00337$, $p = 0.969$). A large, positive Moran's I ($Z = 17.73$, $p < 0.0001$) indicates that inoculum density is spatially autocorrelated and more clustered than would be expected if inoculum were randomly distributed within the field. Nonrandom clustered spatial distribution of inoculum is consistent with the expectation that FOV4 growth and spread occurs in the field, potentially followed multiple introductions of FOV4 from infected seeds. A semivariogram of C_q values was used to estimate the spatial scale at which soilborne FOV4 inoculum density is spatially autocorrelated. The range of spatial autocorrelation using a spherical model was 10.55 m (**Figure 14**), which is approximately the size of two experimental plots in common variety trials conducted in the field.

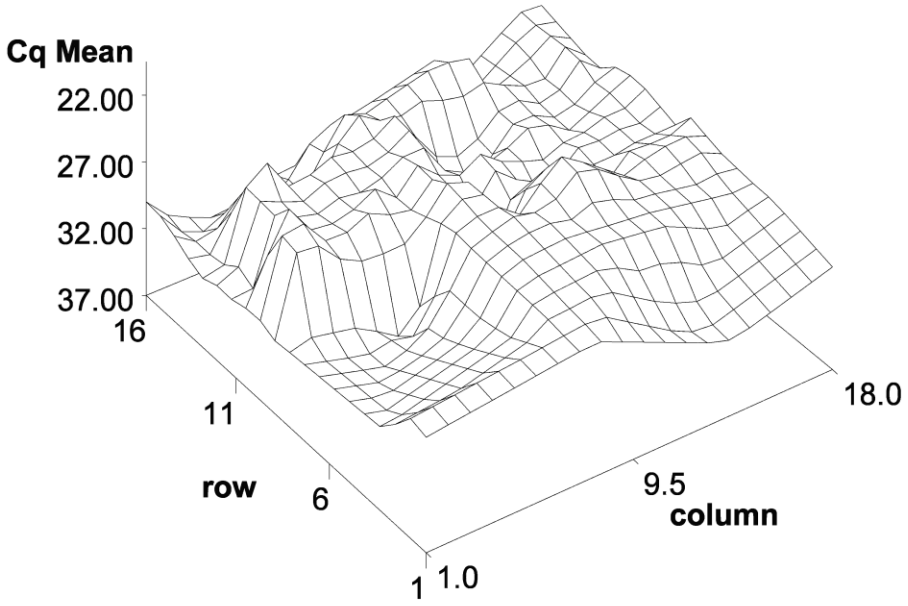

Figure 13. A surface plot depicting the variability of the soilborne inoculum density in July 2020 during a variety trial to assess the susceptibility of cotton cultivars. The large, positive Moran's I ($Z = 17.73$, $p < 0.0001$) indicates that soilborne FOV4 inoculum is more clustered than what would be expected if inoculum arrived randomly in the field.

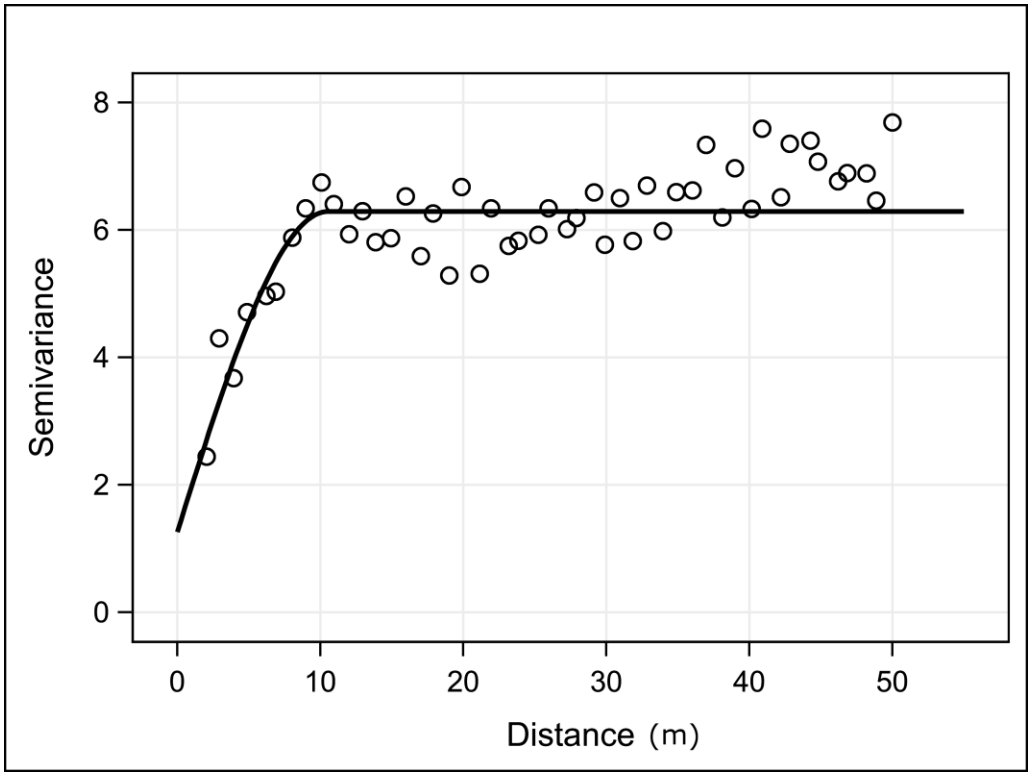

Figure 14. A semivariogram was used to determine the scale at which soilborne FOV4 inoculum density was spatially autocorrelated. An exponential model was used to estimate the range (10.55 m) at which mean C_q data were autocorrelated.

The ten-fold dilution series used to construct the standard curve was used to compare the output from both the qPCR and ddPCR analyses. The results from qPCR proved a good predictor of ddPCR results, the latter of which are expected to be more accurate and precise especially at lower template concentrations (r = -0.998, p = 0.0023) (**Figure 15**). Inhibition of PCR by contents of environmental soils is of major concern when analyzing samples with qPCR, ddPCR lessens the consequence of PCR inhibition (Rački et al. 2014, Wen et al. 2020). Field soil samples were quantified in parallel using ddPCR and qPCR to test for a decrease in qPCR quantitative accuracy in the presence of expected inhibitors. The qPCR results remained highly predictive of ddPCR results in

these comparisons, but variability in qPCR-based quantification led to a decrease in the strength of the correlation between techniques (r = -0.942, p < 0.0001) (**Figure 16**).

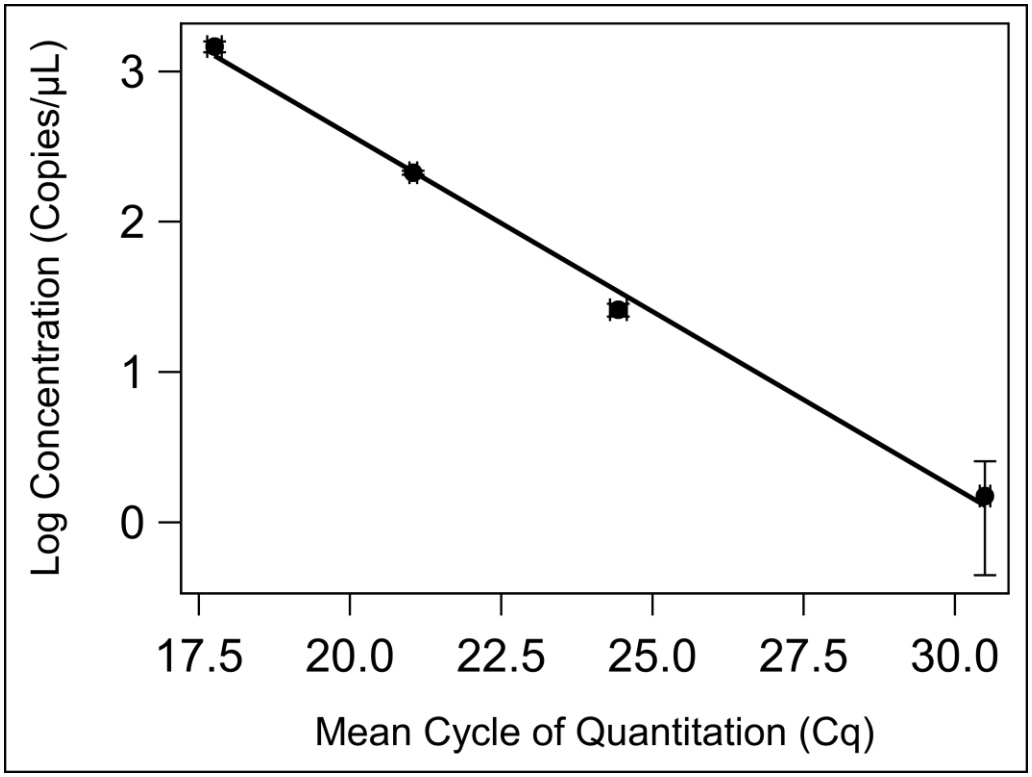

Figure 15. A dilution series was compared between the qPCR and droplet digital PCR (ddPCR). The log normal concentrations of fluorescent genomic DNA, measured in copies per microliter (copies/µL), were correlated with the C_q values of the standard curve (r = -0.994, p = 0.005).

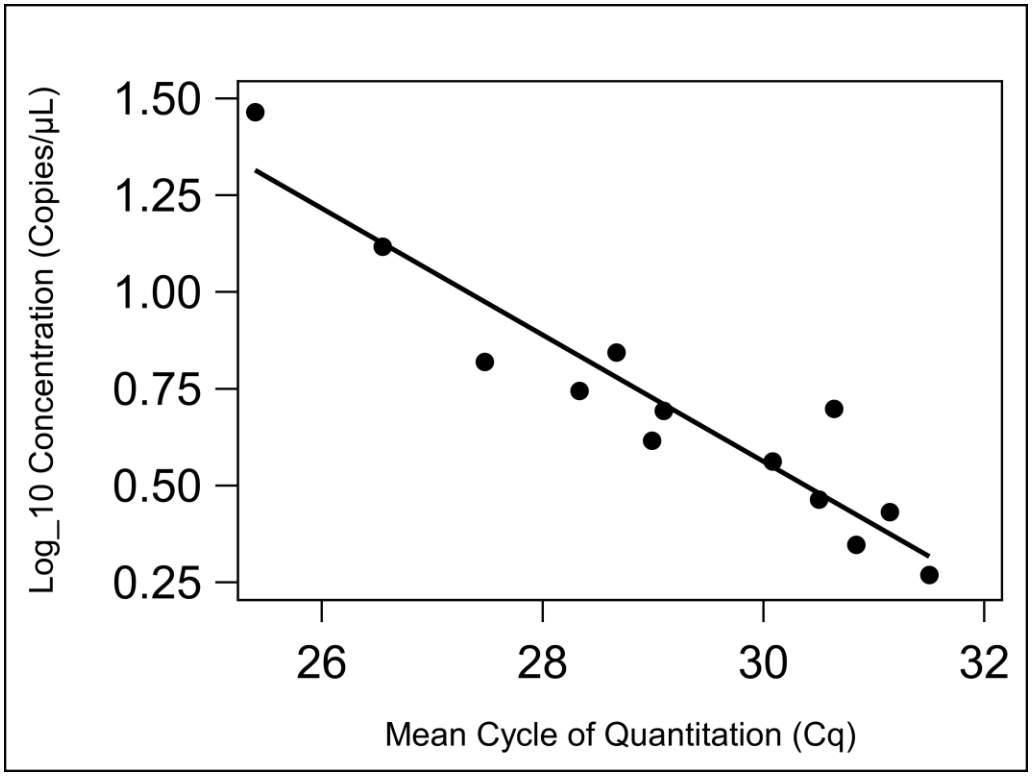

Figure 16. Genomic DNA from soil extractions was compared between qPCR and ddPCR analyses to determine the correlation between these two methods. The log normal transformed average concentrations of genomic DNA quantifed using ddPCR (copies/µL) were correlated with the C_q values from th qPCR output (r = -0.942, p < 0.0001).

Discussion

In agricultural settings, soilborne fungal pathogens present a major threat to crop or fiber yield and the economic viability of cultivating specific crops in heavily-infested areas. This is especially evident with monoculture planting operations where soilborne pathogens are present, and especially consequential where operations involve seed production if seeds can be infected. Many *formae speciales* of the pathogenic soil-inhabiting fungus *Fusarium oxysporum* are responsible for wilting diseases in many large-scale crops, with FOV4 being a current and evolving threat to Pima and Upland

cotton production. FOV4 infects cotton independently of root knot nematodes and survives well in soils as a saprophyte even in the absence of cotton. Because new disease foci can be created by the movement of infested soil or by infected seeds and thereafter become a recalcitrant disease threat to any cotton grown at the affected location, there is value in knowing or estimating the distribution of inoculum in the field prior to investing in cotton production. Inoculum foci are otherwise unknown prior to planting and symptom expression, and the DNA-based method to quantify FOV4 inoculum in field soils described here allowed us to see how variable inoculum density is in a field independently from symptom expression or stand loss.

Seedborne transmission is hypothesized to be a potential long-distance dispersal mechanism for FOV4 (Bennett et al. 2008) and due to the ability of chlamydospores to survive for long periods in infested soils, any movement of soil contaminated equipment, vehicles or other equipment from FOV4-contaminated fields could also introduce the pathogen to cotton production fields in other regions. Through some mechanism, strains with the *Tfo1* insertion in the *PHO84* gene (Ortiz et al. 2017), a sequence unique to California race 4 isolates, may have been introduced to cotton production in West Texas. Primer pairs developed for this study used this sequence because of the likelihood that the Texas isolates would be similar to the California isolate sequences accessioned by Ortiz et al. (2017). Additionally, these sequences were used because the insertion of the *Tfo1* transposon was unique to isolates of FOV4 (Ortiz et al. 2017), and this allowed for primer specificity for FOV4 vs. FOV1. Specificity to FOV4 vs. FOV1 was expected to be most important for this study because FOV1 is present in Texas. The method used in

this study amplified TX FOV4 isolates (classified to the level of race, with the caveat that the Acceler8 kit used to do so may not differentiate between races 3 and 4) specifically enough to afford accurate target quantification in the presence of substantial FOV1 material. Crutcher et al. (2016) demonstrated that the Acceler8 kit returns positive results for Egyptian isolates of FOV3; however, California race 3 and other race 3-like samples did not result in positive results from the kit. A survey conducted in 2013 did not detect FOV3 in Texas (Cianchetta et al. 2015), and description of symptoms associated with the El Paso, Texas FOV isolates used in this study were characteristic of FOV4 infection (Isakeit & Arce, 2020). Multiple sub-racial variants have been identified since our sampling (Diaz et al. 2021) and it is possible that these different sub-racial variants exhibit different in-field host specificity or other characteristics. If this is the case, then spatial variation of inoculum density at the sub-racial level may affect the results reported here, underscoring the need to assume that inoculum density varies in space – perhaps not only in aggregate amount at some taxonomic level, but also in composition. Further research is necessary to describe the variation in symptom expression, if any, that result from genotypic differences between sub-racial variants.

Spatially, soilborne FOV4 inoculum density is heterogeneous due to the existence of multiple disease foci, themselves likely a result of multiple and variable introduction events caused by planting infected seeds and/or the movement of infested soils by field machinery. Temporally, inoculum density varies due to environmental and biotic inputs affecting fungal pathogenic and saprophytic growth, and additional research is necessary to understand these inputs and their consequences. Methods used to confirm

field infestations often and appropriately rely on the observation of symptomatic plants and further confirmation by selective plating and sequencing (Halpern et al. 2017) or by using field diagnostic assays of plant material (Doan et al. 2014). This can be limiting factor concerning FOV4 in fields because symptom expression varies greatly depending on the cultivar and its susceptibility to the pathogen. Indeed, when variation in cultivar susceptibility is the purpose of field research, as is the case in variety trials, the ability to attribute symptom expression to inoculum density vs. cultivar susceptibility is critically important. In other words, as a result of the distribution of FOV4 in soil, symptom expression cannot be used as a reliable predictor of inoculum density unless cultivar response across a range of inoculum densities is understood. Cultivar response across inoculum density, however, is difficult to understand without knowing or controlling inoculum density. Providing information on soilborne inoculum density benefits the design of field trials aimed at differentiating cultivars in terms of susceptibility. Intensive use of densely-interposed known-susceptible cultivars in a field trial as calibration checks (J. Olvey, *pers comm.*) allows spatial resolution of inoculum density to be inferred through symptom expression, provided the density of these "checks" is high enough to not miss high- or low-inoculum spaces between the checks. Spatial autocorrelation of inoculum density at distance of less than 10 m suggests that checks between every approximately 5-meter-long plot may be useful in randomized complete designs for variety trials. Additionally, grid-distributed checks may be used as a basis for generating an interpolated spatial map of infection risk, allowing for symptom variation within plots to be attributed to a gradient of inoculum density, and increasing statistical

power of analysis used during variety trials. A benefit of calibration checks is that they are realistic, and the plants used are subject to the environmental conditions of their neighbors – both of these benefits are uniquely provided by the use of actual plants as checks. A limitation to calibration checks is that they must be assessed after planting and do not provide information on inoculum dynamics after the check plants die – both of these limitations can be partially addressed by molecular quantification of inoculum pre-planting. Thorough use of calibration checks and molecular inoculum quantification where useful can provide researchers conducting variety trials with the information needed to address the recalcitrant and spatially variable problem represented by FOV4 inoculum.

The variability of inoculum raises the question of the amount of sampling necessary to describe field-wise inoculum density. The estimate of Moran's I ($Z = 17.73$, $p < 0.0001$) resulting from sampling the field in 2020 indicates that the distribution of inoculum is nonrandom and clustered. Sampling intensity may be informed by empirically determining the spatial scale at which inoculum density values are correlated, and sampling at scale minimally greater than that. Sampling intensively in a research field at which multiple different cotton varieties (and potentially different inoculum amplification rates associated with those varieties) provided data useful for estimating spatial autocorrelation using semivariance (**Figure 14**). Quantities of soilborne FOV4 inoculum density were spatially autocorrelated at a spatial scale (range) of 10.55 m. A cotton production field, planted uniformly to one variety with minimal variation, may lead to a different degree of spatial autocorrelation, and this is a

consideration that should be attended by researchers using spatially host-heterogeneous fields to develop applications for host-uniform commercial fields.

Standard, uniform spore counts have been used for consistent disease development in greenhouse variety trials, however disease severity varies especially as a function of environmental factors that vary between the field and laboratory. More field work building on a body of knowledge from laboratory and greenhouse research is necessary to understand the inoculum density-dependent susceptibility of cotton cultivars that may have resistance to FOV4. Hao et al. (2009) found that FOV4 inoculum may increase through time in the presence of cultivars that bear infection without dying, suggesting that the use of "tolerant" cultivars may have downstream consequences in terms of FOV4 abundance. Accordingly, research focusing on the temporal dynamics of FOV4 in varying environments and depending on host presence is necessary for understanding potential long-term changes in soilborne inoculum. Neither the spatial extent nor the potential temporal amplification of inoculum have previously been quantified in a host-independent in-field fashion. The utility of this quantification is its facilitating risk assessment, potentially prior to cultivar selection. Because the field we investigated was the site of a variety trial, it stands to reason that in-field FOV4 inoculum density variation may arise as a function of commensurate variation in cotton susceptibility to FOV4 infection, consistent with the laboratory findings by Hao et al. (2009). Additional research is necessary to determine the degree to which cotton cultivar affects inoculum density, and on which to base expectations of inoculum increase or decrease in a given location through time.

CHAPTER IV

COMPARATIVE TEMPORAL VARIATION OF *FUSARIUM OXYSPORUM* F. SP. *VASINFECTUM* RACE 4 IN FIELD SAMPLING AND GROWTH CHAMBER TRIALS

Soilborne inoculum of *Fusarium oxysporum* f. sp. *vasinfectum* race 4 (FOV4) is spatially variable in cotton fields, however the temporal dynamics of the pathogen are not well characterized. Environmental sampling was undertaken to describe the temporal dynamic of soilborne FOV4 inoculum density. The variability of soilborne FOV4 inoculum density was measured in July and December 2020 where the variance of samples collected in the field decreased between the two dates ($\sigma^2_{July} = 5.67$, $\sigma^2_{Dec} = 3.38$). These findings were compared to an experiment carried out under controlled conditions in a growth chamber to identify drivers of temporal variation in inoculum density. In this experiment, organic matter content (0, 5, 25, or 50 g per 100 mL of sand) and the presence or absence of cottonseeds (susceptible or tolerant Pima cotton, or Upland cotton (*G. hirsutum*) of unknown susceptibility), were studied as hypothetical causes of change in inoculum density. No effect of cotton cultivar was detected ($r = 0.212$, $p = 0.2035$) as a cause of amplification of soilborne inoculum. This was supported by results from the field sampling where cotton cultivar was not correlated to inoculum density. Organic matter was found to be a factor affecting the amplification of inoculum in the growth chamber experiment ($r = 0.704$, $p < 0.0001$).

Introduction

Plant pathosystems are complex networks with various, interconnected components that in combination initiate the onset of disease. The manifestation of plant disease is a dynamic process, and the complexities of a given plant pathosystem can be decomposed to attribute epidemiological variation to causes. The disease triangle represents the combined dependence of disease on the co-occurrence of environmental conditions that are conducive for pathogenesis, a virulent pathogen, and a susceptible host (Scholthof 2007). While these factors are necessary for the initiation of infection, many additional elements influence disease progress and severity over the course of a growing season. In soilborne plant pathosystems, inoculum density has a major effect on the progression of plant diseases (Stahr & Quesada-Ocampo 2020). Plant diseases caused by soilborne pathogens are dependent on inoculum density, meaning that the temporal progression of disease is affected by how much inoculum is present in the soil. The importance of inoculum density to disease progress has been empirically substantiated by research suggesting that quantities of soilborne pathogens at the start of the growing season most directly affect the severity of disease (Bailey & Gilligan 1999).

Fusarium oxysporum f. sp. *vasinfectum* (FOV) is a soilborne fungal pathogen that causes Fusarium wilt of cotton (*Gossypium* spp.) and has been identified in all cotton growing regions in the United States (Davis et al. 2006). Most races of FOV require the co-occurrence of the root knot nematode (*Meloidogyne incognita*) to infect cotton, leading to the expression of wilt symptoms (Davis et al. 2006; Kim et al. 2005; Cianchetta and Davis 2015). During the periods between growing seasons, FOV can

persist in soils as chlamydospores, thick-walled resting spores, and on plant debris as a saprophyte (Davis et al. 2006). The highly virulent race 4 (FOV4) is the exception because it can infect cotton and cause symptoms in soils where the root knot nematode is absent (Davis et al. 2006). In the United States, FOV4 was first identified in Pima cotton *(G. barbadense*) fields in California (Kim et al. 2005). The pathogen was later detected in Texas in 2017 (Halpern et al. 2018) and New Mexico in 2019 (Zhu et al. 2020).

The mode of FOV4 introduction to Texas and its initial location has not been confirmed, but infected seed coming from California has nevertheless been implicated as the most likely source of initial inoculum (Bennett et al. 2008). Subsequent spread from the initial introduction, also not confirmed, could be attributed to the movement of infested soil on field implements or through water. As a result of the initial seed introductions or the movement of infested soil thereafter, the distribution of FOV4 in infested fields is characteristically patchy, resulting in uneven cotton stands (Davis et al. 2006). In addition to the seed introductions, the movement of soil and plant debris within fields likely has caused multiple disease foci of varying inoculum density, observable by symptoms of infection, to be distributed throughout infested cotton fields (Davis et al. 2006). The spatial patterns of inoculum are observable by symptom expression, with some research showing a correlation between inoculum density and disease severity in cotton (Hao et al. 2009), however the temporal dynamics of soilborne FOV4 inoculum have not been characterized in the field.

Infection of cotton by FOV4 occurs predominantly during the seedling stage, where damping-off may result depending on susceptibility (Zhang et al. 2020). With the

understanding that this is a monocyclic disease, the temporal dynamics of inoculum can be used to predict severity in subsequent growing seasons if field inoculum is being amplified by tolerant varieties without any visible aboveground symptoms. Observations by Henry et al. (2019) suggest that maintenance of Fusarium wilt population density over time is a function of the saprophytic capabilities of the fungus. Hao et al. (2009) noted an increase in soilborne FOV4 during greenhouse inoculum density assays with a cotton cultivar tolerant to the pathogen, however this result has not been compared to results obtained from field research. As with other soilborne pathogens, such as *Verticillium dahliae* (Berbegal et al. 2007), the effect of inoculum density on infection probability and disease severity varies by host cultivar.

The purpose of this work was to examine the temporal dynamics of FOV4 in relation to inoculum density. The objectives of this research were to (i) quantify FOV4 from field soils using quantitative real-time polymerase chain reaction (qPCR), (ii) describe the temporal dynamics of soilborne FOV4 inoculum using a growth chamber experiment, and to (iii) compare temporal variation in inoculum density between field and growth chamber experiments, and between different quantification techniques.

Materials and Methods

Collection of field soils.

In July and December of 2020, soil samples were collected from a Texas A&M AgriLife Research & Extension field in Fabens, Texas, where Upland cotton variety trials were underway. Cotton plants were present during each sampling dates. Using a

randomized block design, 72 cotton cultivars were planted in 4.9 m length cotton plots, with 1.0 m of spacing between plots in a field consisting of 16 rows and 18 columns; each cultivar was replicated four times in the field (Isakeit & Arce 2021). Soil was collected from 131 plots, where samples was taken from each plot in rows 9 to 13 and randomly sampled from other plots outside of this extent (**Figure 17**). Three, 10 mL soil samples were collected, each corresponding to the front, middle, and end of each field. The sampling depth of 15 cm was used to remain within the root zone of the soil where the likelihood of fungal activity was greatest.

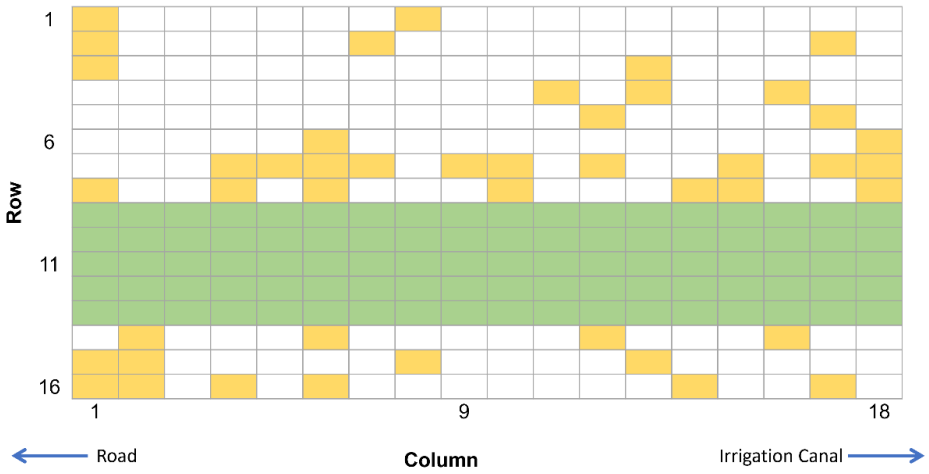

Figure 17. The map of the sampled portion of the field in 2020 where column 1 is nearest the road and column 18 is the end of the variety trial field. Rows 9 to 13 (green cells) were samples across the length of this field. Other plots (yellow cells) were chosen based on the cultivars found within rows 9 to 13.

In November 2021, three soil subsamples were collected from fifteen cotton plots in the Upland cotton variety trial field in Fabens, Texas, where the dimension of the field were 28 rows by 12 columns. Five plots were selected for sampling from the front, middle, and end of the variety trial field to account for spatial variation in inoculum density (**Figure 18**). In a second, smaller field, a single cotton cultivar (**Figure 19**),

Phytogen 400 (PHY400), was coated with each of the eight fungicide treatments in a split plot design, with Delta Pine 340 (DP340), a highly susceptible cultivar, planted in border plots for the field. Three, 10 mL soil samples were collected from each of sixteen plots, where each fungicide treatment was collected twice in each field. Sampling was completed before harvesting occurred. Samples collected from the fields were used for DNA extractions and were subsequently stored at -20°C following use.

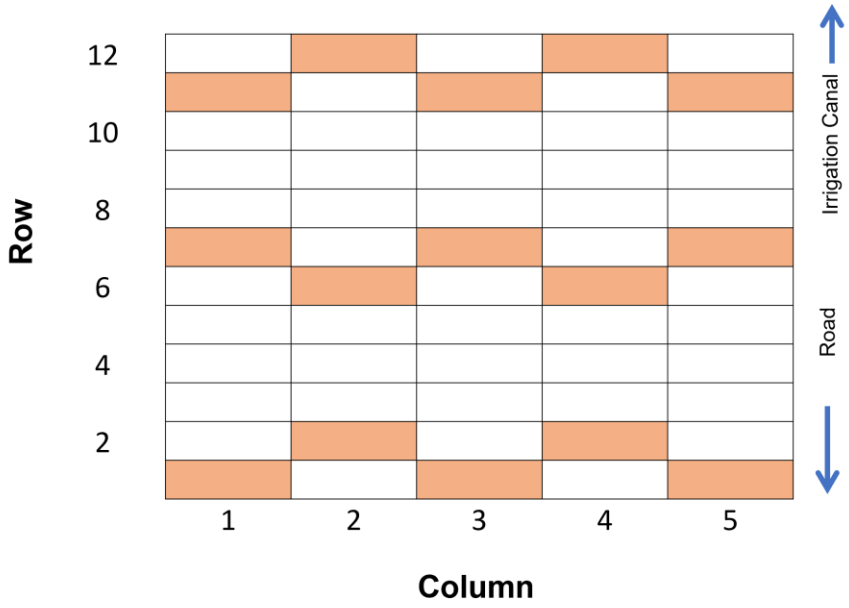

Figure 18. The sampling plan used to collect from a subset of plots in the 2021 variety trial field in the Texas A&M AgriLife Research and Extension field in Fabens, TX. Fifteen plots were sampled three times each to describe the variation in inoculum density in a multiyear cotton variety trial field.

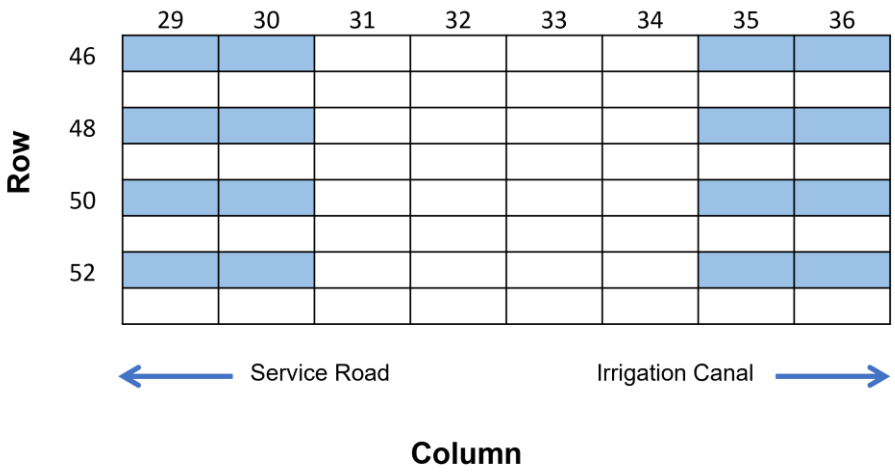

Figure 19. A fungicide seedcoat treatment efficacy trial was ongoing. Soil was sampled from the plots in blue. A single Upland cotton cultivar was planted in this field. Eight different seedcoat fungicide treatments were tested for their resistance to FOV4. Treatments were planted in double plots (for instance row 46 column 29 and row 47 column 29 have the same seedcoat treatment).

Fungal isolate cultures.

Potato dextrose agar (PDA) plates, augmented with lactic acid, were used to culture isolates of FOV4. The fungus was grown for 7 to 10 days at room temperature (22-23°C). Sterile toothpicks were used to scrape mycelia from the plates.

A 500 mL liquid culture of yeast extract peptone dextrose broth was used to grow conidia. The broth was inoculated with four plugs of plate cultured FOV4. After being shaken at room temperature (22-23°C) for four days, one day at 90 rpm and three days at 120 rpm, the broth was filtered through four layers of sterile cheesecloth. The conidia in the resultant suspension were counted using a hemocytometer with an initial inoculum density of 6.75×10^5 conidia/mL. The suspension was diluted twice in sterile water; the

diluted conidia suspension (6.75 x 10^4 conidia/mL) was used for inoculating sorghum grain for growth chamber experimentation.

Growth chamber experiment preparation.

Sorghum grain was used as the organic matter for growth chamber experimentation. About 750 mL of sorghum grain was soaked in, 1000 mL screw cap beakers for six hours. After the water was drained from the beakers, the sorghum grain was autoclaved for one hour at 121°C for two consecutive days. Play sand was also autoclaved on the gravity setting for two consecutive days at 121°C for one hour.

Table 5. Treatments used for the growth chamber experiment.

Organic Matter (g)	Seed Type	DP357	PHY841	PHY499	DP1522
0	None	None	None	None	None
5	Low	Low	Low	Low	Low
25	Medium	Medium	Medium	Medium	Medium
50	High	High	High	High	High

Four treatments, each repeated three times, were used for organic matter (**Table 5**). The treatments consisted of 0, 5, 25, or 50 g of autoclaved sorghum grain. Sorghum grain was inoculated with 1 mL of the conidia suspension and mixed with up to 100 mL of sterile sand. A randomized complete block factorial design was used in a 40-cell seedling tray.Full cells of each treatment type, twelve cells per date, were sampled every ten days for 30 days. Cottonseeds Delta Pine 357 (DP357), Phytogen 841 (Phy841), Phytogen 499 (Phy499), and Deltapine 1522 (DP1522) were surface sterilized in a 10% bleach solution and rinsed twice with sterile deionized water. Cottonseeds were planted after 10 days to mimic the build-up of inoculum in a fallow field. Sand, without organic

matter present, was also inoculated with 1 mL of the conidia suspension. The experiment was repeated twice under the same growth chamber conditions.

Isolation of genomic DNA.

The Qiagen DNeasy PowerSoil Pro kit was used to isolate genomic DNA from 0.25 g of soil, which were homogenized using the Bertin Technology Precellys 24 Lysis & Homogenizer. The extractions followed the manufacturer's protocol. Extracted DNA was suspended in 50 µL of elution buffer, with aliquots of 15 µL stored at 4°C until use, the remaining DNA was stored at -20°C.

Quantification of soilborne inoculum.

Soilborne FOV4 was quantified using qPCR as described in Davis et al. (2022) for both field and growth chamber samples. Briefly, 1 µL of genomic DNA ($1x10^{-7}$ to 0.01 ug/mL) was quantified in a mixture of 5 µL of Bio-Rad SsoAdvanced Universal Inhibitor Tolerant SYBR Green Supermix, 1 µL each of the A3-2018 FOV4 forward and reverse primers (0.001 ug of each), and 2 µL of sterile DNase-free water, per well. The Bio-Rad CFX Connect QX200 Real-Time PCR System was used for quantification using the settings outlined in Chapter III (Davis et al. 2022). A standard curve, consisting of a ten-fold serial dilution of plate culture FOV4 genomic DNA, was used to compare cycle of quantitation (C_q) values of soil samples to known quantities. The Bio-Rad CFX Connect Maestro Software for Windows program collected the output data, which was used for downstream statistical analysis. Output for both the cycle of quantitation (C_q) and the starting quantity (SQ) were used for analysis.

Fungal colony counts.

Colony forming units (CFU) of FOV4 were counted from the growth chamber experiment samples to compare the change in viable conidia between the sampling dates. Subsamples of approximately 0.25 g of soil were weighed and 1 mL of water was added to the tube. A sterile microcentrifuge tube pestle was used to disrupt the contents of the tube, which was followed by briefly vortexing. The first serial dilution of the mixture was spread on three plates each. Colonies were counted two days after inoculation.

Data analysis.

The SAS System version 9.4 (SAS Institute, Cary, NC) was used to analyze data. Data were analyzed using the GLM, G3DGRID, and SGPLOT procedures. The G3D and G3GRID procedures were used for visualization of C_q values as surface plots to describe spatial inoculum density over time. The GLM procedure was used to model the change in starting quantity (SQ) values and to compare between means using the LSMEANS function. PROC SGPLOT was also used for visualization of results as line graphs and as box plots.

Results

Temporal dynamics of soilborne FOV4 inoculum density – environmental samples

Figure 20 compares the ranges of inoculum density in December (*range* = 6.03, σ^2 = 1.57, 95% CI [1.25, 2.02]) and July (*range* = 11.76, σ^2 = 6.20, 95% CI [4.14, 6.73]). Using Levene's test for the homogeneity of variance, the variance in mean C_q between the two sampling dates was determined to be different ($p < 0.0001$). When compared to December, inoculum density was more variable throughout the field in

July. Although the range of mean C_q values is smaller, there is no significant difference between the averaged estimated inoculum density as a function of time. Surface plots generated using PROC G3D and G3GRID were used to visualize the temporal variation in soilborne inoculum density between the July and December sampling dates (**Figure 21)**. Soil samples became more spatially autocorrelated in December (I = 0.114, Z = 29.6, $p < 0.0001$) compared to July (I = 0.073, Z = 17.73, $p < 0.0001$), the positive Z-score indicated spatial autocorrelation. A spatial effect of inoculum density exists between the July and December 2020 sampling dates. There is structure in the inoculum density along the in-field columns when comparing mean C_q (r = 0.741, $p < 0.0001$) between the two sampling dates. There was, however, no structure when comparing rows and mean C_q between the sampling dates (r = 0.342, $p < 0.4241$).

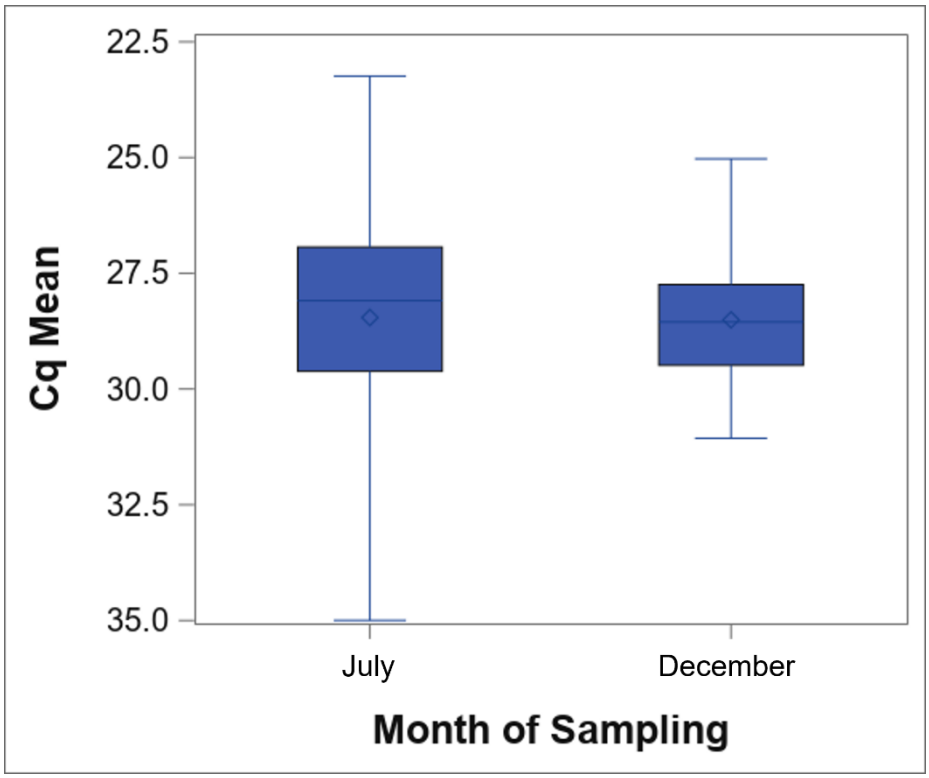

Figure 20. Box plots illustrating the variability of inoculum density between July and December 2020. While there was no difference between the means, the variance of inoculum density decreased between July (*range* = 11.76, σ^2 = 6.20, 95% CI [4.14, 6.73]) than in December (*range* = 6.03, σ^2 = 1.57, 95% CI [1.25, 2.02]).

A

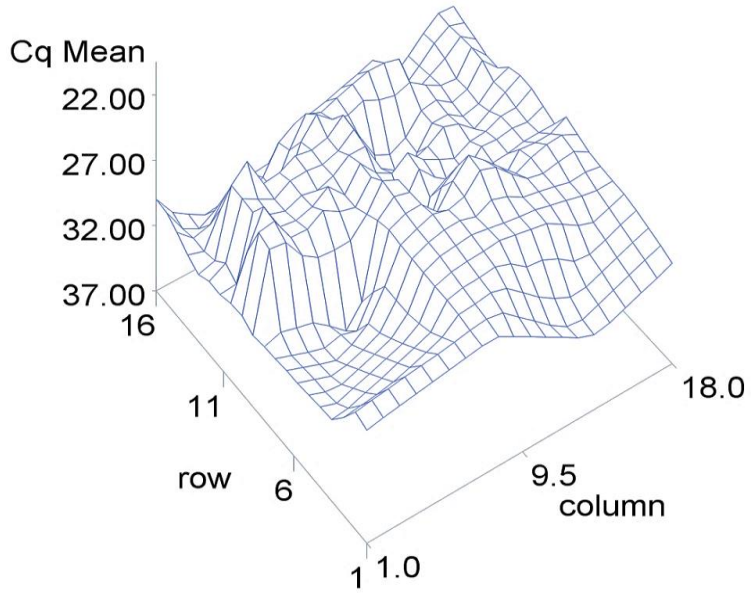

B

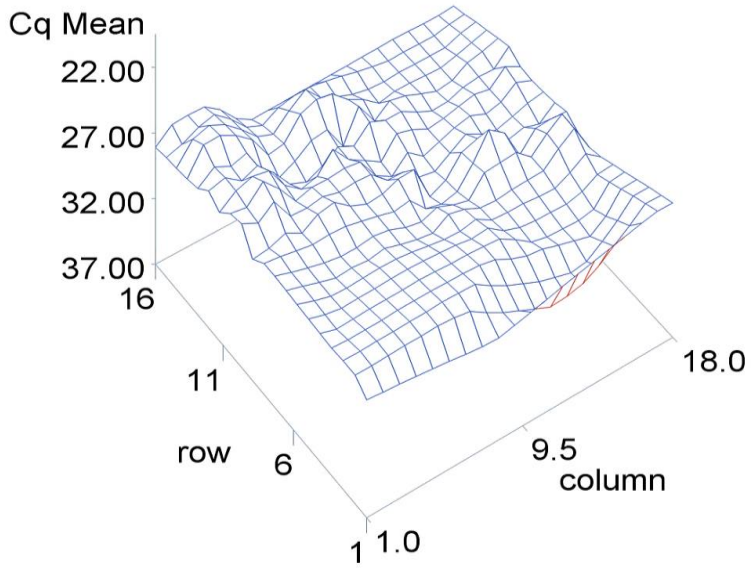

Figure 21. Surface plots visualizing the mean C_q values estimated from soil samples collected from the field in A) July and B) December 2020 to understand the temporal dynamic of soilborne FOV4 inoculum density. The x-axis represents the rows (1 to 16) and the y-axis represents the columns (1-18) that were sampled from the Texas A&M AgriLife Research and Extension experimental field in Fabens, Texas. The z-axis is the mean C_q estimates for each plot. In July, variability of inoculum density was greater throughout the field when compared to December.

Comparative quantification of environmental samples in 2021.

In 2021, soil samples were collected from two fields to examine the differences between a long-term variety trial field, used for testing FOV4 tolerance in cotton plants, and a field that was newly used for seedcoat fungicide trials against FOV4 in 2021 (**Figure 22**). The difference between the averages of the mean C_q values estimated between the two field was significant ($r = 0.379$, $p = 0.0320$). Additionally, the range of Cq values was smaller for samples collected from the fungicide trial.

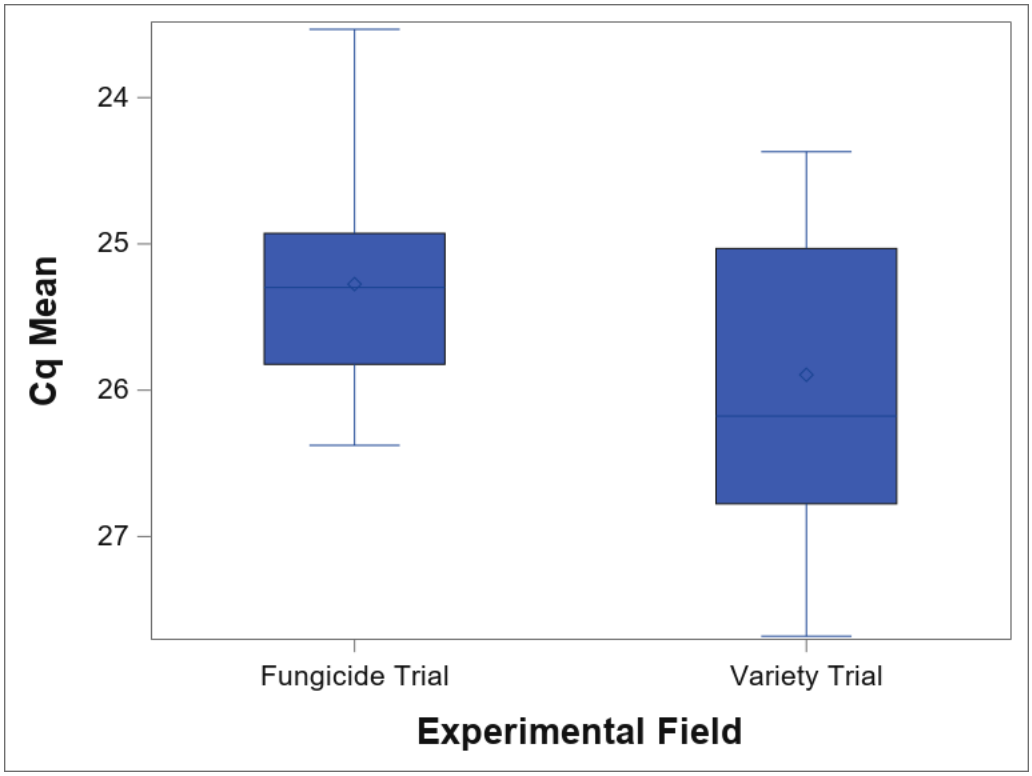

Figure 22. Boxplots show the difference in soilborne inoculum density between two cotton fields where samples were collected in November 2021, when cotton plants were still present in the field. The first, a monoculture field using Phytogen 400 for a seedcoat fungicide trial had newly been used for FOV4 trials in 2021. In the second field, multiyear cotton variety trials had been underway. The difference between the mean C_q values between the two seasons was marginally significant with a small effect size ($r = 0.379$, $p = 0.0320$).

Temporal variation in inoculum density – growth chamber

Baseline quantifications were done on samples before placing the sand-sorghum grain mixture into the germination trays. These quantifications were done to ensure that there was a difference between initial and subsequent sampling dates. In **Figure 23** the mean $\log_2$ SQ of the growth chamber soil samples is shown with the days post inoculation (DPI) on the x-axis ($r = 0.704$, $p < 0.0001$), generated using PROC GLM. Inoculum density, which was represented by the starting quantity (SQ), increased between 0 and 20 dpi for low, medium, and high levels of organic matter. Overall, each organic matter treatment follows the same trend for the first 20 dpi. The greatest increase in inoculum density was between 0 and 10 dpi when FOV4 was most readily colonizing the organic matter in each cell. Inoculum density continued to increase, at a comparatively slower rate between 10 and 20 dpi, until it plateaued, for medium and high treatments, from 20 to 30 dpi.

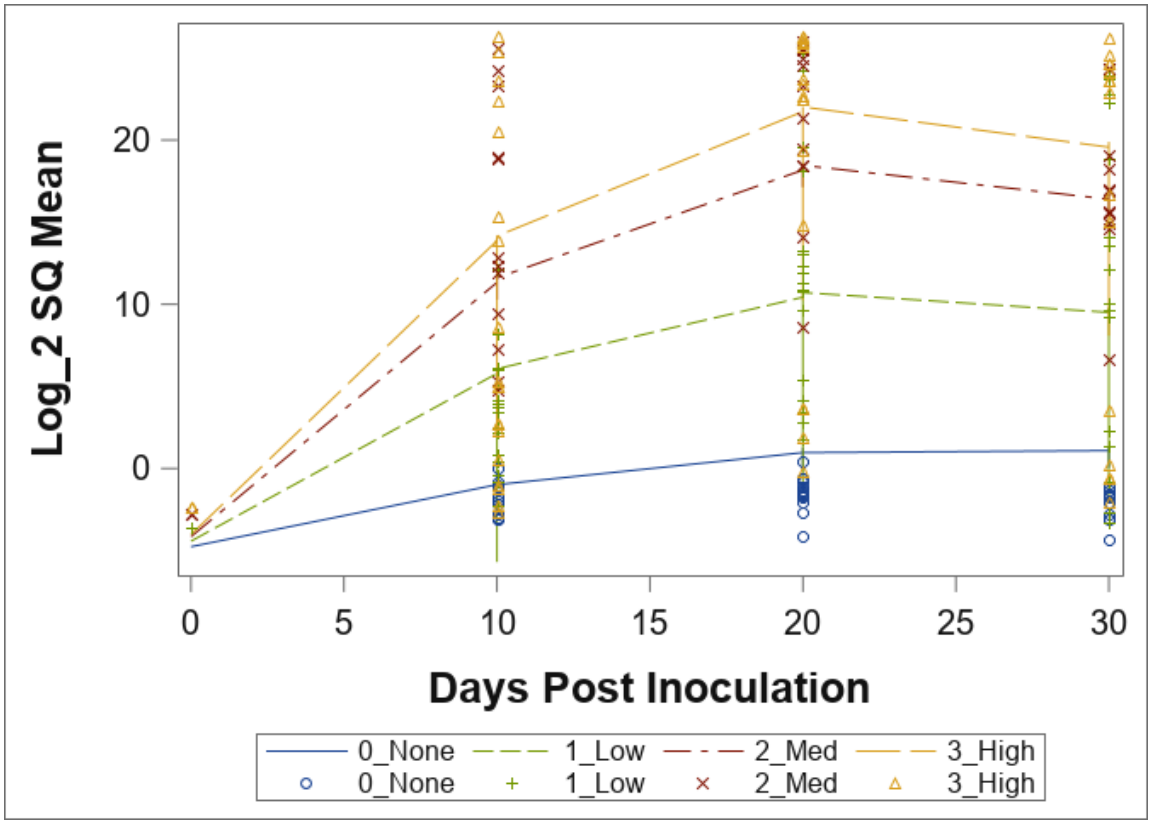

Figure 23. The entire contents of designated cells were collected every ten days over a thirty-day period. Genomic DNA from 0.25 g soil samples were quantified using qPCR. The mean log2 starting quantities (SQ) for the soil samples were used to fit the change in inoculum density over time for each of the organic matter inputs (none, low, medium, and high). A quadratic model best fit the data. The progression of inoculum density was significant with respect to time (r = 0.704, p < 0.0001), with the greatest increase in inoculum density occurring by 10 dpi. Inoculum continued to increase at a slower pace between 10 and 20 DPI. Following this, inoculum density begins to decrease, or it remains relatively steady, based on organic matter content.

Using PROC GLM, a linear regression of mean $\log_2$ SQ against cotton cultivar was fit to determine if there was an effect of cotton cultivar on inoculum density. No effect of cotton cultivar was detected (r = 0.212, p = 0.2035), though PHY499 was found to be significantly different from the no seed treatment and cultivars DP357 and PHY841 (**Figure 24**).

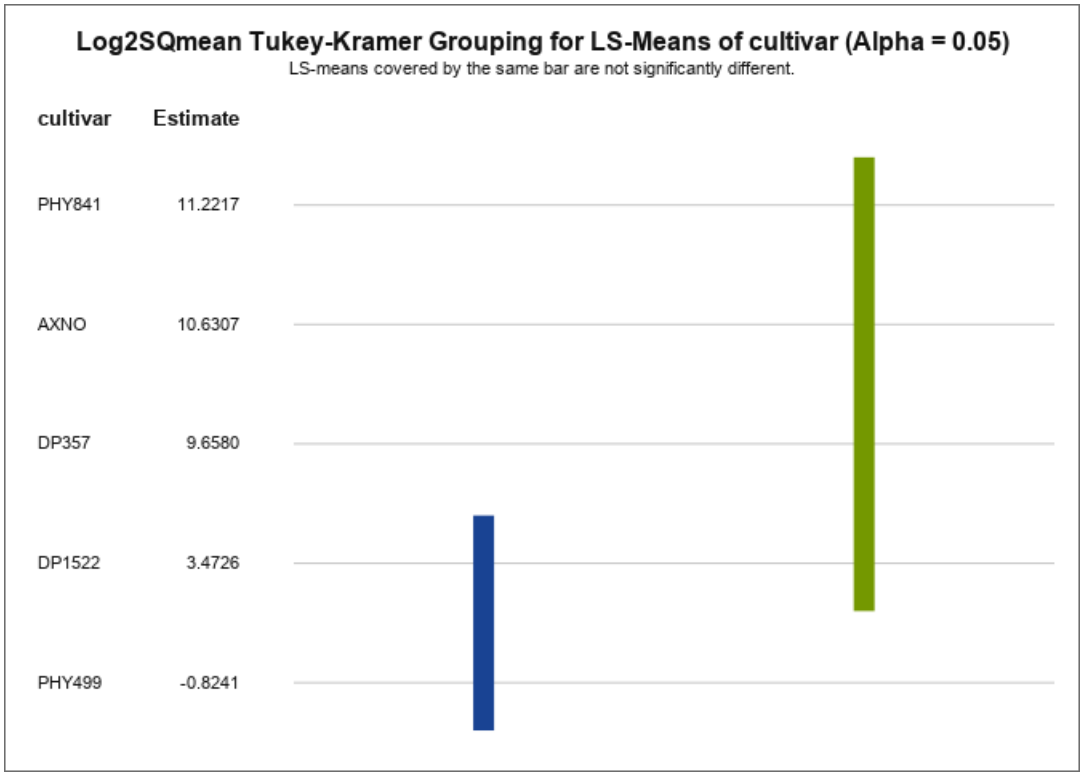

Figure 24. Using a LINES in the LSMEANS statement, the least squares means by cultivar were compared. This graph shows if the estimates of mean log2 SQ were significantly different from the other seed types. The means covered by the same bar were not significantly different. PHY499, an Upland cotton cultivar tolerant to FOV4, was significantly different from the other cottonseed cultivars and the no seed treatment

Fungal colony counts.

Fungal colony forming units (CFUs) were counted on the initial planting date and for each of the sampling dates (**Figure 25**). The $\log_{10}$ of CFUs were calculated and the data were fit over time based on the organic matter level. The counts for each of the treatments increased with respect to time. Medium and high levels of organic matter followed a similar trend between the sampling dates; the low organic matter treatment

experienced the greatest increase in CFUs over the course of the experiment. The change in CFUs over time was significant ($r = 0.647$, $p < 0.0001$).

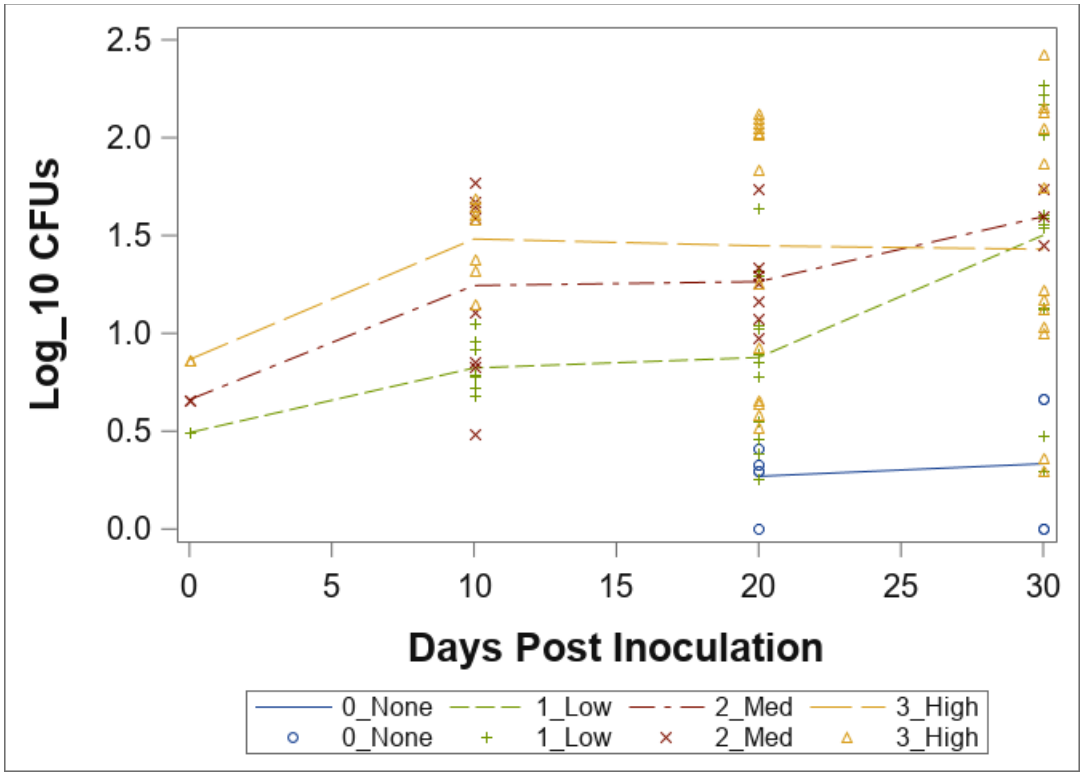

Figure 25. Colony forming units (CFU) of FOV4 were counted on potato dextrose media two days after inoculation. To describe the temporal variation in viable conidia, the change in the mean log_{10} fungal CFUs of each level of organic matter (none, low, medium, and high) was plotted over the 30-day experimental period ($r = 0.647$, $p < 0.0001$). With respect to time, inoculum density increased for each of the treatments over time, with the low inoculum treatment having the greatest increase in viable CFUs over the course of the experiment.

Discussion

In agricultural ecosystems, plant diseases are expected to vary through time as a function of environmental and host-related inputs, as well as variability in the abundance and availability of the pathogen. Under the relevant field conditions, soilborne FOV4

inoculum density is heterogeneous, varying spatially between plots and even at the intra-plot level (Davis et al. 2022, Chapter III). This spatial variability affects the temporality of inoculum density at field scale. Prior FOV4 research has not thoroughly examined how inoculum density changes over time, nor have the drivers of soilborne inoculum density been well characterized for this and many other systems. Researchers have anecdotally observed change in soilborne inoculum density over time, however the environmental or other mechanisms associated with the variation were not characterized. Furthermore, the severity of infection from FOV4 is known to vary because Fusarium wilt of cotton is an inoculum density-dependent disease (Hao et al. 2009). In their greenhouse study, Hao et al. (2009) observed that their resistant cotton cultivar Phytogen 800 may have increased FOV4 inoculum density over the course of their experiment. The result from Hao et al. (2009) raises the question of what actually drives the temporal variation in soilborne FOV4 inoculum density.

In 2020, soil samples were collected in July and December to understand the temporal variation in soilborne inoculum density under the relevant environmental conditions from a cotton field in Fabens, Texas where yearly variety trials, and other FOV4 trials, were performed. This sampling plan was designed to describe the variation over the entire extent of the variety trial field, which spanned 18 columns, approximately 88.2 m. The plots for random sampling (**Figure 17**) were chosen based on the cultivars that were present within the larger sampling block. With this sampling intensity, the heterogeneity of inoculum density was empirically described (Davis et al. 2022; Chapter III). Temporally, there was a change in range of inoculum density between July and

December 2020 (**Figure 21**). The range and variance in inoculum density were greater in July (*range* = 11.76, σ^2 = 6.20, 95% CI [4.14, 6.73]) and decreased in December (*range* = 6.03, σ^2 = 1.57, 95% CI [1.25, 2.02]) (**Figure 20**). Soilborne FOV4 inoculum density in December was more uniform than in July (**Figure 21**). These results can be used to verify that there is temporal variation in inoculum density using the DNA-based approach described in Chapter III. Conversely, these results do not explain how inoculum ends at a relatively uniform level at the end of the season. Despite this result, the mechanisms behind the general uniformity of soilborne inoculum are not well known. There are two possible ways in which this could be explained. The first possible explanation is that soil moved throughout the field during routine tillage could move inoculum from and to different locations creating new foci or expanding previously established foci. The second concerns the flood irrigation practices used in cotton production in this region of Texas. Wang et al. (2004) attributed the spread of FOV in Australia to irrigation practices used in cotton production. If this assumption is correct, then the change in inoculum density detected between the two sampling dates could be a function of both the movement of inoculum through irrigation and the expected amplification in the field over the course of the growing season.

A temporal inoculum density study was undertaken where both cotton cultivar and organic matter content were examined as possible drivers of soilborne inoculum density. These factors were chosen because they could be experimentally manipulated in tandem to determine which is important in inoculum density. Organic matter can mostly be controlled by the amount of debris left in the field from previous growing seasons.

Growers choose cotton cultivars based on yield potential and other factors relating to their hardiness to disease. Not every cotton cultivar, especially many Pima cotton cultivars, can withstand infection by FOV4 during the growing season. The levels of organic matter in fields are influenced by the practices of the growers and whether the previous year's cotton is removed or plowed under. In the experiment, four organic matter treatments, corresponding to 0, 5, 25, or 50 g of sorghum grain, and five seed treatments (no seeds, DP357, Phy841, DP1522, and Phy499) were used, each was replicated three times per tray over three trays (**Table 5**). The seeds used were chosen by susceptibility to FOV4; a known susceptible Pima cultivar, DP357, and Phy841, a Pima cultivar tolerant to FOV4. Two Upland cotton cultivars, Phy499 and DP1522, were also utilized. Despite the aforementioned results of Hao et al. (2009), the results of this study showed that the susceptibility of a given cotton cultivar was not a major factor in increasing soilborne inoculum density ($r = 0.212$, $p = 0.2035$). Instead, organic matter is the factor that most directly increased soilborne inoculum density in this study.

Organic matter content affects the environmental conditions that a microorganism experiences. As observed in this experiment, the greater the amount of organic matter in a pot of soil, the better the soil retained water. Despite the better water retention, germination rates were variable. Mostly PHY499 and DP1522 were able to germinate in the cells with low amounts of organic material. As the fungal mass increased, those tolerant cultivars were unable to withstand the infection. This may be in part due to the concentration of inoculum in a 100 mL cell compared to the relatively more diffuse inoculum in fields. Under artificial conditions, where the disease pressure

is much higher than it would be in the field, the tolerant cultivars were less able to withstand infection.

Over the course of the 30-day growth chamber experiment, for the treatments with differing levels of organic matter, three different inoculum growth rates were observed. The first, from 0 to 10 dpi, FOV4 grew rapidly to colonize the fresh organic matter in each cell. In the period of 10 to 20 dpi, when seeds were added, the rate of growth slowed, however inoculum still increased steadily (**Figure 23**). In the final period until the termination of the experiment, inoculum density was either approaching or had reached a plateau (**Figure 23**). The growth of FOV4 seemed to reach a carrying capacity by the end of the experiment. A carrying capacity can be described as a species maximum population given the environment, resources, and other factors necessary for species survival. Each of the individual FOV4 populations within the cells reached a carrying capacity in part because of the limiting factor in this experiment. This phenomenon can be explained by Liebig's law of the minimum, which states that a population's growth is limited by the scarcest resource in its environment. And in this experiment, the factor that limited population growth was the amount of organic matter in each of the cells, resulting in a variable maximum population size as a function of organic matter abundance. The maximum inoculum density detected by qPCR does not, however, directly equate to the number of viable spores produced. Even if inoculum density reaches maximum at a high level, the qPCR analysis cannot differentiate between living and non-living tissue. To differentiate between these, fungal colony counts were also employed.

The temporal change in viable CFUs was significant with respect to time (r = 0.647, $p < 0.0001$). Over the course of the experiment, low organic matter treatment reaches a level that is equal to that of the medium treatment (**Figure 25**). The low and medium organic matter treatments follow a similar trend throughout the duration of the experiment. The results of this experiment may support the idea that after reaching a carrying capacity, sporulation of FOV4 may occur and account for increase the amount of DNA in soil. Increased sporulation during a period of stress may be similar to stress flowering, where plants prioritize reproduction over vegetative growth (Hatayama & Takeno 2004; Wada & Takeno 2010; Takeno 2016). This type of stress-adaptive prioritization of reproduction has also been documented in bacteria (Ultee et al. 2019). Upon reaching carrying capacity, based on the available organic matter content which promotes mycelial growth, the lack of resources in the soil may induce sporulation (Dahlberg & Van Etten 1982), however this does not necessarily mean that all of the new spores are viable, nor is every spore likely to survive until conditions are more favorable. To this end, the amount of quantified DNA in this growth chamber experiment may relate more to scarcity of usable resources and not the amount viable and infectious propagules. The increased sporulation after reaching a carrying capacity may be what makes up inoculum for the coming season. Instead of producing new spores to infect, the pathogen may be sporulating for survival by creating chlamydospores. The overwintering spores are formed and, upon signaling by newly planted cotton seedlings, they germinate to infect the new seedlings. Further

investigation is required to determine the rates of sporulation, especially in the presence of tolerant cotton cultivars as the organic material for FOV4.

The effect of water on the movement of FOV4 in the variety field may be explained by the fact that there is structure in how inoculum was distributed over time. The surface plot in **Figure 21** shows a relatively even distribution of C_q values across the field. There is a spatial effect of column that persists between the two sampling dates ($r = 0.741$, $p < 0.0001$). The movement of FOV by water has been previously hypothesized in Australia where FOV was found outside of the sites where it was originally detected (Wang et al. 2004). If, after multiple periods of flood irrigation, inoculum is either pushed some distance across the field until it is impeded, or it percolates into the soil, it is possible that movement of soil and fungal spores eventually evens out over the growing season. Using the data acquired from the growth chamber experiment, this result can be further explained. The rate of growth in the first 10 dpi is much more rapid than at any time after for all levels of organic matter. Subsequently, the growth rate slows and eventually decreases. In the field, within the first two weeks following planting, damping-off, one of the characteristic symptoms of FOV4 infection leading to seedlings death, is observed. Damping-off at this time can be attributed to the rapid amplification of inoculum density alongside the growing, but vulnerable seedlings. The seedlings that survive to maturity continue to increase inoculum, but at a slower rate compared to the beginning of the season until a carrying capacity, of sorts, is reached. Then, as the season progresses, inoculum density eventually is relatively level at the end of the season. And because the inoculum levels at the end of the growing season

influence the next, inoculum density quantifications at the end of the growing season may have utility in predicting the next season's inoculum density.

In 2021, soil samples were collected from selected plots in two fields, where a variety trial and a fungicide trial were underway. The purpose of sampling from these fields was to determine if a difference exists between fields dependent on how recently these fields were used for experimentation related to FOV4. The first field examined (**Figure 18**) was the 2021 Upland cotton variety trial field. Multi-year variety trials for both Pima and Upland cotton cultivars have been conducted in this field. The second field (**Figure 19**) held a fungicide trial which tested the efficacy of multiple seed coat treatments against FOV4. Fungicide seedcoat treatments were on Phy500, an Upland cotton cultivar. The 2021 fungicide trial was the first FOV4-related trial to occur in this field.

The first objective of this sampling was to understand whether there was a difference between mean C_q values of the two fields. There was marginal significance and a small effect size ($r = 0.379$, $p = 0.0320$) between the mean C_q values of two field (**Figure 22**). There was more variation in the C_q values corresponding to soilborne inoculum density in the variety trial field, presumably because of the multiyear amplification of inoculum and the multiple, different cultivars planted in that field. The range of mean C_q values in the fungicide trial supports this claim, however the inoculum density measured in this field is consistently and relatively high. As a tolerant Upland cotton cultivar, this high level of inoculum at the end of the season should be expected because of the amount of organic matter present to fuel the growth of FOV4 in the soil

throughout the growing season. Similarly, the sampled portion of the 2021 Upland cotton variety trial field, while more variable, also has a relatively high amount of inoculum. Again, the high levels of inoculum may be a function of these tolerant cultivars acting as organic matter for FOV4.

The results of the growth chamber experiments help to underscore the biological significance of organic matter in fields to soilborne plant pathogens that can also live as saprophytes. As demonstrated here, inoculum density varies as a function of the amount of available organic material, and as abundance of organic matter increases so does the rate at which inoculum density increases. Organic matter also limits the maximum population size of the fungus per unit soil area. In the field, an expectation could be that inoculum density would be greater in plots where a cultivar could withstand the initial infection by FOV4. As the tolerant cultivar grows, FOV4 can sporulate throughout the growing season, though potentially at a slower, more constant, rate than it would at the beginning of the season. Because in this instance organic matter is not a limiting factor, amplification of inoculum continues. If organic matter was scarce, such as in plots where cotton was completely susceptible and died, Liebig's law of the minimum would apply to this limiting factor. In the event of a very susceptible cultivar, organic matter would be the scarcest resource for the growth of FOV4. Instead of vegetative growth, the pathogen would be likely to form chlamydospores until a suitable host is present. Unlike the growth chamber experiment, higher C_q values (less DNA) were estimated from plots where there was no major source of organic matter. This indicates that although

inoculum is not actively being amplified, DNA may still be present, even if there was a relatively lower concentration found in those plots.

The relationship between cultivar susceptibility and inoculum density has been investigated in different *formae speciales* of *Fusarium oxysporum*. For example, lettuce cultivars resistant to *Fusarium oxysporum* f. sp. *latucae*, the causal agent of Fusarium wilt of lettuce, can support the development of the pathogen without expression of symptoms aboveground (Scott et al. 2014). Additional research demonstrated that the persistence of *Fusarium oxysporum* f. sp. *latucae* in soil is driven, in part, by saprophytic growth on debris remaining in the soil (Paugh & Gordon 2021). Research performed by Henry et al. also supports the results of the present study. Asymptomatic growth of *Fusarium oxysporum* f. sp. *fragariae* was investigated to determine if resistant strawberry cultivars and closely related crops affected the persistence of the pathogen in soil (Henry et al. 2019). Their work found that the population densities of *Fusarium oxysporum* f. sp. *fragariae* were higher on the asymptomatic hosts and attributed that to parasitic growth, not pathogenic growth, supporting the long-term survival of the pathogen (Henry et al. 2019).

Mitigation of soil organic matter content, though potentially necessary to decrease the saprophytic survival of FOV4 in fields, may not be entirely feasible. Organic matter that is decomposed in the soil helps to replenish the nutrients that support plant growth. Over the course of the growing season, the organic matter in soil that is actively amplifying the population of the pathogen are the cotton plants. Realistically, the optimal manner through which inoculum density could be managed would be to

remove infected plant debris from fields. This, however, may not be entirely feasible in terms of cost and labor for growers.

The temporal amplification of inoculum has implications for subsequent growing seasons. FOV4 persists indefinitely in soils and the only reliable methods to control spread is sanitation of field implements, such as tractors, (Davis et al. 2006; Cianchetta & Davis 2015). Inoculum is heterogeneously dispersed through fields with some degree of spatial autocorrelation (Davis et al. 2022). Prior to planting, soilborne inoculum could be spread from disease foci throughout the field by practices such as tillage. Relatively high levels of inoculum at different disease foci at the end of the previous season could then be spread within or between fields, thereby determining disease pressure for the next season. FOV4 is an inoculum density dependent disease (Hao et al. 2009). As such, understanding the temporality of inoculum is necessary step in eventually developing strategies to mitigate the spread of FOV4 outside of its current geographic range.

Though this study used one field to describe the temporal variation in soilborne FOV4 inoculum density over time, there is some consistent pattern between the growth chamber and the field results. While additional work is required for characterization of the temporal variation in soilborne inoculum in multiple fields, the results of this study provide preliminary evidence supporting that organic matter is the main driver of the temporal variation in soilborne inoculum density. Future work pertaining to the temporal variation in inoculum density should continue with the methods used here. Incorporation of different tolerant Upland cultivars may also be useful in more accurately describing the potential for those cultivars to amplify inoculum. In particular, using other methods

to either directly inoculate the plants, such as root dip inoculations, or adding plants to inoculated soil at different growth stages. Such experimentation can clarify intricacies of the temporal dynamics of this pathosystem, especially concerning the relationship of infection tolerance as a precursor to the presence of post-cropping organic matter in fields experiencing FOV4 infestation.

CHAPTER V

CONCLUSIONS

The metaphorical arms race between host plants and their pathogens results in new forms of resistance in plants. Pathogens adapt to these new mechanisms of resistance and in turn evolve new mechanisms to evade or suppress host resistance. Coevolution between hosts and pathogens affects plant disease epidemics, especially in agricultural settings. Because plants are sessile organisms, they are forced to continually adapt to the heterogeneity present in their environments throughout their life cycles. Within a single field, nutrient availability or inoculum density can vary greatly depending on growing practices, and to understand how these affect plants, they must be empirically investigated. In this research, three studies were conducted in which spatiotemporal dynamics related to the heterogeneity of phenotypes and inoculum density were studied. These studies answered the three questions outlined in Chapter I concerning the spatial and temporal patterns of inoculum distribution, the processes that may give rise to the patterns, and the interplay between spatial and temporal aspects of the process.

Low altitude remote sensing

Heterogeneity in agricultural systems is not limited to the variation associated with inoculum density or disease. Topographical heterogeneity limits the applicability of some low altitude remote sensing capabilities in fields because a floor must be made prior to and estimations of height as the measurable phenotypic change (for nitrogen or

other nutrient input or for disease progress). The construction of a floor, using GPS control points, removes the variability associated with topography, thereby potentially missing some of the variation associated with plant height present in a field. The unsupervised machine learning technique of finite mixture modeling (FMM) was used to describe phenotypic variation in agricultural fields. Variation in height was used to test the applicability of FMM in large datasets with an unknown number of mixture components. Plant height is a readily apparent phenotype that may vary as a result of different inputs, such as nitrogen input as was used in the rice plots in Chapter II. Here, height was used as the measurable phenotype hypothesized to be affected by differential nitrogen input. Using height to estimate phenotypic variation with FMM is readily applicable to studying crop heterogeneity associated with disease. Stunting, for instance, is a common phenotype that is associated with different types of plant pathogens. Variation in plant height can be used as an indicator for disease presence, and this can inform sampling practices. Using the methods outlined in Chapter II, plant biomass can be quantified by partitioning structure-from-motion or single images and comparing the change in means between observations.

One general utility of unsupervised learning algorithms is their ability to discern patterns within a dataset without requiring training of the algorithm. If a systematic approach were to be taken to a dataset to apply FMM to different sections of an image, patterns in the data would emerge as mixture components. For example, red-green-blue (RGB) color indices are widely used to distinguish healthy and infected plant tissues. Applying FMM to a single color in the images and using a systematic approach to

further subset the image, the algorithm would output graphs that display the relative frequency of the two colors. If two colors, green and yellow, were observed in an image, then there would be two distributions in the output; if only green or only yellow were observed, a single distribution would be in the output instead.

Epidemiological research relies heavily on recognition of patterns in disease through space and time. This method utilizing FMM can be applied to spatial data to observe the change in disease patterns over time. The research described in Chapter II provides a proof of concept for employing FMM for myriad purposes related to precision agriculture.

Spatial dynamics of soilborne FOV4

Soilborne fungal pathogens, like *Fusarium oxysporum* f. sp. *vasinfectum* race 4 (FOV4), persist through a variety of strategies, including using overwinter spores or adopting a saprophytic phase. Though these are known, the spatial distribution of these types of pathogens is difficult to know prior to planting cotton. For a contemporary epidemic like FOV4 in West Texas, the goal of understanding the spatiotemporal dynamics of inoculum is twofold: mitigation and remediation.

Before the spatiotemporal dynamics of inoculum can be described, inoculum must first be quantified. The DNA-based quantitative method described in Chapter III was designed to be preferential to FOV4 and to detect DNA in soil samples. The spatial configuration of inoculum is dependent on the sources of initial inoculum and the modes through which subsequent short-range and long-distance spread occur. Soilborne FOV4 is likely to have first been introduced through infested seeds, and later spread because of

the translocation of soil within and between fields. In individual fields, multiple introductory events are possible. While the modes through which inoculum moves have not been characterized empirically, these results can guide investigation of hypothetical modes that would be expected to result in various patterns of inoculum distribution. In Chapter III, sampling intensity was chosen for the purpose of collecting enough soil in a structured and random pattern to describe the spatial autocorrelation of inoculum. Spatial autocorrelation can in turn be used to not only inform future sampling, but also for designing variety trials with calibration checks (known susceptible or tolerant cultivars) to better connect symptom expression to inoculum density.

Temporal dynamics of FOV4

Study of the spatial dynamics of FOV4 informs study of the temporal dynamics. Spatial and temporal dynamics of inoculum are interdependent, with temporal processes of movement and amplification affecting the spatial distribution of inoculum, and spatial autocorrelation affecting the structure of disease pressure experienced by a host population and therefore the consequent amplification-dependent inoculum distribution across space. Variation in inoculum density at the end of one growing season affects variability at the beginning of the following season. In both July and December 2020, soilborne inoculum has spatially autocorrelated, but the autocorrelation increased at the end of the season as estimated inoculum density leveled off in December, due to the effect of temporal processes on inoculum amplification/decay and movement. In both 2020 and 2021, inoculum densities measured in field in December had comparatively smaller ranges between the highest and lowest C_q values. Inoculum density was

relatively high throughout the time of observation. The amount of organic matter in the soil, from the tolerant Upland cotton cultivars planted in these fields, was the likeliest reason for the levels of inoculum detected. Comparing these results to the results of the growth chamber trial, organic matter was determined to be a driver of inoculum density through time. The rapid increase in inoculum density at the beginning of experimental period was indicative of the hypothesized increase at the beginning of the growing season as new cotton was planted. The reaching of maximum inoculum density toward the end of the experimental period could be seen as a carrying capacity being reached. In terms of Liebig's law of the minimum, the growth-limiting factor in this case was organic matter.

Implications of this research

Dynamic heterogeneity in agricultural fields results from complex and interacting processes. The three research projects described in this dissertation are each related to a different aspect heterogeneity in agricultural ecosystems. Prior to any field studies, the whereabouts and amounts of inoculum are unknown. Describing heterogeneity requires that there is detection of differences at scale, and quantification to know if variation exists. In addition, knowing how these inoculum and disease aggregate, and if the aggregation is sustained or changes, is useful to epidemiological studies that consider space and spatial processes.

Taken together, the techniques described here are useful for the purpose of describing patterns that result from the interplay between spatial and temporal processes, and for the purpose of inferring those processes themselves. Two methods were outlined

discussing how to monitor the spatial distribution of disease or inoculum. The first used the unsupervised machine learning technique FMM to reliably estimate quantitative phenotypic differences in the presence of variation that presents challenges to other techniques. The applications of this method are myriad related to detection and differentiation of distributions latent in datasets. At spatial scale, disease incidence and the variation in disease can be tracked over time using FMM in addition to the different types of image analysis techniques (RGB, multispectral, structure-from-motion). The analytical pipeline developed here opens the possibility for expedited routine monitoring of spatial and temporal variation.

In the prior literature, FOV4 was noted to be an inoculum density-dependent disease (Hao et al. 2009), with the anecdotal knowledge surrounding the epidemiology of FOV4 focused mostly on using the aboveground symptoms of disease to predict severity. In California, where the pathogen was first detected in the United States, Pima cotton was the main cultivar planted. Inoculum density was expected to be high, however quantification of inoculum density relied exclusively on the severity of symptoms, which are unreliable due to the differential expression of symptoms based on the cultivar and its susceptibility. By developing a DNA-based metric to quantify soilborne FOV4, inoculum density measurements are empirically substantiated, and the autocorrelation of inoculum is knowable. The results of Chapter III are taken form a single field, but these results can be used to inform sampling patterns, and when used in tandem with Chapter IV, these results are useful in determining the patterns associated with soilborne FOV4 inoculum density. Specifically, there is spatial autocorrelation,

organic matter is a driver of the increase in inoculum density, and the movement of inoculum may be dependent on initial inoculum. These results not only inform sampling, but also inform management practices related to limiting the spread of inoculum within and between fields.

Spatial and temporal variation in inoculum density, and other factors leading to heterogeneity, are related to each other. The temporality of disease is directly affected by the spatial configuration of inoculum. Inoculum could be moved, new foci established, amplified, or any combination of these due to both pathogen related and external factors. These, in turn, determine disease pressure over the course of the current season and future growing seasons. Furthermore, knowledge of how inoculum survives, and if it is being amplified during the time between seasons is necessary to understanding the epidemiology of a disease outside of the constraints of the disease triangle. Importantly, this research describes methods that can be used as tools to help decompose the complexities of the pathogen side of a plant pathosystem to learn about the dynamics of inoculum and disease. Aspects such as spatial and temporal variation affect every pathosystem in different ways and understanding these and their interactions is an important step in developing better models of plant disease epidemics.

REFERENCES

1. Alexander. H. M. 1989. Spatial heterogeneity and disease in natural populations. In *Spatial Components of Plant Disease Epidemics*. ed. Michael J. Jeger. Prentice Hall Inc., p. 144-164.
2. Al-Hiary, H., Bani-Ahmad, S., Reyalat, M., Braik, M., A. L., Rahamneh, Z. 2011. Fast and accurate detection and classification of plant diseases. *Int. J. Comput. Appl*. 17: 31–38, Doi: 10.5120/2183-2754.
3. Altschul, S. F., Gish, W., Miller, W., Myers, E. W., and Lipman, D. J. 1990. Basic local alignment search tool. *J. Mol. Biol*. 215:403-410.
4. Anbessa, Y. and Juskiw, P. 2012. Nitrogen fertilizer rate and cultivar interaction effects on nitrogen recovery, utilization efficiency, & agronomic performance of spring barley. *ISRN Agron*. Doi: 10.5402/2012/531647.
5. Anderson, J. P., Gleason, C. A., Foley, R. C., Thrall, P. H., Burdon, J. B., and Singh, K. B. 2010. Plant versus pathogens: an evolutionary arms race. *Funct. Plant Biol.* 37: 499-512. Doi: 10.1071/FP09304.
6. Armstrong, G. M., and Armstrong, J. K. 1960. American, Egyptian, and Indian cotton-wilt Fusaria: their pathogenicity and relationship to other wilt Fusaria. U.S. Dep. Agric. Tech. Bull. 1219:1-19.
7. Araus, J. L., Kefauver, S. C., Zaman-Allah, M., Olsen, M.S., and Cairns, J.E. 2018. Translating high-throughput phenotyping into genetic gain. *Trends Plant Sci*. 23(5). Doi: 10.1016/j.tplants.2018.02.001.

8. Araus, J. L. and Cairns, J.E. 2014. Field high-throughput phenotyping: The new crop breeding frontier. *Trends Plant Sci*. 19(1). Doi: 10.1016/j.tplants.2013.09.008.
9. Bailey, D. J. and Gilligan, C. A. 1999. Dynamics of primary and secondary infection in take-all epidemics. *Phytopath.* 89: 84-91. Doi: 10.1094/PHYTO.1999.89.1.84.
10. Ballestrini, R., Lumini, E., Borriello, R., and Bianciotto, V. 2015. Plant-Soil Biota Interactions. In *Soil Microbiology, Ecology, and Biochemistry*. ed. Eldor A. Paul. Academic Press, Elsevier Inc., p. 311-338.
11. Bell, A. A., Gu, A., Olvey, J., Wagner, T. A., Tashpulatov, J. J., Prom, S., Quintana, J., Nichols, R. L., and Liu, J. 2019. Detection and characterization of *Fusarium oxysporum* f. sp. *vasinfectum* VCG0114 (race 4) isolates of diverse geographical origin. *Plant Dis.* 103:1998-2009. Doi: 10.1094/PDIS-09-18-1624-RE.
12. Bendig, J., Bolten, A., and Bareth, G. 2013. UAV-based imaging for multi-temporal, very high resolution crop surface models to monitor crop growth variability. *PFG.* 6: 551–562. Doi: 10.1127/1432-8364/2013/0200.
13. Bennett, R. S., Hutmacher, R. B., and Davis, R. M. 2008. Seed transmission of *Fusarium oxysporum* f. sp. *vasinfectum* race 4 in California. *J. Cotton Sci.* 12:160-164.

14. Bennett, R. S., and Colyer, P. D. 2010. Dry heat and hot water treatments for disinfesting cottonseed of *Fusarium oxysporum* f. sp. *vasinfectum. Plant Dis.* 94:1469-1475. Doi: 10.1094/PDIS-01-10-0052.

15. Bennett, A. J., Bending, G. D., Chandler, D., Hilton, S., and Mills, P. 2011. Meeting the demand for crop production: the challenge of yield decline in crops grown in short rotations. *Biol. Rev.* 87(1): 52-71. Doi: 10.1111/j.1469-185X.2011.00184.x.

16. Bennett, R. S., Spurgeon, D. W., DeTar, W. R., Gerik, J. S., Hutmacher, R. B., and Hanson, B. D. 2011. Efficacy of four soil treatments against *Fusarium oxysporum* f. sp. *vasinfectum* race 4 on cotton. *Plant Dis.* 95(8):967-976. Doi: 10.1094/PDIS-09-10-0696.

17. Bennett, R. S. 2012. Survival of *Fusarium oxysporum* f. sp. *vasinfectum* chlamydospores under solarization temperatures. *Plant Dis.*96:1564-1568. Doi: 10.1094/PDIS-09-11-0812-RE.

18. Berbegal, M., Ortega, A., García-Jiménez, J. and Armengol, J. 2007. Inoculum density-disease development relationship in Verticillium wilt of artichoke caused by *Verticillium dahliae*. *Plant Dis*. 91:1131-1136. Doi: 10.1094/PDIS-91-9-1131.

19. Borra-Serrano, Pena, J.M.; Torres-Sanchez, J.; Messa-Carracosa, F.J.; Lopez-Granados, F. 2015. Spatial quality evaluation of resampled unmanned aerial vehicle-imagery for weed mapping. *Sensors*. (12) 19688–19708. Doi: 10.3390/s150819688.

20. Brown, J. 1997. Survival and dispersal of plant parasites: general concepts. In *Plant Pathogens and Plant Disease.* Ed. J. F. Brown and H. J. Ogle. 195-206.

21. Bruns, H. A. 2017. Southern corn leaf blight: a story worth retelling. *Agron. J.* 109: 1-7. Doi: 10.2134/agronj2017.01.0006.

22. Burdon, J. J. and Thrall, P.H. 1999. Spatial and temporal patterns in coevolving plant and pathogen associations. *Am Nat.* 153: S15-S33. Doi: 10.1086/303209.

23. Burdon, J. J. and Thrall, P. H. 2003. The fitness costs to plants of resistance to pathogens. *Genome Biol.* 4:227. Doi: 10.1186/gb-2003-4-9-227.

24. Burdon, J. J., Thrall, P. H., and Ericson, L. 2005. The current and future dynamics of disease in plant communities. *Annu. Rev. Phytopathol.* 44: 19-39. Doi: 10.1146/annurev.phyto.43.040204.140238.

25. Burdon, J. J. and Thrall, P. H. 2007. Pathogen evolution across the agro-ecological interface: implications for disease management. *Evol. App.* 1:57-68. Doi: 10.1111/j.1752-4571.2007.00005.x.

26. Burdon, J. J. and Thrall, P. H. 2009. Coevolution of plants and their pathogens in natural habitats. *Science*. 324: 755-756. Doi: 10.1126/science.1171663.

27. Burkhardt, A., Ramon, M. L., Smith, B., Koike, S. T., and Martin, F. 2018. Development of molecular methods to detect *Marcrophomina phaseolina* from strawberry plants and soil. *Phytopath.* 108: 1386-1394. Doi. 10.1094/PHYTO-03-18-0071-R.

28. Chappelka, A. H. and Grulke, N. E. 2015. Disruption of the ‘disease triangle’ by chemical and physical environmental change. *Plant Biol.* 18: 5-12. Doi: 10.1111/plb/12353.

29. Cianchetta, A. N., Allen, T. W., Hutmacher, R. B., Kemerait, R. C., Kirkpatrick, T. L., Lawrence, G. W., Lawrence, K. S., Mueller, J. D., Nichols, R. L., Olsen, M. W., Overstreet, C. Woodward. J. E., and Davis, R. M. 2015. Survey of *Fusarium oxysporum* f. sp. *vasinfectum* in the United States. *J. Cotton Sci*. 19:328-336.

30. Cianchetta, A. N. and Davis, R. M. 2015. Fusarium wilt of cotton: management strategies. *J. Crop Prot.* 73: 40-44. Doi: 10.1016/j.cropro.2015.01.014.

31. Chawla, S., Woodward, J. E., Wheeler, T. A., and Wright, R. J. 2012. Effect of *Fusarium oxysporum* f. sp. *vasinfectum* inoculum density, *Meloidogyne incognita* and cotton cultivar on Fusarium wilt development. *Texas Journal Agriculture and Natural Resources.* 25:45-56.

32. Chenu, C., Rumpel, C., and Lehmann, J. 2015. Methods for Studying Soil Organic Matter: Nature, Dynamics, Spatial Accessibility, and Interactions with Minerals. In *Soil Microbiology, Ecology, and Biochemistry*. ed. Eldor A. Paul. Academic Press, Elsevier Inc., p. 383-420.

33. Christiansen, M. P., Laursen, M. S., Jorgensen, R. N., Skovsen, S., and Gislum, R. 2017. Designing and testing a UAV mapping system for agricultural field surveying. *Sensors.* 17: 2703. Doi: 10.3390/s171122703.

34. Cox, K. L. Jr., Babilonia, K., Wheeler, T. A., He, P. and Shan, L. 2019. Return of old foes – recurrence of bacterial blight and Fusarium wilt of cotton. *Curr. Opin. Plant Biol*. 50:95-103. Doi: 10.1016.j.pbi.2019.03.012.

35. Crutcher, F. K., Doan, H. K., Bell, A. A., Davis, R. M., Stipanovic, R. D., Nichols, R. L., and Liu, J. 2016. Evaluation of methods to detect the cotton wilt pathogen *Fusarium oxysporum* f. sp. *vasinfectum* race 4. *Eur. J. Plant Pathol.* Doi: 10.1007/s10658-015-0763.

36. Citavello, D. J., Cohen, J., Fatima, H., Halstead, N. T., Liriano, J., McMahon, T. A., Ortega, C., N. Saure, E. L., Sehgal, T., Young, S., and Rohr, J. R. 2015. Biodiversity inhibits parasites: broad evidence for the dilution effect. *PNAS*. 112: 8867-8671. Doi: 10.1073/pnas.1506279112.

37. Dahlberg, K. R. and Van Etten, J. L. 1982. Physiology and biochemistry of fungal sporulation. *Ann. Rev. Phytopathol.* 20: 281-301. Doi: 10.1146/annurev.py.20.090182.001433.

38. Davis, R. M., Colyer, P. D., Rothrock, C. S., and Kochman, J. K. 2006. Fusarium wilt of cotton: population diversity and implication for management. *Plant Dis.* 90(6):692-703.

39. Davis II, R. L**.**, Greene, J. K., Dou, F., Jo, Y. K., and Chappell, T. M. 2020. A practical application of unsupervised machine learning for analyzing plant image data collected using unmanned aircraft systems. *Agronomy*. Doi: 10.3390/agronomy10050633.

40. Davis II, R. L., Isakeit, T., Chappell, T. M. 2022. DNA-based quantification of *Fusarium oxysporum* f. sp. *vasinfectum* in environmental soils to describe spatial variation in inoculum density. *Plant Dis*. Doi: 10.1094/PDIS-08-21-1664-RE.

41. DeVay, J. E., Gutierrez, A. P., Pullman, G. S., Wakeman, R. J., Garber, R. H., Jeffers, D. P., Smith, S. N., Goodell, P. B., and Roberts, P. A. 1997. Inoculum densities of *Fusarium oxysporum* f. sp. *vasinfectum* and *Meloidogyne incognita* in relation to the development of Fusarium wilt and the phenology of cotton plants (*Gossypium hirsutum*). *Phytopathology*. 87(3):341-346.

42. Diaz, J., Garcia, J., Lara, C., Hutmacher, R. B., Ulloa, M., Nichols, R. L., and Ellis, M. 2021. Characterization of current *Fusarium oxysporum* f. sp. *vasinfectum* isolates from cotton in the San Joaquin Valley of California and Lower Valley El Paso Texas. *Plant Dis.* Doi: 10.1094/PDIS-05-20-1038-RE.

43. Diaz-Varela, R. A., De la Rosa, R., Léon, L., and Zarco-Tejada, P. J. 2015. High-Resolution Airborne UAV Imagery to Assess Olive Tree Crown Parameters Using 3D Photo Reconstruction: Application in Breeding Trials. *Remote Sens*. 7(4). Doi: 10.3390/rs70404213.

44. Doan, H. K., Zhang, S., and Davis, R. M. 2014. Development and evaluation of AmplifyRP Accerer8 Diagnostic Assay for the detection of *Fusarium oxysporum* f. sp. *vasinfectum* race 4 in cotton. *Plant Health Progress.* 15(1):48-52. Doi: 10.1094/PHP-RS-13-0115.

45. Eversmeyer, M. G., and Kramer, C. L. 2000. Epidemiology of wheat leaf rust and stem rust in the Central Great Plains of the USA. *Annu. Rev. Phytopathol.* 38: 491-513. Doi: 10.1146/annurev.phyto.38.1.491.

46. Gordon, T. R. 2017. *Fusarium oxysporum* and the *Fusarium* wilt syndrome. *Annu. Rev. Phytopathol.* 55:23-29. Doi: 10.1146/annurev-phyto-080615-095919.

47. Gracia-Romero, A., Kefauver, S. C., Vegara-Diaz, O., Zaman-Allah, M. A., Prsanna, B. M., Cairns, J. E., and Araus, J. L. 2017. Comparative performance of ground vs. aerially assessed RGB and multispectral indices for early-growth evaluation of maize performance under phosphorus fertilization. *Front. Plant Sci*. 8: 2004. Doi: 10.3389/fpls.2017.02004.

48. Grulke, N. E. 2011. The nexus of host and pathogen phenology: understanding the disease triangle with climate change. *New Phytol.* 189: 8-11. Doi: 10.1111/j.1469-8137.2010.03568.x.

49. Haghighattalab, A., Perez, L. G., Mondal, S., Singh, D., Schinstock, D., Rutkoski, J., Ortiz-Monasterio, I., Singh, R. P., Goodin, D., and Poland, J. 2016. Application of unmanned aerial systems for high throughput phenotyping of large wheat breeding nurseries. *Plant Methods*. 12: 35. Doi: 10.1186/s13007-016-0134-6.

50. Halpern, H. C., Bell, A. A., Wagner, T. A., Liu, J., Nichols, R. L., Olvey, J., Woodward, J. E., Sanogo, S., Jones, C. A., Chan, C. T., and Brewer, M. T. 2017. First report of Fusarium wilt of cotton caused by *Fusarium oxysporum* f. sp. *vasinfectum* race 4 in Texas, U.S.A. DOI: 10.1094/PDIS.07.17.1084-PDN.

51. Hansen, J. G. 1991. Use of multispectral radiometry in wheat yellow rust experiments. *EPPO Bull*. 21: 651–658.

52. Hao, J. J., Yang, M. E., and Davis, R. M. 2009. Effect of soil inoculum density of *Fusarium oxysporum* f. sp. *vasinfectum* race 4 on disease development in cotton. *Plant Dis.* 93(12):1324-1328. Doi: 10.1094/PDIS-93-12-1234.

53. Henry, P. M., Pastrana, A. M., Leveau, J. H. L., and Gordon, T. R. 2019. Persistence of *Fusarium oxysporum* f. sp. *fragariae* in soil through asymptomatic colonization of rotation crops. *Phytopath.* 109:770-779. Doi: 10.1094/PHYTO-11-18-0418-R.

54. Hindson, B. J., Ness, K. D., Masquelier, D. A. et al. 2011. High-throughput droplet digital PCR system for absolute quantitation of DNA copy number. *Anal. Chem.* 83:8604-8610. Doi: 10.1021/ac202028g.

55. Honkavaara, E., Kaivosoja, J., Pellikka, I., Pesonen, L., Saari, H., Hakala, T., Marklelin, L., and Rosnell, T. 2012. Hyperspectral reflectance signatures and point clouds for precision agriculture by light weight UAV imaging systems. *ISPRS Ann. Photogramm. Remote Sens. Spat. Inf. Sci*. 7: 353–358.

56. Hutmacher, R. B., Ulloa, M., Wright, S. D., et al. 2013. Elite upland cotton germplasm-pool assessment of Fusarium wilt resistance in California. *Agron.* 105(6):1635-1644. Doi: 0.2134/agronj2013.0264.

57. Isakeit, T., and Arce, J. 2021. Evaluation of commercial Upland cotton varieties for reaction to *Fusarium oxysporum* f. sp. *vasinfectum* race 4 in Texas. 2021 Proc. Beltwide Cotton Conf., pp. 488-491.

58. Jeger, M. J. 2020. The epidemiology of plant viruses: towards a new synthesis. *Plants.* 9:1768. Doi: 10.3390/plants9121768.

59. Jimenez-Brenes, F. M., Lopez-Granados, F., de Castro, A. I., Torres-Sanchez, J., Serrano, N., and Peña, J. M. 2017. Quantifying pruning impacts on olive tree architecture and annual canopy growth by using UAV-based 3D modelling. *Plant Methods.* 13: 55. Doi:10.1186/s13007-017-0205-3.

60. Kalischuk, M., Paret, M. L., Freeman, J. H., Raj, D., Da Silva, S., Eubanks, S., Wiggins, D. J., Lollar, M., Marois, J. J., Mellinger, H. C., and Das, J. 2019. An improved crop scouting technique incorporating unmanned aerial vehicle-assisted multispectral crop imaging into conventional scouting practices for gummy stem blight in watermelon. *Plant Dis.* 103:1642-1650. Doi: 20.094/PDIS-08-18-1373-RE. *PLoS One*. 8(5): e63003.

61. Keesing, F., Holt, R. D., and Ostfeld, R. S. Effects of species diversity on disease risk. *Ecol. Lett.* 9: 485-498. Doi: 10.1111/j.1461-0248.2006.00885.x.

62. Kefauver, C., Vicente, R., Vergara-Diaz, O., Ferdandez-Gallego, J. A., Kerfal, S., Lopez, A., Melichar, J. P. E., Serret Molins, M. D., and Araus, J.L. 2017. Comparative UAV and field phenotyping to assess yield and nitrogen use efficiency in hybrid and conventional barley. *Front. Plant Sci*. 8: 1733. Doi: 10.3389/fpls.2017.01733.

63. Khanna, R., Möller, M., Pfeifer, J., Liebisch, F., Walter, A., and Siegwart, R. 2015. Beyond point clouds—3D mapping and field parameter measurements

using UAVs. In Proceedings of the EEE 20th Conference on Emerging Technology & Factory Automation, Luxembourg, 8-11 September 2015.

64. Kim, Y., Hutmacher, R. B., and Davis, R. M. 2005. Characterization of California isolates of *Fusarium oxysporum* f. sp. *vasinfectum. Plant Dis*. 89:366-372. Doi: 10.1094/PD-89-0366.
65. Leclerc, M., Doré, T., Gilligan, C. A., Lucas, P., and Filipe, J. A. N. 2013. Host growth can cause invasive spread of crops by soilborne pathogens. Doi: 10.1371/journal.pone.0063003.
66. Li, F., Piasecki, C., Millwood, R. J., Wolfe, B., Mazarei, M., and Stewart Jr., N. C. 2020. High-throughput switchgrass phenotyping and biomass modeling by UAV. *Front Plant Sci.* 11: 574073. Doi:10.33898/fpls.2020.574073.
67. Liebisch, F., Kirchgessner, N., Schneider, D., Walter, A., and Hund, A. 2015. Remote, aerial phenotyping of maize traits with a mobile multi-sensor approach. *Plant Methods*. 11: 9. Doi: 10.1186/s13007-015-0048-8.
68. Liu, W., Cao, X., Fan, J., Wang, Z., Yan, Z., Luo, Y., West, J. S., Xu, X., and Zhou, Y. 2018. Detecting wheat powdery mildew and predicting grain yield using unmanned aerial photography. *Plant Dis.* 102:1981-1988. Doi: 10.1094/PDIS-12-17-1893-RE.
69. Liu, Y. and He, F. 2019. Incorporating the disease triangle framework for testing the effect of soil-borne pathogens on tree species diversity. *Funct. Ecol.* 33: 1211-1222. Doi: 10.1111/1365-2435.13345.

70. Madden, L. V. 1989. Dynamic nature of within-field disease and pathogen distribution. In *Spatial Components of Plant Disease Epidemics*. ed. Michael J. Jeger. Prentice Hall Inc., p. 85-95.

71. Madec, S., Baret, F., de Solan, B., Thomas, S., Dutarte, D., Jezequel, S., Hemmerlé, M., Colombeau, G., and Comar, A. 2017. High-throughput phenotyping of plant height: Comparing unmanned aerial vehicle and ground LiDAR estimates. *Front. Plant Sci*. 8: 2002. doi:10.3389/fpls.2017.02002.

72. Maes, W. H. and Steepe, K. 2019. Perspective for remote sensing with unmanned aerial vehicles in precision agriculture. *Trends Plant Sci*. 24: 2. Doi: 10.1016/j.tplants.2018.11.007.

73. National Agricultural Statistics Service, Southern Plains Region: *Annual Cotton Review*. [https://www.nass.usda.gov/Statistics_by_State/Texas/Publications/Current_News_Release/2020_Rls/tx-cotton-review-2020.pdf]. 2020.

74. Ojiambo, P. S., Yuen, J., van den Bosch, F., and Madden, L. V. 2017. Epidemiology: past, present, and future impacts on understanding disease dynamics and improving plant disease: management – a summary of focus issue articles. *Phytopath.* 107: 1092-1094. Doi: 10.1094/PHYTO-07-17-0248-FI.

75. Ortiz, C. S., Bell, A. A., Magill, Clint, and Liu, J. 2017. Specific PCR detection of *Fusarium oxysporum* f. sp. *vasinfectum* California race 4 based on a unique *Tfo1* insertion event in the *PHO* gene. *Plant Dis*. 101(1):34-44. Doi: 10.1094/PDIS-03-16-0332-RE.

76. Ostfeld, R. S. and Keesing F. 2012. Effect of host diversity on infectious disease. *Annu. Rev. Ecol. Evol. Syst*. 43: 157-182. Doi: 10.1146/annurev-ecolsys-102710-1450022.

77. Ota, T., Ogawa, M., Shimizu, K., Kajisa, T., Mizoue, N., Yoshida, S, Takao, G., Hirata, Y., Furuya, N., Sano, T., et al. 2015. Aboveground biomass estimation using structure from motion approach with aerial photographs in a seasonal tropical forest. *Forests.* 6: 3882–3898. Doi: 10.3390/f6113882.

78. Papaix, J., Burdon, J. J., Zhan, J., and Thrall, P. H. 2015. Crop pathogen emergence and evolution in agro-ecological landscapes. *Evol. Appl.* 8: 385-402Doi: 10.1111/eva.12251.

79. Paugh, K. R. and Gordon, T. R. 2021. Survival of *Fusarium oxysporum* f. sp. *latucae* on crop residue in soil. *Plant Dis*. 105: 912-918. Doi: 10.1094/PDIS-07-20-1464-RE.

80. Pena, J. M., Torres-Sanchez, J., de Castro, A. I., Kelly, M., and Lopez-Granados, F. 2013. Weed mapping in early-season maize fields using object-based analysis of unmanned aerial vehicle (UAV) images. *PLoS One*. 8: e77151. Doi: 10.1371/journal.pone.0077151.

81. Pix4Dmapper 4.1 User Manual. Available online: https://support.pix4d.com/hc/en-us/articles/204272989-Offline-Getting-Started-and-Manual-pdf (accessed: 18 November 2018).

82. Plantegenest, M., Le May, C., Fabre, F. 2007. Landscape epidemiology of plant diseases. *J. r. Soc. Interface*. 4:963-972. Doi: 10.1098/rsif.2007.1114.

83. Rački, N., Dreo, T., Gutierrez-Aguirre, I., Blejec, Ravnikar, M. 2014. Reverse transcriptase droplet digital PCR shows high resilience to PCR inhibition from plant, soil, and water samples. *Plant Methods.* 10:42. Doi: 10.1186/s13007-014-0042-6.

84. Sanogo, S., and Zhang, J. 2016. Resistance sources, resistance screening techniques and disease management for Fusarium wilt in cotton. *Euphytica.* 207:255-271. Doi: 10.1007/s10681-015-1532-y.

85. Santoyo, G., Moreno-Hagelsieb, G., Orozco-Mosqueda, M. C., and Glick, B. R. 2016. Plant growth-promoting bacterial endophytes. *Microbiol Res.* 183:92-99. Doi: 10.1016/j.micres.2015.11.00.

86. SAS Institute Inc., SAS 9.4 Help and Documentation, Cary, NC: SAS Institute Inc., 2002-2014.

87. Scholthof, K. B. S. 2007. The disease triangle: pathogens, the environment and society. *Nat. Rev. Microbiol.* 5: 152-156. Doi: 10.1038/nrmicro1596.

88. Scott, J. C., McRoberts, D. N., and Gordon, T. R. 2014. Colonization of lettuce cultivars and rotation crops by *Fusarium oxysporum* f. sp. *latucae*, the cause of fusarium wilt of lettuce. *Plant Pathol.* 63: 548-553. Doi: 10.1111/ppa.12135.

89. Seabloom, E. W., Borer, E. T., Gross, K., Kendig, A. E., Lacroix, C., Mitchell, C. E., Mordecai, E. A., and Power, A. G. 2015. The community ecology of pathogens,: coinfection, coexistence, and community composition. *Ecol. Lett.* 18: 401-415. Doi: 10.1111/ele.12418.

90. Seo E., Yoon Y., Kim K., Shim W.B., Kuzmina N., Oh K.S., Lee J.O., Kim D.S., Suh J., Lee S.H., Chung K.H., and Chung DH. 2009. Fumonisins B1 and B2 in agricultural products consumed in South Korea: an exposure assessment. *J Food Prot*. 72(2):436-40. Doi: 10.4315/0362-028x-72.2.436.

91. Shan, L., He, P., and Sheen, J. 2007. Endless hide-and-seek: dynamic co-evolution in plant-bacterium warfare. *J Int. Plant Biol.* 49(1): 105-111. Doi: 10.1111/j.1744-7909.2006.00409.x.

92. Shi, Y., Thomasson, J. A., Murray, S. C., Pugh, N. A., Rooney, W.,L., Shafian, S., Rana, A., et al. 2016. Unmanned aerial vehicles for high-throughput phenotyping and agronomic research. *PLoS One*. 11: e0159781. Doi: 10.1371/journal.pone.01599781.

93. Stahr, M and Quesada-Ocampo, L. M. 2020. Assessing the role of temperature, inoculum density, and wounding on disease progression of the fungal pathogen *Ceratocystis fimbriata* causing black rot in sweetpotato. *Plant Dis.* 104:930-937. Doi: 10.1094/PDIS-12-18-2224-RE.

94. Starr, J. L., Jeger, M. J., Martyn, R. D., and Schilling, K. 1989. Effects of *Meloidogyne incognita* and *Fusarium oxysporum* f. sp. *vasinfectum* on plant mortality and yield of cotton. *Phytopathology*. 79:640-646.

95. Stevens, R. B. (1960). Cultural practices in disease control. In J. G. Horsfall, & A. E. Dimond (eds.), Plant pathology, an advanced treatise (Vol 3. pp. 357–429). New York: Academic Press.

96. Su, J., Liu, C., Coombes, M., Hu, X., Wang, C., Xu, X., Li, Q., Guo, L., and Chen, W.H. 2018. Wheat yellow rust monitoring by learning from multispectral UAV aerial imagery. *Compt. Electron. Agric*. 155: 157-166. Doi: 10.1016/j.compag.2018.10.017.

97. Takeno, K. 2016. Stress-induced flowering: the third category of flowering response. *J. Exp. Bot*. 67(17): 4925-4934. Doi: 10.1093/jxb/erw272.

98. Termorshuizen, A. J. 2016. Ecology of fungal plant pathogens. *Microbiol. Spectrum.* 4(6): 1-11. Doi: 10.1128/microbiolspec.FUNK-0013-2016.

99. Torres-Sanchez, J., López-Granados, F., Serrano, N., Arquero, O., and Peña, J.M. 2015. High-throughput 3-D monitoring of agricultural-tree plantations with unmanned aerial vehicle (UAV) technology. *PLoS One*. 2015. 10: e0130479. Doi: 10.137/journal.pone.0130479.

100. Thrall, P. H. and Burdon, J. J. 2002. Evolution of gene-for-gene systems in metapopulations: the effect of spatial scale of host and pathogen dispersal. *Plant Pathol.* 51: 169-184. Doi:

101. Thrall, P. H., Oakeshott, J. G., Fitt, G., Southerton, S., Burdon, J. J., Sheppard, A., Russell, R. J., Zalucki, M., Heino, M., and Denison, R. F. *Evol. App.* 4: 200-215. Doi: 10.1111/j.1752-4571.2010.00179.x.

102. Thrall, P. H., Barrett, L. G., Dodds, P. N., and Burdon, J. J. 2016. Epidemiological and evolutionary outcomes in gene-for-gene and matching allele models.

103. Turechek, W. W. and McRoberts, N. 2013. Considerations of scale in the analysis of spatial patterns of plant disease epidemics. *Annu. Rev. Phytopathol.* 51:453-472. Doi: 10.1146/annurev-phyto-081211-173017.

104. Ulloa, M., Hutmacher, R. B., Davis, R. M., Wright, S. D., Percy, R., and Marsh, B. 2006. Breeding for Fusarium wilt race 4 resistance in cotton under field and greenhouse conditions. *J Cotton Sci.* 10(2):114-127.

105. Ulloa, M., Hutmacher, R. B., Roberts, P. A., Wright, S. D., Nichols, R. L., and Davis, R. M. 2013. Inheritance and QTL mapping of Fusarium wilt race 4 resistance in cotton. *Theor. Appl. Genet.* 126:1405-1418. Doi: 10.1007/s00122-013-2061-5.

106. Ulloa, M., Hutmacher, R. B., Schramm, T., Ellis, M. L., Nichols, R., Roberts, P. A., and Wright, S. D. 2020. Sources, selection and breeding of Fusarium wilt (*Fusarium oxysporum* f. sp. *vasinfectum*) race 4 (FOV4) resistance in Upland (*Gossypium hirsutum* L.) cotton. *Euphytica*. 216:109. Doi: 10.1007/s10681-020-02643-5.

107. Ultee, E., Ramijan, K., Dame, R. T., Briegel, A., and Claessen, D. 2019. Stress-induced adaptive morphogenesis in bacteria. *Adv. Microb. Physiol*. 74: 97-141. Doi: 10.1016/bs.ampbs.2019.02.001.

108. Vanegas, F., Bratanov, D., Powell, K., Weiss, J., and Gonzalez, F. 2015. A novel methodology for improving plant pest surveillance in vineyards and crops using UAV-based hyperspectral and spatial data. *Sensors*. 18: 260. Doi: 10.3390/s18010260.

109. Vegara-Diaz, O., Zaman-Allah, M. A., Masuka, B., Hornero, A., Zarco-Tejada, P., Prasanna, B. M., Cairns, J. E., and Araus, J. L. 2016. A novel remote sensing approach for prediction of maize under different nitrogen fertilizations. *Front. Plant Sci*. 7: 666. Doi: 10.3389/fpls.2016.00666.

110. Voroney, R. P. and Heck, R. J. 2015. The Soil Habitat. In *Soil Microbiology, Ecology, and Biochemistry*. ed. Eldor A. Paul. Academic Press, Elsevier Inc., p. 15-40.

111. Wada, K. C., and Takeno, K. 2010. Stress-induced flowering. *Plant Signaling Behav*. 5(8): 944-947. Doi: 10.4161/psb.5.8.11826.

112. Wang, C., Ulloa, M., Duong, T., and Roberts, P. A. 2018. Quantitative trait loci mapping of multiple independent loci for resistance to *Fusarium oxysporum* f. sp. *vasinfectum* race 1 and 4 in an interspecific cotton population. *Phytopathology*. 108:759-767. Doi: 10.1094/PHYTO-06-17-0208-R.

113. Wani, Z. A., Ashraf, N., Mohuiddin, T., and Riyaz-Ul-Hassan, S. 2015. Plant-endophyte symbiosis, an ecological perspective. *Appl Microbiol Biotechnol*. 99:2955-2965. Doi: 10.1007/s00253-015-6487-3.

114. Watanabe, K., Guo, W., Arai, K., Takanashi, H., Kajiya-Kanegae, H., Kobayashi, M., Yano, K., Tokunaga, T., Fujiwara, T., Tsutsumi, N., et al. 2017. High-throughput phenotyping of sorghum plant height using an unmanned aerial vehicle and its application to genomic prediction modeling. *Front. Plant Sci*. 8: 421. Doi: 10.3389/fpls.2017.00421.

115. Way, M. O., McCauley, G. M., Zhou, X. G., Wilson, L. T., and Morace, B. 2014. Texas Rice Production Guidelines. Available online: https://beaumont.tamu.edu/eLibrary/Bulletins/2014_Rice_Produdution_Guidelines.pdf (accessed on 15 December 2018).

116. Wen, R., Lee, J., Chu, M., Tonu, N., Dumonceaux, T., Gossen, B. D., Yu, F., and Peng, G. 2020. Quantification of *Plasmodiophora brassicae* resting spores in soils using droplet digital PCR (ddPCR). 104:1188-1194. Doi: 10.1094/PDIS-03-19-0584-RE.

117. Westoby, M. J., Brasington, J., Glasser, N. F., Hambrey, and M. J., Reynolds, J. M. 2012. 'Structure-from-motion' photogrammetry: A low-cost, effective tool for geoscience applications. *Geomorphology*. 179, 300–314, Doi: 10.1016/j.geomorph.2012.08.021.

118. White, J. W., Andrade-Sanchez, P., Gore, M. A., Bronson, K. F., Cofflet, T. A., Conley, M. M., Feldmann, K. A., French, A. N., Heun, J. T., Hunsaker, D. J. et al. 2012. Field-based phenomics for plant genetics research. *Field Crop Res*. 133: 110–112. Doi: 10.1026/j/fcr/2012.04.003.

119. Yamamoto, K., Togami, T., and Yamaguchi, N. 2017. Super-resolution of plant disease images for the acceleration of image-based phenotyping and vigor diagnosis in agriculture. *Sensors*. 17: 2557. Doi: 10.3390/s17112557.

120. Yang, G., Liu, J., Zhao, C., Li, Z., Huang, Y., Yu, H., Xu, B., Yang, X., Zhu, D., Zhang, X., et al. 2017. Unmanned aerial vehicle remote sensing for

field-based crop phenotyping: Current status and perspectives. *Front. Plant Sci*. 8: 1111. Doi: 10.3389/fpls.2017.01111.

121. Yin, X., McClure, A., Jaja, N., Tyler, D. D., and Hayes, R. M. 2011. In-season prediction of corn yield using plant height under major production systems. *Agron. J.* 103: 923–929. Doi: 10.2134/agronj2010.0450.

122. Young, H. S., Parker, I. M., Gilbert, G. S., Gurerra, A. S., and Nunn, C. L. 2017. Introduced species, disease, ecology, and biodiversity – disease relationships. *Trends Ecol. Evol.* 32(1): 41-54. Doi: 10.1016/j.tree.2016.09.008.

123. Yuen, J. and Mila, A. 2015. Landscape-scale disease risk quantification and prediction. *Annu. Rev. Phytopathol.* 51:453-472. Doi: 10.1146/annurev-phyto-080614-120406.

124. Zhang, C. and Kovacs, J. M. 2012. The application of small unmanned aerial systems for precision: a review. *Precision Agric*. 13: 693–712. Doi: 10.1007/s11119-012-9274-5.

125. Zhang, C., Walters, D., and Kovacs, J. M. 2014. Applications of low altitude remote sensing in agriculture upon farmers' requests- a case study in northeastern Ontario, Canada. *PLoS One*. 9: e112894. Doi: 10.1371/journal.pone.0112894.

126. Zhang, D., Zhou, X., Zhang, J., Lan, Y., Xu, C., and Liang, D. 2018. Detection of rice sheath blight using an unmanned aerial system with high-resolution color and multispectral imaging. *PLoS One*. 13: e0187470. Doi: 10.1371/journal.pone.018740.

127. Zhang, J., Abdelraheem, A., Zhu, Y., Wheeler, T. A., Dever, J. K., Frelichowski, J., Love, J., Ulloa, M., Jenkins, J. N., McCarty, J. C. Jr., Nichols, R., and Wedegaertner, T. 2020. Assessing genetic variation for Fusarium wilt race 4 resistance in tetraploid cotton by screening over three thousand germplasm lines under greenhouse or controlled conditions. *Euphytica*. 216(108). Doi: 10.1007/s10681-020-02646-2.

128. Zheng, Q.; Huang, W.; Cui, X.; Liu, L. 2018. New spectral index for detecting wheat yellow rust using sentinel-2 multispectral imagery. *Sensors*. 18: 868. Doi: 10.3390/s18030868.

129. Zhu, Y., Lujan, P. A., Wedegaertner, T., Nichols, R. L., Abdelraheem, A., Zhang, J. F., and Sanogo, S. 2020. First report of *Fusarium oxysporum* f. sp. *vasinfectum* race 4 causing Fusarium wilt of cotton in New Mexico, U.S.A. Doi: 10.1094/PDIS-06-19-1170-PDN.

APPENDIX A

SUPPLEMENTAL FIGURES AND TABLE CHAPTER II

Table 6. Nitrogen application tables for field N-1 and field N-6. Nitrogen was applied at four relative time points pre-planting (APP-1), pre-flooding (APP-2), midseason (APP-3), and heading (APP-4). Treatments were replicated four times in each field.

Relative Nitrogen (kg/ha) Applications					
Field N-1					
Trt#	APP-1	APP-2	APP-3	APP-4	Total N
1	0	0	47	0	47
2	0	62	47	0	109
3	0	96	47	0	143
4	0	130	47	0	177
5	0	163	47	0	210
6	59	0	47	0	106
7	59	62	47	0	168
8	59	96	47	0	202
9	59	130	47	0	235
10	59	163	47	0	269
Field N-6					
Trt#	APP-1	APP-2	APP-3	APP-4	Total N
11	0	0	0	34	34
12	0	135	0	34	168
13	0	168	0	34	202
14	0	202	0	34	235
15	0	235	0	34	269
16	59	0	0	34	92
17	59	135	0	34	227
18	59	168	0	34	261
19	59	202	0	34	294
20	59	235	0	34	328

Table 7. Fit statistics for the selection of effective components in the FMM distributions of the four soybean fields.

Fit Statistics for Soybean Field				
	Field 1	**Field 2**	**Field 3**	**Field 4**
-2 Log Likelihood	-3601.5	-3999.8	471.6	-2111.8
AIC	-3591.5	-3985.8	481.6	-2101.8
AICC	-3591.5	-3985.8	481.6	-2101.8
BIC	-3557.8	-3938.4	515.6	-2066.6
Pearson Statistic	6205.0	6510.0	6716.0	8388.0
Effective Parameters	5	7	5	5
Effective Components	2	2	2	2

Table 8. Fit statistics for a grain sorghum field at the Edisto REC in Blackville, SC. The effective components are the number of latent classes found in data subpopulations.

Fit Statistics for a Sorghum Field				
	32m^2	**16m^2**	**8m^2**	**4m^2**
-2 Log Likelihood	34300.9	12074.8	-823.6	-49.4737
AIC	34316.9	12096.8	-801.6	-39.4737
AICC	34316.9	12096.8	-801.4	-39.2967
BIC	34375.9	12166.5	-745.3	-20.2560
Pearson Statistic	11852.1	4188.0	1239.0	345.0
Effective Parameters	8	11	11	5
Effective Components	3	4	4	2

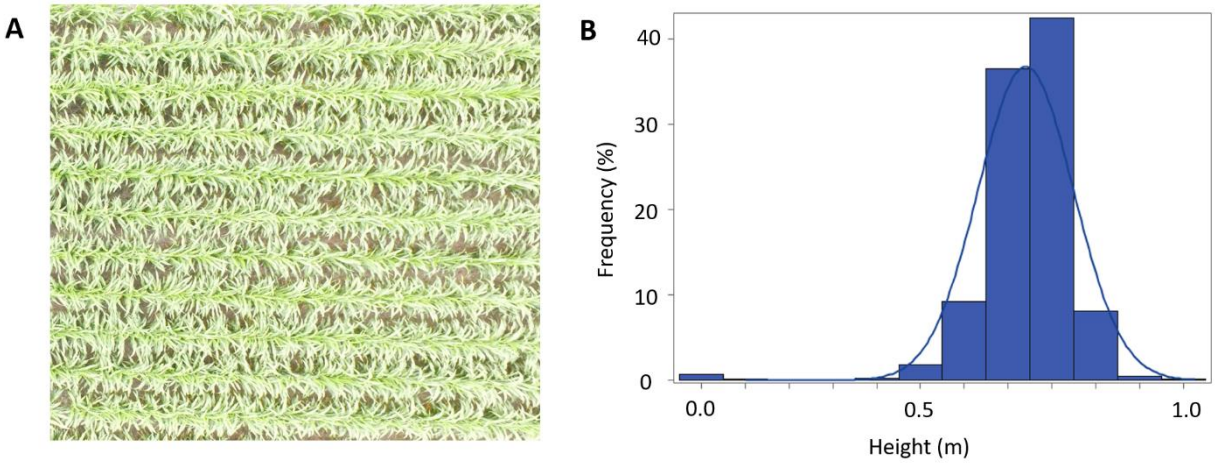

Figure 26. A) Aerial imagery of sorghum, showing dense plant biomass and limited visibility of the ground. B) Histogram of height variation in 3D point cloud derived from imagery of sorghum, and Finite Mixture Model fit to data, showing that only one mixture component is estimated, preventing the estimation of average height by comparing two component distribution means.